DESIGN OF A PRIVATE PASSAGEWAY FUSION RECEPTOR FOR SENSITIVE CONTROL OF ADOPTIVE CELL THERAPIES

by

Boning Zhang

A Dissertation

Submitted to the Faculty of Purdue University

In Partial Fulfillment of the Requirements for the degree of

Doctor of Philosophy

Department of Chemistry

West Lafayette, Indiana

August 2019

THE PURDUE UNIVERSITY GRADUATE SCHOOL
STATEMENT OF COMMITTEE APPROVAL

Dr. Philip S. Low, Chair
Department of Chemistry
Dr. Andrew Mesecar
Department of Chemistry
Dr. Kavita Shah
Department of Chemistry
Dr. Seung-oe Lim
Department of Medicinal Chemistry and Molecular Pharmacology

Approved by:

Dr. Christine Hrycyna
Head of the Graduate Program

To my mum and dad

ACKNOWLEDGMENTS

First and foremost, I would like to express my sincere appreciation to my advisor, Dr. Philip S. Low, who encouraged and guided my research with his profound knowledge, unmet enthusiasm about science, and generous support for the past six years. The completion of a Ph.D. is rarely a smooth journey, and I thank Dr. Low especially for supporting me through the challenges I met in the process of completing these projects. Step-by-step, Dr. Low taught me how to identify a question and how to interpret and learn from the unexpected results that often occur in science. "First, make sure whether there is a question or not," and "Try to turn a lemon into lemonade," he would always say. His insightful vision and broad understanding for translational research have influenced me a great deal and will always guide me in the future whenever I embark on new areas of research or techniques. His rigorous attitude regarding scientific writing has also provided a great model for me. Just as Dr. Low says, "How often do you have the chance to solve a mystery in real life?" Science is an endless puzzle and thanks to Dr. Low, I have gradually learned the joy of solving it.

I would also like to thank the rest of my advisory and thesis committee members, Dr. Kavita Shah, Dr. Timothy Ratliff, Dr. Andrew Mesecar and Dr. Seung-Oe Lim, for the insightful comments, encouragement, and guidance.

Many thanks also go to my former and current colleagues in the Low group. Thanks to Dr. Haiyan Chu and Dr. Yonggu Lee for their hands-on guidance with my CAR T projects. Their hardworking attitude has had a very positive influence on my work. Thanks to my collaborators, Dr. John Victor and Xin Liu. for the CAR T and influenza project, (respectively), I could not finish my work without their help in chemistry. Thanks to Dr. Bingbing Wang and Dr. Fenghua Zhang for sharing their knowledge of the MDSC and TAM. And my thanks go to every other member in

the lab: Weichuan, Qian, Rami, Estela, Suraj, Lindeman, Gardeen, Stew, Jeff, Madduri, Karson, Mingding, Yingwen, Jyoti, Isaac, Mark, and Ian as well as other former lab members, for making such a big and happy family in the lab. My thanks also go to Patti Cauble for taking care of the lab and always being there to listen.

Last but not the least, I would like to thank my parents for their endless love and support throughout my Ph.D. study. As the only child, I have received unconditional love and support from them for every decision I have made in life. I would not have been able to finish my study without their understanding and support.

TABLE OF CONTENTS

LIST OF TABLES 9
LIST OF FIGURES 10
ABSTRACT 12
CHAPTER 1. HISTORY AND DEFICIENCIES IN CURRENT CHIMERIC ANTIGEN RECEPTOR (CAR) T CELL THERAPIES 14
1.1 Introduction 14
1.2 Design and Use of Current CAR T Cell Methodologies in Clinical Cancer Treatment 17
1.3 Side Effects and Limitations of Current CAR T Cell Therapies 24
1.4 Current Approaches to Improve CAR T Cell Design for Better Control and Efficacy of CAR T Cell Activity 26
1.4.1 Current Approaches for Better Control of CAR T Cell Activity 26
1.4.2 Current Approaches for Improving Efficacy of CAR T Cell Therapies in Solid Tumors 30
1.5 References 34
CHAPTER 2. A NOVEL METHOD FOR CONTROL OF CAR T CELL OVERACTIVATION USING A PRIVATE PASSAGEWAY FUSION RECEPTOR 43
2.1 Introduction 43
2.2 Materials and Methods 44
2.2.1 Cell Lines and Human T Cells 44
2.2.2 Synthesis of Private Passageway Substrates 45
2.2.3 Preparation of Lentiviral Vectors Encoding anti-CD19 CAR T2A FKBP-FR and anti-CD19 CAR T2A FITC-FR 47
2.2.4 Use of Lentiviral Vectors Encoding anti-CD19 CAR T2A FKBP-FR and anti-CD19 CAR T2A FITC-FR to Transduce to Human T Cells 48
2.2.5 Analysis of Private Passageway Fusion Receptor Binding and Internalization 49
2.2.6 Quantification of Expression Level of Fusion Receptors Using FA-^{99m}Tc 50
2.2.7 Formulation and Labeling of FITC-^{99m}Tc 50
2.2.8 Measurement of Internalized and Membrane-Bound FITC-^{99m}Tc after Various Periods of Continuous Incubation 50

2.2.9 Characterization of FITC-FR and FKBP-FR Fusion Receptor Molecular Weights by Western Blotting 51
2.2.10 FITC-/FK506-Cytotoxic Payload Mediated Killing of Fusion Receptor Positive Cells 51
2.2.11 Inhibition of Human T Cell Lysis via Private Passageway Delivery of an Immunosuppressant/Kinase Inhibitor Payload 51
2.2.12 Evaluation of FITC-DM4 and FITC-FK506 on FITC-FR CAR T Cell in Raji Tumor Model 52
2.3 Results 54
2.3.1 Design of Private Passageway Fusion Receptors 54
2.3.2 Generation and Characterization of Fusion Receptors 57
2.3.2.1 Stable Surface Expression of Fusion Receptors in Multiple Cell Lines 57
2.3.2.2 Binding Affinities of Folic Acid, Fluorescein and FK506 For Their Corresponding Binding Domains of the Fusion Receptors 60
2.3.2.3 Internalization of Fusion Receptors 61
2.3.3 Inhibition of Cytokine Release Syndrome through Private Passageway Fusion Receptor Mediated Delivery of a Cytotoxic Drug Payload 62
2.3.4 Inhibition of Cytokine Release Syndrome through Private Passageway Fusion Receptor Mediated Delivery of Either an Immunosuppressant or Kinase Inhibitor Payload 63
2.3.4.1 Screening for Potential Small Molecule Inhibitors of CAR T Cell Activity 63
2.3.4.2 FK506 as a Proof-of-Concept Immunosuppressant Payload 65
2.3.4.3 Systemic Control of CAR T Cell Number and/or Activity Using Private Passageway Fusion Receptor 66
2.4 Discussion 67
2.5 References 84
CHAPTER 3. IN VIVO LOCATIONLIZATION AND REJUVENATION OF CAR T CELLS USING A PRIVATE PASSAGEWAY FUSION RECEPTOR 91
3.1 Introduction 91
3.2 Materials and Methods 92
3.2.1 Cell Lines and Human T Cells 92

3.2.2 Biodistribution and SPECT Imaging of Fusion Receptor Positive T Cells Detected by FITC-^{99m}Tc 92
3.2.3 Evaluation of Potential Payloads for in vitro Rejuvenation of Exhausted CAR T Cells 93
3.2.4 Evaluation of FITC-TLR7 Agonist on FITC-FR CAR T Cell in MDA-MB-231 Tumor Model 93
3.3 Results 94
3.3.1 Evaluation of Fusion Receptor Positive CAR T Cells Homing in Solid Tumor by a FITC-^{99m}Tc Radio-Imaging Agent 94
3.3.2 Evaluation of the Ability of Phosphatase Inhibitors and TLR7 Agonists to Rejuvenate Exhausted CAR T cells 96
3.3.3 Evaluation of the Ability of FITC-TLR7 Agonists to Rejuvenate Exhausted CAR T Cells in a Solid Tumor Model 99
3.4 Discussion 101
3.5 References 113
VITA 118
PUBLICATIONS 119

LIST OF TABLES

Table 1 Summary of current approaches using an ON/OFF control switch for CAR T cell therapy ……..……..…33

LIST OF FIGURES

Figure 1-1 Diagram of endogenous TCR (left) and three generations of CAR constructs (right). 16
Figure 1-2 amino acid sequence of anti-CD19 CAR T (CTL019) with each domain annotated. 16
Figure 1-3 Current CAR T cells being tested in clinical trials. 23
Figure 2-1 Design of FKBP-FR and FITC-FR fusion receptors and corresponding targeting ligands. 71
Figure 2-2 Stable expression and localization of FKBP-FR and FITC-FR fusion receptor to the cell surface. 72
Figure 2-3 Structural interference between FR and FKBP in FKBP-FR fusion receptor. 73
Figure 2-4 Optimization of co-expression of fusion receptor and anti-CD19 CAR using a T2A self-cleavage linker in between. 74
Figure 2-5 Private passageway fusion receptors preserve good binding affinity for the corresponding targeting ligands property. 75
Figure 2-6 Preservation and specificity of the binding of FK506-Rhodmaine to FKBP-FR fusion receptor in whole blood. 76
Figure 2-7 Structure and binding affinity of SLF-FITC for FKBP-FR fusion receptor. 77
Figure 2-8 Evaluation and Quantification of FITC-FR and FKPB-FR fusion receptors internalization. 78
Figure 2-9 Quantification of FITC-FR fusion receptor internalization by FITC-^{99m}Tc. 79
Figure 2-10 Effect of FITC-cytotoxic payload on FITC-FR positive human T cells. 80
Figure 2-11 Screening of potential payloads for inhibition of CAR T cell lysis effect. 81
Figure 2-12: Effect of targeting ligand-immunosuppressant conjugates on fusion receptor positive anti-CD19 CAR T cells. 82
Figure 2-13 FITC-DM4 and FITC-FK506 alleviate the CRS by decreasing CAR T cell number and/or cytokine release level in mice bearing Raji tumor cell. 83
Figure 3-1 in vivo localization of CAR T cells using FITC-^{99m}Tc imaging agents. 106
Figure 3-2 in vitro model for the induction of CAR T cell exhaustion. 107
Figure 3-3 Evaluation of TLR7 agonist and PTP1b inhibitor effect on rejuvenation of exhausted CAR T cells. 108

Figure 3-4 Evaluation of potential derivatization sites of the TLR7 agonist for non-releasable ligand targeted delivery. 109
Figure 3-5 Design and evaluation of releasable and non-releasable targeted delivery of TLR7 agonist using FITC as a targeting ligand. 110
Figure 3-6 Evaluation of a potential rejuvenation effect of the releasable FITC-TLR7 agonist in an MDA-MB-231 $CD19^{+}$ solid tumor model. 111
Figure 3-7 Chemical linkers of variable rigidity and hydrophobicity available for usage in the design of targeting ligand-payload conjugates. 112

ABSTRACT

Author: Zhang, Boning. PhD
Institution: Purdue University
Degree Received: August 2019
Title: Design of a Private Passageway Fusion Receptor for Sensitive Control of Adoptive Cell Therapies
Committee Chair: Philip Low

Most Adoptive Cell Therapies (ACT), including CAR T cell therapies, suffer failure because of the severe side effects due to loss-of-control of the therapeutic cells once they are inside the patient's body, suggesting that novel strategies must be developed for a better in vivo control of these engineered cells. In the meantime, CAR T cell therapies targeting solid tumors have not experienced the remarkable success achieved with hematopoietic cancers, mainly due to continuous tumor antigen exposure and a suppressive tumor microenvironment. Here we designed a private passageway fusion receptor, which is composed of a ligand binding domain and a glycosylphosphatidylinositol (GPI) anchoring domain, to be expressed and localized to the surface of CAR T cells independently to the classical CAR T construct. These ligand binding domains preserve high binding affinity towards their cognate ligands and are only expressed on the CAR T cells that have been transduced. Therefore, cytotoxic drugs or immunosuppressants linked to the corresponding targeting ligands are shown to be specifically delivered to these fusion receptor positive CAR T cells for lowering the activity of the over-activated CAR T cells. On the other hand, we discovered that a potent TLR7 agonist is able to enhance the lysis effect of the exhausted CAR T cells in a co-culture model. Serial releasable and non-releasable targeted TLR7 agonists were prepared and tested. Based on these data, we suggest that our secret passageway fusion receptor platform provides a better control of the activity of CAR T cells using the corresponding

targeting ligand-payload conjugates in a dose dependent manner and function as a doorway for the delivery of instructions to CAR T cells for versatile purposes.

CHAPTER 1. HISTORY AND DEFICIENCIES IN CURRENT CHIMERIC ANTIGEN RECEPTOR (CAR) T CELL THERAPIES

1.1 Introduction

There has been a long-lasting interest in using intact human cells to treat various diseases. Among these, stem cell therapy and Adoptive Cellular Therapy (ACT) are the two most well-developed approaches in the last few decades. Induced Pluripotent Stem Cells (iPSC) are being differentiated into cardiomyocytes for the compensation of damaged heart tissues from myocardial infarction[1], islet cells for the treatment of type I diabetes[2], and retinal cells for the replacement of defective retinal pigment epithelial cells[3]. Alternatively, ACT focuses on using immune cells from patients or healthy donors for the treatment of cancer. There are many ways to empower one's own immune system to fight against cancer cells, including peptide-based vaccines, checkpoint inhibitors and ACT. Several reviews have covered the history and development of cancer vaccines and checkpoint inhibitors, and this chapter will focus only on immune cell-based ACT. Early attempt for ACT includes using dendritic cells (DC) that are primed ex vivo with tumor antigens and then transferring them back to patients. This method can target not only surface tumor antigens, but also intracellular ones. In detail, DCs can be loaded with specific antigens, such as MAGE-1, gp100, tyrosinase, Melan-A/Mart-1[4-5], PSA[6] and PSCA[7], or tumor lysates and apoptotic tumor cells. In 2010, FDA approved the first dendritic cell vaccine Sipuleucel-T, based on DCs loaded with prostatic acid phosphatase (PAP) and GM-CSF[8].

T cells are capable of killing cells through many different mechanisms, such as release of Perforin, Granzyme and cytokines. Therefore, they have been used as a platform for artificially designed immune pathways toward tumor cells for long time. Tumor antigens are presented through the MHC molecules expressed on Antigen Presenting Cells (APC) and the complex will then dock

with certain endogenous TCR on T cells. The activation of T cells is a complicated process that requires both the docking of TCR/MHC as well as the engagement of co-activation molecules, such as CD28, 4-1BB with CD80/86 on the APC[9]. Since there is almost no structural difference between a TCR and an antibody for the antigen binding domain, in 1980s, Zelig Eshhar and his colleges tried to substitute the antigen binding part of TCR with an antibody, while keeping the rest of the TCR the same, resulting in the first functional chimeric TCR that is MHC independent[10]. However, this construct turns out to be poorly persistent in mice due to a lack of co-activation signals (TCR docking without a secondary activation signal can result in an anergic condition or activation induced cell death[11]). To improve this, Michel Sadelain and his colleagues incorporated the intracellular CD28 domain into the CAR construct and proofed its better survival and lysis effect[12]. During that time, the phage display technique for the screening of antibodies with higher affinity was gradually developed, and the concept of merging the variable domains of light and heavy chains into one single chain was tested[13]. The resulting single chain fusion protein is called short chain variable fragment (scFv) and can be generated towards any antigens based on the original high affinity antibody. These scFvs are therefore used as the antigen binding domain of the CAR construct while the rest of the signaling domains remain the same. The evolution process of the basic CAR T construct is shown in Figure 1-1. The amino acid sequence of CAR for Kymriah, one of the two FDA-approved anti-CD19 CAR T cell, with each domain annotated, is shown in Figure 1-2.

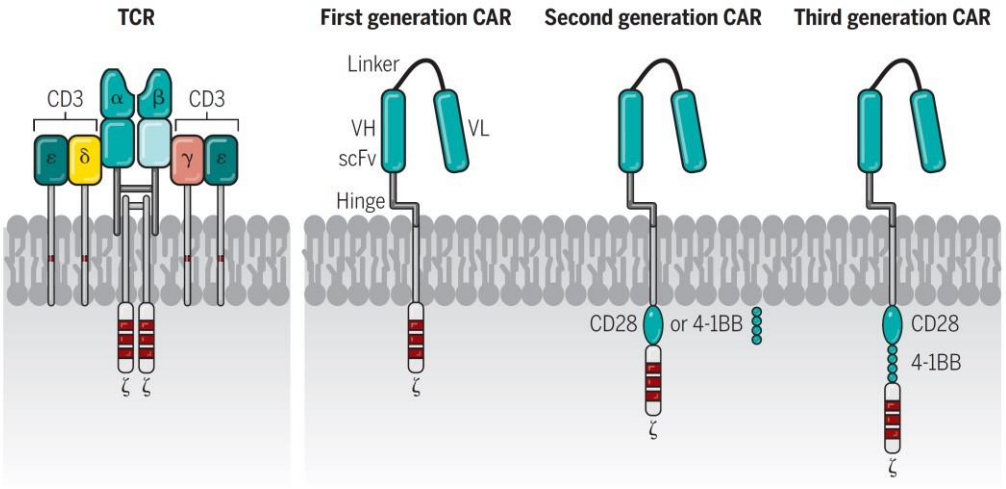

Figure 1-1 Diagram of endogenous TCR (left) and three generations of CAR constructs (right). While there is no difference for the extracellular domains, first generation CARs contain only CD3ζ intracellularly, while 2nd and 3rd generation of CAR include one or two co-stimulatory domains, including CD28 and 4-1BB, in frame. Reprinted from Science, 359(6382), pp.1361-1365.

Figure 1-2 amino acid sequence of anti-CD19 CAR T (CTL019) with each domain annotated. FMC63: scFv against human CD19.

1.2 Design and Use of Current CAR T Cell Methodologies in Clinical Cancer Treatment

The foremost step of any targeted approach for cancer treatment, either through Antibody Drug Conjugate (ADC), vaccines, or CAR T cell therapy, is to find a suitable biomarker as the target[14]. The most important criterion for a good biomarker is to have an abundant or over-expression level in malignant tissues while having a relatively low or no expression level in normal tissues. In some cases, although the expression levels are similar, the difference of the expression form, modification, and surface location of certain antigens can also lower the potency of on-target off-tumor side effects.

The first successful biomarker that is used for CAR T therapy is CD19, a B cell marker that is highly overexpressed in malignant B cells. Since CD19 is also expressed, although at lower level, in normal B cells, patients treated with anti-CD19 CAR T cells will have hypogammaglobulinemia due to B cell aplasia and need to be dosed with IgG that are isolated from healthy donors during and after treatment[15]. Excepting CD19, CD20[16], CD22[17] and CD123[18] all are potent biomarkers and utilized as targets for CAR T cell therapies for hematopoietic malignant diseases, including Acute Myeloid Leukemia (AML), Chronic Lymphocytic Leukemia (CLL), and Acute Lymphocytic Leukemia (ALL) etc.[19] Although most of them are still in the clinical trial phase, CAR T cells therapy for hematopoietic cancer are seeing a significantly better survival rate and less side effects compared to traditional chemotherapies.

The expansion of biomarkers also opens doors for CAR T cells in solid tumors. Currently there are approximately 20 biomarkers for solid tumors that are being explored by many different targeted therapeutic drugs[20-21], including Folate Receptor alpha (FRα), Her2, EGFR, PSMA etc. Among them, Trastuzumab emtansine, a Her2 targeted antibody drug conjugate (ADC), has been approved by the FDA for breast cancer treatment[22]. However, intrinsic mechanism differences

exist between ADC and CAR T cell therapy: only small numbers (at the magnitude of 200) of antigens are required to form the immune synapse and pass the threshold for triggering T cell activation in CAR T therapy[23]. The potency of ADC, however, strongly depends on the expression level of antigens, with a higher expression level directly correlates with the amount of drugs that could be delivered inside the targeted cell[24]. Therefore, biomarkers that have been proved to be safe for ADC may not be suitable for CAR T cell approach, as in the case of Her2[25], CA IX[26] etc. Other than Her2 and CA IX, Mesothelin[27] and Fibroblast activation protein (FAP)[28] for pleural mesothelioma, the prostate stem cell antigen (PSCA) for pancreatic cancer, prostate specific membrane antigen (PSMA)[29] for prostate cancer, and the EGFRVIII[30] for glioblastoma are all currently being evaluated as targets for CAR T cell therapies in clinical trials (Figure 1-3).

Since the current lab has been focused on small molecule targeted cancer diagnosis and treatment for FR, PSMA, CA IX and MUC1 for the past decades and has accumulated substantial knowledge of their expression profile and function, the current landscape of CAR T cell therapy for these antigens will be discussed in more detail below.

- Folate Receptor

The folate receptor family consists of four known members (α, β, γ and δ). FRα, FRβ and FRδ are glycosylphosphatidylinositol-linked membrane proteins, while FRγ is secreted[31]. FRα has a high affinity for folate acid and a high internalization rate, therefore, it can efficiently deliver folate acid into cells and recycle back to the cell surface. FRα is overexpressed in various epithelial malignancies including ovarian, breast, and renal cancers, while normal tissues do express FRα, but only at a lower level or at the apical surfaces of polarized epithelial cells (such as in kidney)[32]. Several antibody-based therapies towards FRα have been developed, including therapeutic antibody[33-35] and ADC. Since Folate Acid (FA) is the natural ligand for FRα, the current lab has

utilized FA[36] as a small molecule targeting ligand and linked it with a cytotoxic drug payload for the treatment of FRα cancers[37-38]. This approach has several advantages compared to antibody-based ones: better tissue penetration[39], better PK/PD, shorter half-life, and lower by-stander effect[40]. With the powerful platform of the CAR T cell therapy, several CAR constructs with different scFvs against FRα have been tested in preclinical mouse models and no severe side effects were observed[41-42]. Another isoform of FR, FRβ, is primarily found on myeloid lineage hematopoietic cells; it can be upregulated in 70% of primary Acute Myeloid Lymphoma (AML) patient tumors and can be increased on AML by all-trans retinoic acid treatment[43]. Therefore, FRβ serves as a promising target for CAR T cells for the treatment of AML and other myeloid lineage malignancies. Daniel Powell, et al. fused FRβ targeting scFv (m909) with a 2nd generation CAR construct and observed a moderate effect of anti-FRβ CAR T cells in a THP-1 tumor model[44]. Since m909 is of mouse origin, it may require a humanization process to reduce immunogenicity before it can be tested on humans. Another potential application of anti-FRβ CAR T cells is to eliminate tumor associated macrophages (TAM) in the tumor microenvironment. These macrophages, usually characterized as CD11b+Gr1-, are known to secrete IL10, GM-CSF, NO and other immunosuppressive cytokines and factors that suppress other nearby immune cells, such as APC, neutrophil, and T cell function. More interestingly, these macrophages have also been shown to overexpress FRβ[45]. Therefore, FRβ targeted CAR T cells may argument the tumor microenvironment by direct killing of TAMs to fight against cancer cells. This potential application has been briefly explored by Jianyin Shen, et al. using an FA-FITC adaptor CAR T cell approach in cell-based assays[46] and is currently pursued in immuno-sufficient mouse models in the current lab.

- PSMA

The prostate specific membrane antigen (PSMA), also known as folate hydrolase I or glutamate carboxypeptidase II, is a type I membrane protein. It is overexpressed in the majority of prostate cancers as well as the neovasculature of other solid tumors, with a limited expression in other normal tissues, such as kidney, nervous system glia, and small intestine[47-48]. The current lab has pioneered the use of a low molecular weight, urea-based inhibitor of PSMA for the targeted drug delivery[49], as well as radioisotope imaging[50]. For immunotherapy approaches, PSMA targeted ADC was first described by Eva Corey, et al.[51] and was recently tested in a phase I clinical trial[52]. Antonio Rosato, et al. first demonstrated the 2nd and 3rd generation anti-PSMA CAR T effect in an NSG mouse model and no side effects were reported[53].

- CA IX

The hypoxia condition is a hallmark of the solid tumor that results in acid metabolites and decreased intracellular pH. To compensate for this, almost all solid tumor cells overexpress carbonic anhydrase IX (CA IX), which reversibly catalyzes CO_2 and water to form $H^+ + HCO_3^-$; the resulting bicarbonate can be transported into the cell, therefore neutralizing the intracellular acid metabolites that would have otherwise inhibited many metabolic pathways[54]. Therefore, CA IX serves as an ideal target for broad spectrum coverage of solid tumor types for targeted drug delivery. The specificity of CA IX targeting, either with the small molecule or antibody approach, is of great importance because there are 14 known carbonic anhydrases exist in humans. Four of them are membrane associated (CA IV, IX, XII, XIV) and widely expressed on normal organs and tissues (including the GI tract, kidney, heart, skeletal muscles and brain)[55-56]. Even when specificity is solved, the widespread expression of CA IX itself still poses great safety concerns,

especially for CAR T cell therapy, as one of the CA IX CAR T therapy trials in renal cell carcinoma showed development of cholestasis due to CA IX expression on the bile duct epithelium[57].

- MUC1

As mentioned above, in some cases, although the same protein is widely expressed in many tissues, different forms and post-translational modifications, such as glycosylation of the protein, can help in differentiating normal surface proteins and tumor associated antigens. Mucin 1 (MUC1) is a good example of this category. MUC1 is ubiquitously expressed on the apical surface of epithelial cells in the lungs, stomach, intestines, eyes and several other organs, as well as many types of malignant cells. Interestingly, MUC1 is a highly glycosylated protein and different patterns of glycosylation among healthy and malignant tissues have been observed. The most prevalent aberrant glycoforms found in cancer are the Tn (GalNAcα1-O-Ser/Thr) and sialyl-Tn (STn) (NeuAcα2-6-GalNAcα1-O-Ser/Thr) glycoforms[58]. Both of these have been found in the N-terminal tandem repeat domain of MUC1 that are overexpressed in malignant cells. Carl June, et al. demonstrated that Tn-MUC1 can be safely used as a tumor antigen and recognized by the therapeutic 5E5 IgG antibody[59]. Next, they utilized the antigen recognition domain of 5E5 to construct a CAR T cell and demonstrated the elimination of Tn-MUC1 tumors in mouse models of leukemia and pancreatic cancer. Other than specific glycosylation patterns, tumor-associated MUC1 also distinguishes itself from mucin expressed in epithelial cells by MMPs mediated cleavage and the shedding of the N-terminal tandem repeat domain. There are several cleavage positions reported for truncated MUC1, resulting in different sizes of C terminal fragments. These fragments include MUC1-C, MUC1* or MUC1-CTF_{15}[58]. To date, no CAR T cell designs specific to these truncated MUC1s have been reported. One potential hurdle for MUC1 as a target is that truncated MUC1 isoforms have also been found in serum in the form of secreted proteins and used

as tumor diagnostic markers[60], therefore these soluble forms of MUC1 may block the scFv binding site of the anti-MUC1 CAR construct.

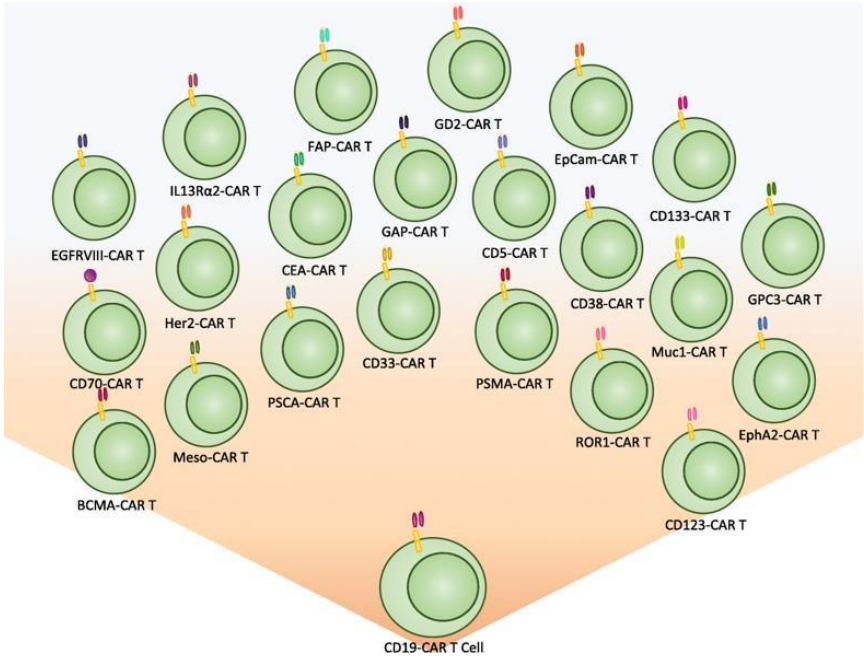

Figure 1-3 Current CAR T cells being tested in clinical trials.
Expansion of biomarkers facilitate the discovery of CAR T cells for both hematopoietic and solid tumors. Reprinted from the Journal of Experimental & Clinical Cancer Research, 2018, 37(1), p.163.

1.3 Side Effects and Limitations of Current CAR T Cell Therapies

The side effects of CAR T therapy in clinic can be briefly divided into two categories: whether it depends on the specific antigen it targets or not. Antigen dependent side effects mainly refer to the on-target off-tumor effect, as mentioned above for CD19, Her2, CA IX etc. Regarding antigen independent side effects, the two major ones are the risk of insertional oncogenesis and the overactivation of the CAR T cell. Both types of side effects are related to the uniqueness of cell therapy compared to traditional therapeutics and will be discussed in detail below.

The risk of insertional oncogenesis has been studied extensively in gene therapies, especially for hematopoietic stem cells for X linked SCID[61]. Viral based gene chromosomal insertion guarantees transgene maintenance during clonal amplification. Insertion also more likely takes place in euchromatin, due to its improved accessibility, and results in increased risk in transcriptionally active regions of chromosomal DNA[62]. In reality, such insertions are unlikely to be directly oncogenic for the following reasons: 1. Retrovirus vector insertion is almost always monoallelic, while most malignant mutations are recessive rather than dominant; 2. Cancer is a multi-gene, multi-level regulated biological event, where a single insertion/mutation usually is not sufficient to develop a malignant phenotype[63]. To date, no cases of malignant transformation have been reported for genetically modified T cells. An alternative strategy to avoid virus related oncogenesis would be the use of mRNA as the gene coding material for the expression of CAR. mRNA has a short half-life, no genome integration, and can potentially reduce the production time of the CAR T cell[64]. At the same time, however, mRNA CAR T cells do have a shorter persistence in vivo, as seen in GD2[65] and EGFR[66] targeted mRNA CAR T cells. Recently, Ruella Macro, et al. reported another form of oncogenesis resulting from CAR T therapy. They observed one patient's relapse of a $CD19^-$ leukemia that aberrantly expressed the anti-CD19 CAR after the

CTL019 treatment[67]. This collapse resulted from the unintentional incorporation of an anti-CD19 CAR gene into a single leukemia B cell during T cell manufacturing, and the CAR bounds to the CD19 epitope on the surface of the same cell, masking it from recognition by the real CAR T cells. All of these rare but life-threatening side-effects call for a safety switch to be incorporated into the design of CAR T cells. The current methods used to solve these rare but life-threatening problems are discussed in chapter 1.4.1.

The second most prevalent side effect of CAR T cell therapy in current clinical applications, especially for hemopoietic cancers, is the overactivation of CAR T cells and the resulting Cytokine Release Syndrome (CRS). CRS has also been reported previously following the infusion of therapeutic monoclonal antibodies[68], IL2, and macrophage-based therapy. The hallmark of CRS in all scenarios is the systemically elevated cytokines production and release. For clinical management, CRS is graded into 3 scales including: 1) mild (constitutional symptoms and/or grade-2 organ toxicity); 2) moderate (some signs of organ dysfunction); and 3) severe (grade >3 organ toxicity, aggressive clinical intervention, and/or potentially life threatening). The clinical phenotype includes: fever, fatigue, nausea, anorexia, tachycardia/hypotension, capillary leaking, renal impairment, cardiac dysfunction, and hepatic failure[69-70]. Another clinical condition that shares a similar clinical phenotype and biomarker signature is cytokine storm. These two terms have been used interchangeably in the literature describing the side effects of CAR T cell therapy but in fact they need to be distinguished from each other[71]. Cytokine storm was first described more than 25 years ago in patients receiving T cell activating antibodies such as OKT3[72], and later anti-CD28 mAb TGN1412[73]. The over-activated inflammation effect can manifest within hours after dosing, with elevated cytokines such as Tumor Necrosis Factor (TNF)-α and INFγ, and symptoms can be resolved by corticosteroids. In contrast, cytokine release syndrome can be

delayed until days or weeks after treatment, depending on the kinetics of the T cell activation with IL-6 as the key mediator. Therefore, symptoms can be resolved not only by corticosteroids, but also the IL6R antibody, tocilizumab.

Another side effect of current CAR T cell therapy in clinics is neurological toxicity in the anti-CD19 CAR T cell treatment for hematopoietic malignancies. Clinical features include confusion, delirium, seizure, and obtundation[74]. The causative pathophysiology of these neurological side effects is still unknown, and whether they are antigen dependent and specific for CD19 (unpublished work by Avery Posey, et al., personal communication) or not is under debate.

1.4 Current Approaches to Improve CAR T Cell Design for Better Control and Efficacy of CAR T Cell Activity

1.4.1 Current Approaches for Better Control of CAR T Cell Activity

As earlier mentioned, some of the side effects of CAR T cell therapy result from the limited specificity of targeted antigens. Although the number of biomarkers for cancer cells are expanding, the number of suitable biomarkers for one certain type of tumor that can be safely differentiated from normal tissue is still limited. On the other hand, tumor heterogenicity is a well-recognized problem for targeted therapy, where one antigen may not be able to cover every tumor cell for even one single patient or one locus. Therefore, the challenge presented here is to design a CAR T cell that has limited on-target off-tumor effect and at the same time cover as much of the malignant tissues as possible using the current repertoire of biomarkers. First, researches have been undertaken the attempt to design CAR T cells that can recognize the density difference of certain antigens between normal and malignant tissues by tuning the affinity of scFv. Therefore, tumors that have a higher antigen density are still being recognized by low affinity CAR, while normal tissues are avoided. This approach has been tested for Her2[75], FRα, FRβ and EGFR targeted CAR

T cells. Secondly, Wendell Lim, et al. utilized the SynNotch system developed by their lab 20 years ago for the design of a logically gated CAR T cell to avoid targeting normal tissues[76]. The first proof-of-concept is an AND gate CAR T that requires combinatorial antigens to present for the activation of CAR T cells[77]. Explained in more detail, a T cell circuit is built in which engagement of the extracellular recognition domain of the synthetic Notch (SynNotch) receptor for the first antigen induces the expression of CAR for the second antigen. These CAR T cells significantly lowered the by-stander effects on single antigen positive normal tissues. However, this strategy may also worsen or hasten the process of antigen loss, which has been seen in the relapse of CD19 negative ALL under anti-CD19 CAR T cell treatment. One potential way to overcome this effect is through the use of NOT gates. In contrast to the AND gate, the NOT gate becomes active through single antigen binding but will be inactivated if the second inhibitory receptor docks with its own target, ideally a protein that specifically marks normal tissues. This has been tested as a proof-of-concept by using a scFv towards PSMA linked with the intracellular domain of PD-1, which contains a co-inhibitory signaling domain. When co-expressed with an anti-CD19 CAR on the same T cell, this CAR T cell was able to lyse $CD19^+$ $PSMA^-$ efficiently, but not $CD19^+PSMA^+$ tumors[78].

To control the antigen-independent side effects, that are tumorigenesis and overactivation, of CAR T cells, many groups have developed safety switch systems that can be incorporated into the CAR construct. The most prevalent approach is to integrate a “suicide gene” for the depletion of CAR T when oncogenesis or CRS occurs. The first suicide gene evaluated in humans was the herpes simplex virus thymidine kinase (HSV-TK)[79], which sensitizes modified cells to ganciclovir, an acyclic nucleoside analog. HSV-TK catalyzes phosphorylation of ganciclovir and this product competes with guanosine for DNA synthesis[80]. However, since HSV-TK originates from the

herpes virus, immunogenicity is a big concern and may result in immuno-rejection of the engineered cells. Moreover, the prodrug, ganciclovir, is a widely used antiviral agent and continuous dosing results in toxicity to by-stander cells[81]. Recently, a more human-compatible suicide gene, called inducible caspase 9 (iCasp9), has been described[82]. Its platform is composed from a dimerizable receptor that contains a FK506 binding protein (FKBP12 or the F36V mutant) linked with caspase 9 as a whole protein and a corresponding small molecule dimerizing agent AP1903 (a FK506 dimer). Crystallographic data indicates that dimerization of inactive caspase 9, an important player in the lower caspase dependent apoptosis pathway, leads to conformational change-induced activation. Controllable dimerization of caspase 9 and activation of the caspase pathway is achieved by fusing it with one FKBP, while two FKBPs in a row give more spontaneous dimerization and ligand independent apoptosis. The first test in humans shows that a single dose of AP1903 depletes 90% of the iCasp9 modified donor T cells within 30 minutes of administration in a Hematopoietic stem cell transplantation (HSCT) patient model[83]. For CAR T cell and NK CAR cell therapy, iCasp9 has been widely tested for different antigens both preclinically and in clinical trials. One concern regarding iCasp9, however, is the re-proliferation of the residual irresponsible population, around 1-10% of modified T cells. This problem could be overcome by tag based positive selection during the manufacturing process of CAR T cells for a relatively high expression level of iCasp9.

Another way to selectively eliminate CAR T cells in vivo is to incorporate a tag on the surface of CAR T cell that can be targeted by therapeutic drugs. Theoretically, the extracellular domain of any tumor surface antigens that have a well-developed targeting antibody/ligand can be used for this purpose. Two examples have been tested in detail, CD20 with Rituximab[84] and truncated EGFR with Cetuximab[85]. Both antibodies have been approved by the FDA and therefore provide

physicians more information and experience regarding their safety and dosing. Treatment of Cetuximab sufficiently deplete truncated EGFR+ anti-CD19 CAR T cells through antibody Fc domain mediated cytotoxic effects. Concerns relative to the on-target off-tumor effect of this approach do exist, since CD20 is expressed in all except the first and last stages of B cell development, while truncated EGFR is more specific to cancer cells.

Other than suicide gene switches and elimination tags, which may only control the CAR T cell in a live/dead two-way manner, many groups have worked on a more tunable switch that can increase/decrease CAR T activity in a dose dependent manner. First, Wendell Lim, et al. attempted to separate the intracellular activation domains of CAR into two proteins that contain dimerization domains and to control their association through a chemically induced dimerization (CID) system, similar to iCas9 system: one receptor contains the antigen recognition domain and FKBP, the other contains the rest part of CAR including 4-1BB and CD3ζ, as well as FRB[86]. In the presence of the targeted antigen as well as the dimerization agent AP21967 (a rapamycin analog), these two receptors will then come together and activate the CAR T cells. A similar design put the FKBP and FRB domains at the extracellular hinge region of the two separate CARs, destabilizing their cell-surface expressions due to increased distance of the scFv from the cell membrane. The addition of rapamycin or its analogs then brings together and stabilizes the two separate CAR receptors, and turns on the activity of CAR T cells. In summary, these "ON-switch" designs have established a platform where the activity of CAR T cells can be controlled by a safe and biologically inert small molecule in a dose dependent manner. One of the major concerns regarding these strategies is their leakage signal: the basal level of activation in the absence of the dimerization agents. To overcome this problem, another "ON-switch" is designed by using a small molecule Shield-1 (FK506 derivative) to stabilize the CAR construct which has been fused to a

destabilizing domain (DD, L106P FKBP or other double or triple FKBP mutants)[87]. In the absence of the Shield-1, the fusion protein containing the CAR and DD will go to proteasome for degradation, while the addition of Shield-1 at approximately 3 μM promotes the stable expression of the CAR-DD fusion protein to the T cell surface. Two major concerns regarding this approach are the relatively high concentration required for the stabilizing agents as well as whether the mutant destabilizing domain will be immunogenic or not in humans.

1.4.2 Current Approaches for Improving Efficacy of CAR T Cell Therapies in Solid Tumors

Due to the tremendous success of CAR T therapy in hemopoietic malignancies, especially in B cell malignancies, as well as the achievement of CAR T in solid tumors in preclinical studies, more than 100 CAR T cell clinical trials targeting solid tumors are currently in progress all around the world. However, multiple unique hurdles face the application of CAR T cells to solid tumors compared to B cell malignancies, including physical barriers, suppressive tumor microenvironment, and continuous antigen exposure. Therefore, many groups have been working to empower CAR T cells with new functional moieties to overcome these hurdles. First, to enhance the trafficking of CAR T cells in a solid tumor, a recombinant chemokine receptor ligand (CCR2) was introduced into CAR -T cells in addition to the classical antigen targeting part[88]. CCL2, the ligand for CCR2, is highly secreted by the tumor microenvironment in several types of cancers, including ovarian, prostate, sarcoma and breast cancer. The production of CCL2 is closely associated with increased TAM and higher immune suppression in the tumor. Transgenic expression of CXCR2 and CCR4 have all been known to enhance the migration of T cells to tumor sites and therefore may be incorporated into CAR T cells for better trafficking. Second, even if CAR-T cells are successfully trafficked to the tumor sites, the interaction between the immunosuppressive immune cells, such as TAM, and the CAR T cells would re-educate T cells

into an anergic or exhausted phenotype or T regulatory (Treg) cells. To break these interactions, several cell engineering approaches to silence or block the co-inhibitor receptors, such as PD-1, CTLA-4, have been tested. These include co-expression of the anti-PD-1 neutralizing antibody with the classical CAR construct, a CRISPR knockout of PD-1, or swapping the intracellular domain of PD-1 with the co-activation molecule CD28[89]. In addition to this, an inducible expression of pro-inflammation cytokines using the above-mentioned SynNotch has also been tested[91]. Finally, it's well known that the tonic signaling of the CAR from continuous exposure to antigens in solid tumors significantly exhaust CAR T cells' potential. Therefore, controlled resting period of CAR signaling is reasoned to preserve CAR T cells for a better overall efficacy in the long run. Indeed, using the destabilizing domain mediated "ON switch" system, Crystal Mackall, et al. achieved a more potent CAR T cell phenotype after multiple antigen stimulation by giving a periodical break to the CAR T cells through controlled addition of the stabilization molecule (Shield-1).

One unique and universal approach to control the activity of the CAR T cells and solve the many problems mentioned above is the bispecific adaptor-based CAR T therapy that has been developed in the Low lab[90]. This CAR T cell contains a scFv for fluorescein (FITC) and the intracellular T cell activation domains of 4-1BB and CD3ζ. The formation of the immune synapse is mediated by the engagement of the FITC-targeting ligand with both the anti-FITC CAR and the antigen positive tumor cells as a ternary complex, similar to the way bi-specific antibodies work. Therefore, the activation of CAR T cells against tumor associated antigens is specifically controlled by the bispecific adaptor in a dose dependent manner, limiting the onset of CRS and the overactivation of CAR T cells in hematopoietic cancer treatments. Although similar designs using FITC-antibody adapters have been previously described[91-92], the small molecule-based approach

may have several advantages in comparison. First, the molecular weight of small molecule adaptors is approximately 1000, more than 10 times smaller than the antibody (MW around 150,000); it therefore presents better tissue penetration in solid tumors. This improved tissue penetration has been confirmed visually by comparing folic acid-based imaging agents with their anti-FR antibody counterparts. Secondly, small molecule adaptors are cleared of receptor negative tissue with a half-life of about 90 minutes while therapeutic antibodies usually have half-lives of approximately 3 days. Thus, a quicker response rate is guaranteed by small molecule adaptors for the timely control of CAR T activity. Thirdly, several studies have shown that the length hinge domain between the scFv and the transmembrane domain in CAR is critical for T cell activity. While it is difficult to predict and modify the structure of antibodies and antibody conjugates, the length of small molecule adaptors can be easily altered by modifying the linker between FITC and the targeting ligands. Another hurdle mentioned above for CAR T therapy is heterogeneity, which is found in almost all solid tumors. This can also be overcome by the bi-specific adaptor strategy which works by simply switching different targeting ligands at one end of the adaptor, while keeping the FITC end and the CAR T cells unchanged. One may argue that given the increasing number of biomarkers available for targeting therapy, FITC-antibody adaptors are easier to generate using phage display or similar techniques, while the development of small molecule targeting ligands is more cumbersome. However, this difficulty can be mitigated by carefully choosing antigens and targeting ligands as a combination panel to cover a wider spectrum of all cancers. CA IX, as earlier mentioned, is upregulated in almost all solid tumors due to hypoxia conditions. PSMA is not only overexpressed on approximately 90% of prostate cancer cells, but also on the neovascular of other solid tumors. The FRα overexpression represents 40% of all human tumors and FRβ is upregulated in tumor associated macrophages (TAM) and myeloid-

derived suppressor cells (MDSC), both of which facilitate cancer cell growth and negatively correlate with patient survival rates. To date, the combination of these three antigens targeted bi-specific adaptors for anti-FITC CAR T cells has been tested, and results show that this panel can cover a great percentage of all solid tumors.

Table 1 Summary of current approaches using an ON/OFF control switch for CAR T cell therapy

Approaches	ON/OFF switch	Rejuvenation	References
EGFRt	Cetuximab mediated depletion	No	87
Inducible caspase9	Chemical induced dimerization of caspase 9	No	84
Destabilizing domain	Chemical induced stabilization and activation	Rest period of CAR T	89
Separated activation domain	Chemical induced dimerization and activation	Rest period of CAR T	88
Bispecific adaptor CAR	Adaptor mediated formation of immune synapse	Rest period of CAR T	92,93,94

In summary, CAR T cell therapies have been constantly evolving over the last few decades. As the most sophisticated and complicated therapeutic method approved by the FDA so far, every moiety in design and every step during production and manufacturing can be and should be optimized. The recent development of off-the-shelf CAR T will definitely hasten the turnover time and lower the cost of this cell-based therapy, and therefore open doors to patients that may not been qualified earlier, such as patients with acute infectious and autoimmune disease, with the help of the discovery of targetable receptors on the surface of disease cells.

1.5 References

1. Funakoshi, S.; Miki, K.; Takaki, T.; Okubo, C.; Hatani, T.; Chonabayashi, K.; Nishikawa, M.; Takei, I.; Oishi, A.; Narita, M.; Hoshijima, M.; Kimura, T.; Yamanaka, S.; Yoshida, Y., Enhanced engraftment, proliferation, and therapeutic potential in heart using optimized human iPSC-derived cardiomyocytes. *Scientific reports* **2016,** *6*, 19111.

2. Ramiya, V. K.; Maraist, M.; Arfors, K. E.; Schatz, D. A.; Peck, A. B.; Cornelius, J. G., Reversal of insulin-dependent diabetes using islets generated in vitro from pancreatic stem cells. *Nature medicine* **2000,** *6* (3), 278-82.

3. Souied, E.; Pulido, J.; Staurenghi, G., Autologous Induced Stem-Cell-Derived Retinal Cells for Macular Degeneration. *The New England journal of medicine* **2017,** *377* (8), 792.

4. Slingluff, C. L., Jr.; Petroni, G. R.; Yamshchikov, G. V.; Hibbitts, S.; Grosh, W. W.; Chianese-Bullock, K. A.; Bissonette, E. A.; Barnd, D. L.; Deacon, D. H.; Patterson, J. W.; Parekh, J.; Neese, P. Y.; Woodson, E. M.; Wiernasz, C. J.; Merrill, P., Immunologic and clinical outcomes of vaccination with a multiepitope melanoma peptide vaccine plus low-dose interleukin-2 administered either concurrently or on a delayed schedule. *Journal of clinical oncology : official journal of the American Society of Clinical Oncology* **2004,** *22* (22), 4474-85.

5. Terheyden, P.; Schrama, D.; Pedersen, L. O.; Andersen, M. H.; Kampgen, E.; thor Straten, P.; Becker, J. C., Longitudinal analysis of MART-1/HLA-A2-reactive T cells over the course of melanoma progression. *Scand J Immunol* **2003,** *58* (5), 566-71.

6. Rožková, D.; Tišerová, H.; Fučíková, J.; Lašťovička, J.; Podrazil, M.; Ulčová, H.; Budínský, V.; Prausová, J.; Linke, Z.; Minárik, I., FOCUS on FOCIS: combined chemo-immunotherapy for the treatment of hormone-refractory metastatic prostate cancer. *Clinical immunology* **2009,** *131* (1), 1-10.

7. Koh, Y. T.; Gray, A.; Higgins, S. A.; Hubby, B.; Kast, W. M., Androgen ablation augments prostate cancer vaccine immunogenicity only when applied after immunization. *The Prostate* **2009,** *69* (6), 571-84.

8. Anassi, E.; Ndefo, U. A., Sipuleucel-T (provenge) injection: the first immunotherapy agent (vaccine) for hormone-refractory prostate cancer. *P T* **2011,** *36* (4), 197-202.

9. Beyersdorf, N.; Kerkau, T.; Hunig, T., CD28 co-stimulation in T-cell homeostasis: a recent perspective. *Immunotargets Ther* **2015,** *4*, 111-22.

10. Gross, G.; Waks, T.; Eshhar, Z., Expression of immunoglobulin-T-cell receptor chimeric molecules as functional receptors with antibody-type specificity. *Proceedings of the National Academy of Sciences of the United States of America* **1989,** *86* (24), 10024-8.

11. Snow, A. L.; Pandiyan, P.; Zheng, L.; Krummey, S. M.; Lenardo, M. J., The power and the promise of restimulation-induced cell death in human immune diseases. *Immunological reviews* **2010,** *236*, 68-82.

12. Krause, A.; Guo, H. F.; Latouche, J. B.; Tan, C.; Cheung, N. K.; Sadelain, M., Antigen-dependent CD28 signaling selectively enhances survival and proliferation in genetically modified activated human primary T lymphocytes. *The Journal of experimental medicine* **1998,** *188* (4), 619-26.

13. Ponsel, D.; Neugebauer, J.; Ladetzki-Baehs, K.; Tissot, K., High affinity, developability and functional size: the holy grail of combinatorial antibody library generation. *Molecules* **2011,** *16* (5), 3675-700.

14. Townsend, M. H.; Shrestha, G.; Robison, R. A.; O'Neill, K. L., The expansion of targetable biomarkers for CAR T cell therapy. *J Exp Clin Cancer Res* **2018,** *37* (1), 163.

15. Doan, A.; Pulsipher, M. A., Hypogammaglobulinemia due to CAR T-cell therapy. *Pediatric blood & cancer* **2018,** *65* (4).

16. Chen, F.; Fan, C.; Gu, X.; Zhang, H.; Liu, Q.; Gao, X.; Lu, J.; He, B.; Lai, X., Construction of Anti-CD20 Single-Chain Antibody-CD28-CD137-TCRzeta Recombinant Genetic Modified T Cells and its Treatment Effect on B Cell Lymphoma. *Medical science monitor : international medical journal of experimental and clinical research* **2015,** *21*, 2110-5.

17. Fry, T. J.; Shah, N. N.; Orentas, R. J.; Stetler-Stevenson, M.; Yuan, C. M.; Ramakrishna, S.; Wolters, P.; Martin, S.; Delbrook, C.; Yates, B.; Shalabi, H.; Fountaine, T. J.; Shern, J. F.; Majzner, R. G.; Stroncek, D. F.; Sabatino, M.; Feng, Y.; Dimitrov, D. S.; Zhang, L.; Nguyen, S.; Qin, H.; Dropulic, B.; Lee, D. W.; Mackall, C. L., CD22-targeted CAR T cells induce remission in B-ALL that is naive or resistant to CD19-targeted CAR immunotherapy. *Nature medicine* **2018,** *24* (1), 20-28.

18. Ruella, M.; Barrett, D. M.; Kenderian, S. S.; Shestova, O.; Hofmann, T. J.; Perazzelli, J.; Klichinsky, M.; Aikawa, V.; Nazimuddin, F.; Kozlowski, M.; Scholler, J.; Lacey, S. F.; Melenhorst, J. J.; Morrissette, J. J.; Christian, D. A.; Hunter, C. A.; Kalos, M.; Porter, D. L.; June, C. H.; Grupp, S. A.; Gill, S., Dual CD19 and CD123 targeting prevents antigen-loss relapses after CD19-directed immunotherapies. *The Journal of clinical investigation* **2016,** *126* (10), 3814-3826.

19. Zhao, Z.; Chen, Y.; Francisco, N. M.; Zhang, Y.; Wu, M., The application of CAR-T cell therapy in hematological malignancies: advantages and challenges. *Acta Pharm Sin B* **2018,** *8* (4), 539-551.

20. Lambert, J. M.; Morris, C. Q., Antibody-Drug Conjugates (ADCs) for Personalized Treatment of Solid Tumors: A Review. *Adv Ther* **2017,** *34* (5), 1015-1035.

21. Garber, K., Driving T-cell immunotherapy to solid tumors. *Nature biotechnology* **2018,** *36* (3), 215-219.

22. Barok, M.; Joensuu, H.; Isola, J., Trastuzumab emtansine: mechanisms of action and drug resistance. *Breast cancer research : BCR* **2014,** *16* (2), 209.

23. Stone, J. D.; Aggen, D. H.; Schietinger, A.; Schreiber, H.; Kranz, D. M., A sensitivity scale for targeting T cells with chimeric antigen receptors (CARs) and bispecific T-cell Engagers (BiTEs). *Oncoimmunology* **2012,** *1* (6), 863-873.

24. Chalouni, C.; Doll, S., Fate of Antibody-Drug Conjugates in Cancer Cells. *J Exp Clin Cancer Res* **2018,** *37* (1), 20.

25. Liu, X.; Zhang, N.; Shi, H., Driving better and safer HER2-specific CARs for cancer therapy. *Oncotarget* **2017,** *8* (37), 62730-62741.

26. Lamers, C. H.; Sleijfer, S.; van Steenbergen, S.; van Elzakker, P.; van Krimpen, B.; Groot, C.; Vulto, A.; den Bakker, M.; Oosterwijk, E.; Debets, R.; Gratama, J. W., Treatment of metastatic renal cell carcinoma with CAIX CAR-engineered T cells: clinical evaluation and management of on-target toxicity. *Molecular therapy : the journal of the American Society of Gene Therapy* **2013,** *21* (4), 904-12.

27. Moon, E. K.; Carpenito, C.; Sun, J.; Wang, L. C.; Kapoor, V.; Predina, J.; Powell, D. J., Jr.; Riley, J. L.; June, C. H.; Albelda, S. M., Expression of a functional CCR2 receptor enhances tumor localization and tumor eradication by retargeted human T cells expressing a mesothelin-specific chimeric antibody receptor. *Clinical cancer research : an official journal of the American Association for Cancer Research* **2011,** *17* (14), 4719-30.

28. Petrausch, U.; Schuberth, P. C.; Hagedorn, C.; Soltermann, A.; Tomaszek, S.; Stahel, R.; Weder, W.; Renner, C., Re-directed T cells for the treatment of fibroblast activation protein (FAP)-positive malignant pleural mesothelioma (FAPME-1). *BMC cancer* **2012,** *12*, 615.

29. Narayan, V.; Gladney, W.; Plesa, G.; Vapiwala, N.; Carpenter, E.; Maude, S. L.; Lal, P.; Lacey, S. F.; Melenhorst, J. J.; Sebro, R., A phase I clinical trial of PSMA-directed/TGFβ-insensitive CAR-T cells in metastatic castration-resistant prostate cancer. American Society of Clinical Oncology: 2019.

30. Shen, C. J.; Yang, Y. X.; Han, E. Q.; Cao, N.; Wang, Y. F.; Wang, Y.; Zhao, Y. Y.; Zhao, L. M.; Cui, J.; Gupta, P.; Wong, A. J.; Han, S. Y., Chimeric antigen receptor containing ICOS signaling domain mediates specific and efficient antitumor effect of T cells against EGFRvIII expressing glioma. *Journal of hematology & oncology* **2013,** *6*, 33.

31. Ledermann, J. A.; Canevari, S.; Thigpen, T., Targeting the folate receptor: diagnostic and therapeutic approaches to personalize cancer treatments. *Annals of oncology : official journal of the European Society for Medical Oncology* **2015,** *26* (10), 2034-43.

32. Cheung, A.; Bax, H. J.; Josephs, D. H.; Ilieva, K. M.; Pellizzari, G.; Opzoomer, J.; Bloomfield, J.; Fittall, M.; Grigoriadis, A.; Figini, M.; Canevari, S.; Spicer, J. F.; Tutt, A. N.; Karagiannis, S. N., Targeting folate receptor alpha for cancer treatment. *Oncotarget* **2016,** *7* (32), 52553-52574.

33. Vergote, I.; Armstrong, D.; Scambia, G.; Teneriello, M.; Sehouli, J.; Schweizer, C.; Weil, S. C.; Bamias, A.; Fujiwara, K.; Ochiai, K.; Poole, C.; Gorbunova, V.; Wang, W.; O'Shannessy, D.; Herzog, T. J., A Randomized, Double-Blind, Placebo-Controlled, Phase III Study to Assess Efficacy and Safety of Weekly Farletuzumab in Combination With Carboplatin and Taxane in Patients With Ovarian Cancer in First Platinum-Sensitive Relapse. *Journal of clinical oncology : official journal of the American Society of Clinical Oncology* **2016,** *34* (19), 2271-8.

34. van Zanten-Przybysz, I.; Molthoff, C.; Gebbinck, J. K.; von Mensdorff-Pouilly, S.; Verstraeten, R.; Kenemans, P.; Verheijen, R., Cellular and humoral responses after multiple injections of unconjugated chimeric monoclonal antibody MOv18 in ovarian cancer patients: a pilot study. *Journal of cancer research and clinical oncology* **2002,** *128* (9), 484-92.

35. Moore, K. N.; Martin, L. P.; O'Malley, D. M.; Matulonis, U. A.; Konner, J. A.; Perez, R. P.; Bauer, T. M.; Ruiz-Soto, R.; Birrer, M. J., Safety and Activity of Mirvetuximab Soravtansine (IMGN853), a Folate Receptor Alpha-Targeting Antibody-Drug Conjugate, in Platinum-Resistant Ovarian, Fallopian Tube, or Primary Peritoneal Cancer: A Phase I Expansion Study. *Journal of clinical oncology : official journal of the American Society of Clinical Oncology* **2017,** *35* (10), 1112-1118.

36. Scaglione, F.; Panzavolta, G., Folate, folic acid and 5-methyltetrahydrofolate are not the same thing. *Xenobiotica; the fate of foreign compounds in biological systems* **2014,** *44* (5), 480-8.

37. Reddy, J. A.; Dorton, R.; Bloomfield, A.; Nelson, M.; Dircksen, C.; Vetzel, M.; Kleindl, P.; Santhapuram, H.; Vlahov, I. R.; Leamon, C. P., Pre-clinical evaluation of EC1456, a folate-tubulysin anti-cancer therapeutic. *Scientific reports* **2018,** *8* (1), 8943.

38. Vlahov, I. R.; Leamon, C. P., Engineering folate-drug conjugates to target cancer: from chemistry to clinic. *Bioconjugate chemistry* **2012,** *23* (7), 1357-69.

39. Kennedy, G. T.; Okusanya, O. T.; Keating, J. J.; Heitjan, D. F.; Deshpande, C.; Litzky, L. A.; Albelda, S. M.; Drebin, J. A.; Nie, S.; Low, P. S.; Singhal, S., The Optical Biopsy: A Novel Technique for Rapid Intraoperative Diagnosis of Primary Pulmonary Adenocarcinomas. *Ann Surg* **2015,** *262* (4), 602-9.

40. Rao, S. I.; Pugh, M.; Nelson, M.; Reddy, J. A.; Klein, P. J.; Leamon, C. P., Development and validation of a UPLC-MS/MS method for the novel folate-targeted small molecule drug conjugate EC1456 and its metabolites in tumor homogenates from mice. *Journal of pharmaceutical and biomedical analysis* **2016,** *122*, 148-56.

41. Kershaw, M. H.; Westwood, J. A.; Parker, L. L.; Wang, G.; Eshhar, Z.; Mavroukakis, S. A.; White, D. E.; Wunderlich, J. R.; Canevari, S.; Rogers-Freezer, L.; Chen, C. C.; Yang, J. C.; Rosenberg, S. A.; Hwu, P., A phase I study on adoptive immunotherapy using gene-modified T cells for ovarian cancer. *Clinical cancer research : an official journal of the American Association for Cancer Research* **2006,** *12* (20 Pt 1), 6106-15.

42. Kim, M.; Pyo, S.; Kang, C. H.; Lee, C. O.; Lee, H. K.; Choi, S. U.; Park, C. H., Folate receptor 1 (FOLR1) targeted chimeric antigen receptor (CAR) T cells for the treatment of gastric cancer. *PloS one* **2018,** *13* (6), e0198347.

43. Wang, H.; Zheng, X.; Behm, F. G.; Ratnam, M., Differentiation-independent retinoid induction of folate receptor type beta, a potential tumor target in myeloid leukemia. *Blood* **2000,** *96* (10), 3529-36.

44. Lynn, R. C.; Poussin, M.; Kalota, A.; Feng, Y.; Low, P. S.; Dimitrov, D. S.; Powell, D. J., Jr., Targeting of folate receptor beta on acute myeloid leukemia blasts with chimeric antigen receptor-expressing T cells. *Blood* **2015,** *125* (22), 3466-76.

45. Shen, J.; Putt, K. S.; Visscher, D. W.; Murphy, L.; Cohen, C.; Singhal, S.; Sandusky, G.; Feng, Y.; Dimitrov, D. S.; Low, P. S., Assessment of folate receptor-beta expression in human neoplastic tissues. *Oncotarget* **2015,** *6* (16), 14700-9.

46. Chu, W.; Zhou, Y.; Tang, Q.; Wang, M.; Ji, Y.; Yan, J.; Yin, D.; Zhang, S.; Lu, H.; Shen, J., Bi-specific ligand-controlled chimeric antigen receptor T-cell therapy for non-small cell lung cancer. *Biosci Trends* **2018,** *12* (3), 298-308.

47. Troyer, J. K.; Beckett, M. L.; Wright, G. L., Jr., Detection and characterization of the prostate-specific membrane antigen (PSMA) in tissue extracts and body fluids. *International journal of cancer* **1995,** *62* (5), 552-8.

48. Carter, R. E.; Feldman, A. R.; Coyle, J. T., Prostate-specific membrane antigen is a hydrolase with substrate and pharmacologic characteristics of a neuropeptidase. *Proceedings of the National Academy of Sciences of the United States of America* **1996,** *93* (2), 749-53.

49. Leamon, C. P.; Reddy, J. A.; Bloomfield, A.; Dorton, R.; Nelson, M.; Vetzel, M.; Kleindl, P.; Hahn, S.; Wang, K.; Vlahov, I. R., Prostate-Specific Membrane Antigen-Specific Antitumor Activity of a Self-Immolative Tubulysin Conjugate. *Bioconjugate chemistry* **2019,** *30* (6), 1805-1813.

50. Kularatne, S. A.; Zhou, Z.; Yang, J.; Post, C. B.; Low, P. S., Design, synthesis, and preclinical evaluation of prostate-specific membrane antigen targeted (99m)Tc-radioimaging agents. *Molecular pharmaceutics* **2009,** *6* (3), 790-800.

51. DiPippo, V. A.; Olson, W. C.; Nguyen, H. M.; Brown, L. G.; Vessella, R. L.; Corey, E., Efficacy studies of an antibody-drug conjugate PSMA-ADC in patient-derived prostate cancer xenografts. *The Prostate* **2015,** *75* (3), 303-13.

52. Petrylak, D. P.; Kantoff, P.; Vogelzang, N. J.; Mega, A.; Fleming, M. T.; Stephenson, J. J., Jr.; Frank, R.; Shore, N. D.; Dreicer, R.; McClay, E. F.; Berry, W. R.; Agarwal, M.; DiPippo, V. A.; Rotshteyn, Y.; Stambler, N.; Olson, W. C.; Morris, S. A.; Israel, R. J., Phase 1 study of PSMA ADC, an antibody-drug conjugate targeting prostate-specific membrane antigen, in chemotherapy-refractory prostate cancer. *The Prostate* **2019,** *79* (6), 604-613.

53. Zuccolotto, G.; Fracasso, G.; Merlo, A.; Montagner, I. M.; Rondina, M.; Bobisse, S.; Figini, M.; Cingarlini, S.; Colombatti, M.; Zanovello, P.; Rosato, A., PSMA-specific CAR-engineered T cells eradicate disseminated prostate cancer in preclinical models. *PloS one* **2014,** *9* (10), e109427.

54. Chiche, J.; Ilc, K.; Laferriere, J.; Trottier, E.; Dayan, F.; Mazure, N. M.; Brahimi-Horn, M. C.; Pouyssegur, J., Hypoxia-inducible carbonic anhydrase IX and XII promote tumor cell growth by counteracting acidosis through the regulation of the intracellular pH. *Cancer research* **2009,** *69* (1), 358-68.

55. McKenna, R.; Frost, S. C., Overview of the carbonic anhydrase family. *Subcell Biochem* **2014,** *75*, 3-5.

56. Wistrand, P. J.; Knuuttila, K. G., Renal membrane-bound carbonic anhydrase. Purification and properties. *Kidney Int* **1989,** *35* (3), 851-9.

57. Lamers, C. H.; Sleijfer, S.; Vulto, A. G.; Kruit, W. H.; Kliffen, M.; Debets, R.; Gratama, J. W.; Stoter, G.; Oosterwijk, E., Treatment of metastatic renal cell carcinoma with autologous T-lymphocytes genetically retargeted against carbonic anhydrase IX: first clinical experience. *Journal of clinical oncology : official journal of the American Society of Clinical Oncology* **2006,** *24* (13), e20-2.

58. Haugstad, K. E.; Hadjialirezaei, S.; Stokke, B. T.; Brewer, C. F.; Gerken, T. A.; Burchell, J.; Picco, G.; Sletmoen, M., Interactions of mucins with the Tn or Sialyl Tn cancer antigens including MUC1 are due to GalNAc-GalNAc interactions. *Glycobiology* **2016,** *26* (12), 1338-1350.

59. Posey, A. D., Jr.; Schwab, R. D.; Boesteanu, A. C.; Steentoft, C.; Mandel, U.; Engels, B.; Stone, J. D.; Madsen, T. D.; Schreiber, K.; Haines, K. M.; Cogdill, A. P.; Chen, T. J.; Song, D.; Scholler, J.; Kranz, D. M.; Feldman, M. D.; Young, R.; Keith, B.; Schreiber, H.; Clausen, H.; Johnson, L. A.; June, C. H., Engineered CAR T Cells Targeting the Cancer-Associated Tn-Glycoform of the Membrane Mucin MUC1 Control Adenocarcinoma. *Immunity* **2016,** *44* (6), 1444-54.

60. Treon, S. P.; Maimonis, P.; Bua, D.; Young, G.; Raje, N.; Mollick, J.; Chauhan, D.; Tai, Y. T.; Hideshima, T.; Shima, Y.; Hilgers, J.; von Mensdorff-Pouilly, S.; Belch, A. R.; Pilarski, L. M.; Anderson, K. C., Elevated soluble MUC1 levels and decreased anti-MUC1 antibody levels in patients with multiple myeloma. *Blood* **2000,** *96* (9), 3147-53.

61. Wu, C.; Dunbar, C. E., Stem cell gene therapy: the risks of insertional mutagenesis and approaches to minimize genotoxicity. *Front Med* **2011,** *5* (4), 356-71.

62. Nisha, P.; Plank, J. L.; Csink, A. K., Analysis of chromatin structure of genes silenced by heterochromatin in trans. *Genetics* **2008,** *179* (1), 359-73.

63. Baum, C.; Dullmann, J.; Li, Z.; Fehse, B.; Meyer, J.; Williams, D. A.; von Kalle, C., Side effects of retroviral gene transfer into hematopoietic stem cells. *Blood* **2003,** *101* (6), 2099-114.

64. Foster, J. B.; Barrett, D. M.; Kariko, K., The Emerging Role of In Vitro-Transcribed mRNA in Adoptive T Cell Immunotherapy. *Molecular therapy : the journal of the American Society of Gene Therapy* **2019,** *27* (4), 747-756.

65. Singh, N.; Liu, X.; Hulitt, J.; Jiang, S.; June, C. H.; Grupp, S. A.; Barrett, D. M.; Zhao, Y., Nature of tumor control by permanently and transiently modified GD2 chimeric antigen receptor T cells in xenograft models of neuroblastoma. *Cancer immunology research* **2014,** *2* (11), 1059-70.

66. Caruso, H. G.; Torikai, H.; Zhang, L.; Maiti, S.; Dai, J.; Do, K. A.; Singh, H.; Huls, H.; Lee, D. A.; Champlin, R. E.; Heimberger, A. B.; Cooper, L. J., Redirecting T-Cell Specificity to EGFR Using mRNA to Self-limit Expression of Chimeric Antigen Receptor. *Journal of immunotherapy* **2016,** *39* (5), 205-17.

67. Ruella, M.; Xu, J.; Barrett, D. M.; Fraietta, J. A.; Reich, T. J.; Ambrose, D. E.; Klichinsky, M.; Shestova, O.; Patel, P. R.; Kulikovskaya, I.; Nazimuddin, F.; Bhoj, V. G.; Orlando, E. J.; Fry, T. J.; Bitter, H.; Maude, S. L.; Levine, B. L.; Nobles, C. L.; Bushman, F. D.; Young, R. M.; Scholler, J.; Gill, S. I.; June, C. H.; Grupp, S. A.; Lacey, S. F.; Melenhorst, J. J., Induction of resistance to chimeric antigen receptor T cell therapy by transduction of a single leukemic B cell. *Nature medicine* **2018,** *24* (10), 1499-1503.

68. Teachey, D. T.; Rheingold, S. R.; Maude, S. L.; Zugmaier, G.; Barrett, D. M.; Seif, A. E.; Nichols, K. E.; Suppa, E. K.; Kalos, M.; Berg, R. A.; Fitzgerald, J. C.; Aplenc, R.; Gore, L.; Grupp, S. A., Cytokine release syndrome after blinatumomab treatment related to abnormal macrophage activation and ameliorated with cytokine-directed therapy. *Blood* **2013,** *121* (26), 5154-7.

69. Lee, D. W.; Gardner, R.; Porter, D. L.; Louis, C. U.; Ahmed, N.; Jensen, M.; Grupp, S. A.; Mackall, C. L., Current concepts in the diagnosis and management of cytokine release syndrome. *Blood* **2014,** *124* (2), 188-95.

70. Frey, N. V.; Porter, D. L., Cytokine release syndrome with novel therapeutics for acute lymphoblastic leukemia. *Hematology Am Soc Hematol Educ Program* **2016,** *2016* (1), 567-572.

71. Porter, D.; Frey, N.; Wood, P. A.; Weng, Y.; Grupp, S. A., Grading of cytokine release syndrome associated with the CAR T cell therapy tisagenlecleucel. *Journal of hematology & oncology* **2018,** *11* (1), 35.

72. Chatenoud, L.; Ferran, C.; Legendre, C.; Thouard, I.; Merite, S.; Reuter, A.; Gevaert, Y.; Kreis, H.; Franchimont, P.; Bach, J. F., In vivo cell activation following OKT3 administration. Systemic cytokine release and modulation by corticosteroids. *Transplantation* **1990,** *49* (4), 697-702.

73. Suntharalingam, G.; Perry, M. R.; Ward, S.; Brett, S. J.; Castello-Cortes, A.; Brunner, M. D.; Panoskaltsis, N., Cytokine storm in a phase 1 trial of the anti-CD28 monoclonal antibody TGN1412. *The New England journal of medicine* **2006,** *355* (10), 1018-28.

74. Tasian, S. K.; Gardner, R. A., CD19-redirected chimeric antigen receptor-modified T cells: a promising immunotherapy for children and adults with B-cell acute lymphoblastic leukemia (ALL). *Therapeutic advances in hematology* **2015,** *6* (5), 228-41.

75. Liu, X.; Jiang, S.; Fang, C.; Yang, S.; Olalere, D.; Pequignot, E. C.; Cogdill, A. P.; Li, N.; Ramones, M.; Granda, B.; Zhou, L.; Loew, A.; Young, R. M.; June, C. H.; Zhao, Y., Affinity-Tuned ErbB2 or EGFR Chimeric Antigen Receptor T Cells Exhibit an Increased Therapeutic Index against Tumors in Mice. *Cancer research* **2015,** *75* (17), 3596-607.

76. Morsut, L.; Roybal, K. T.; Xiong, X.; Gordley, R. M.; Coyle, S. M.; Thomson, M.; Lim, W. A., Engineering Customized Cell Sensing and Response Behaviors Using Synthetic Notch Receptors. *Cell* **2016,** *164* (4), 780-91.

77. Roybal, K. T.; Rupp, L. J.; Morsut, L.; Walker, W. J.; McNally, K. A.; Park, J. S.; Lim, W. A., Precision Tumor Recognition by T Cells With Combinatorial Antigen-Sensing Circuits. *Cell* **2016,** *164* (4), 770-9.

78. Kloss, C. C.; Condomines, M.; Cartellieri, M.; Bachmann, M.; Sadelain, M., Combinatorial antigen recognition with balanced signaling promotes selective tumor eradication by engineered T cells. *Nature biotechnology* **2013,** *31* (1), 71-5.

79. Tiberghien, P.; Ferrand, C.; Lioure, B.; Milpied, N.; Angonin, R.; Deconinck, E.; Certoux, J. M.; Robinet, E.; Saas, P.; Petracca, B.; Juttner, C.; Reynolds, C. W.; Longo, D. L.; Herve, P.; Cahn, J. Y., Administration of herpes simplex-thymidine kinase-expressing donor T cells with a T-cell-depleted allogeneic marrow graft. *Blood* **2001,** *97* (1), 63-72.

80. Bonini, C.; Ferrari, G.; Verzeletti, S.; Servida, P.; Zappone, E.; Ruggieri, L.; Ponzoni, M.; Rossini, S.; Mavilio, F.; Traversari, C.; Bordignon, C., HSV-TK gene transfer into donor lymphocytes for control of allogeneic graft-versus-leukemia. *Science* **1997,** *276* (5319), 1719-24.

81. Greco, R.; Oliveira, G.; Stanghellini, M. T.; Vago, L.; Bondanza, A.; Peccatori, J.; Cieri, N.; Marktel, S.; Mastaglio, S.; Bordignon, C.; Bonini, C.; Ciceri, F., Improving the safety of cell therapy with the TK-suicide gene. *Frontiers in pharmacology* **2015,** *6*, 95.

82. Straathof, K. C.; Pule, M. A.; Yotnda, P.; Dotti, G.; Vanin, E. F.; Brenner, M. K.; Heslop, H. E.; Spencer, D. M.; Rooney, C. M., An inducible caspase 9 safety switch for T-cell therapy. *Blood* **2005,** *105* (11), 4247-54.

83. Zhou, X.; Dotti, G.; Krance, R. A.; Martinez, C. A.; Naik, S.; Kamble, R. T.; Durett, A. G.; Dakhova, O.; Savoldo, B.; Di Stasi, A.; Spencer, D. M.; Lin, Y. F.; Liu, H.; Grilley, B. J.; Gee, A. P.; Rooney, C. M.; Heslop, H. E.; Brenner, M. K., Inducible caspase-9 suicide gene controls adverse effects from alloreplete T cells after haploidentical stem cell transplantation. *Blood* **2015,** *125* (26), 4103-13.

84. Philip, B.; Kokalaki, E.; Mekkaoui, L.; Thomas, S.; Straathof, K.; Flutter, B.; Marin, V.; Marafioti, T.; Chakraverty, R.; Linch, D.; Quezada, S. A.; Peggs, K. S.; Pule, M., A highly compact epitope-based marker/suicide gene for easier and safer T-cell therapy. *Blood* **2014,** *124* (8), 1277-87.

85. Wang, X.; Chang, W. C.; Wong, C. W.; Colcher, D.; Sherman, M.; Ostberg, J. R.; Forman, S. J.; Riddell, S. R.; Jensen, M. C., A transgene-encoded cell surface polypeptide for selection, in vivo tracking, and ablation of engineered cells. *Blood* **2011,** *118* (5), 1255-63.

86. Wu, C. Y.; Roybal, K. T.; Puchner, E. M.; Onuffer, J.; Lim, W. A., Remote control of therapeutic T cells through a small molecule-gated chimeric receptor. *Science* **2015,** *350* (6258), aab4077.

87. Weber, E. W.; Lynn, R. C.; Malipatlolla, M.; Sotillo, E.; Xu, P.; Mackall, C. L., Abstract LB-111: Precise regulation of CAR signaling prevents and reverses CAR T cell exhaustion. AACR: 2018.

88. Jin, H.; Vicario, P. P.; Zweerink, H.; Goyal, S.; Hanlon, W. A.; Dorn, C. P.; Mills, S. G.; DeMartino, J. A.; Cascieri, M. A.; Struthers, M., Expression and characterization of the chemokine receptor CCR2B from rhesus monkey. *Biochemical pharmacology* **2003,** *66* (2), 321-30.

89. Rupp, L. J.; Schumann, K.; Roybal, K. T.; Gate, R. E.; Ye, C. J.; Lim, W. A.; Marson, A., CRISPR/Cas9-mediated PD-1 disruption enhances anti-tumor efficacy of human chimeric antigen receptor T cells. *Scientific reports* **2017,** *7* (1), 737.

90. Lee, Y. G.; Marks, I.; Srinivasarao, M.; Kanduluru, A. K.; Mahalingam, S. M.; Liu, X.; Chu, H.; Low, P. S., Use of a Single CAR T Cell and Several Bispecific Adapters Facilitates Eradication of Multiple Antigenically Different Solid Tumors. *Cancer research* **2019,** *79* (2), 387-396.

91. Tamada, K.; Geng, D.; Sakoda, Y.; Bansal, N.; Srivastava, R.; Li, Z.; Davila, E., Redirecting gene-modified T cells toward various cancer types using tagged antibodies. *Clinical cancer research : an official journal of the American Association for Cancer Research* **2012,** *18* (23), 6436-45.

92. Viaud, S.; Ma, J. S. Y.; Hardy, I. R.; Hampton, E. N.; Benish, B.; Sherwood, L.; Nunez, V.; Ackerman, C. J.; Khialeeva, E.; Weglarz, M.; Lee, S. C.; Woods, A. K.; Young, T. S., Switchable control over in vivo CAR T expansion, B cell depletion, and induction of memory. *Proceedings of the National Academy of Sciences of the United States of America* **2018,** *115* (46), E10898-E10906.

CHAPTER 2. A NOVEL METHOD FOR CONTROL OF CAR T CELL OVERACTIVATION USING A PRIVATE PASSAGEWAY FUSION RECEPTOR

2.1 Introduction

Great advances have been made in the cell therapy field, pioneered by the approval of the CTL019 CAR T therapy in 2017. Unfortunately, this product was halted soon after its release due to an unexpected patient death. This again draws attention to the severe side effects of CD19 CAR T therapy, including acute cytokine storm and long-term hypo-gammaglobulinemia. Although neutralization therapy exists in clinics, such as use of the IL6R antibody and steroids, a finer control of the CAR T cell activity is greatly needed, either to dampen its killing effect in the case of the cytokine storm, or to terminate its activity for the B cell recovery. Another long-lasting concern in cell-based therapy in general, is the tumorigenic potential of these transplanted cells. Therefore, it would be ideal if researchers had the choice to terminate the adopted cells in case they become malignant.

Several controlled CAR T cell designs have been reported. Most of them have focused on the ON/OFF switch by incorporating either a Boolean gate or a cascade pathway for T cell activation. Although all of them can induce the termination of the CAR T cell, none of them have the ability to fine tune the activity of the CAR T cell in situ efficiently if needed. Here the current study presents a novel platform for controlling the transplanted cells by genetically incorporating a membrane-anchored two-part-fusion receptor. The first part of the fusion receptor is responsible for mediating specifically high affinity ligand binding, while the second part is responsible for the internalization of the complex through a GPI anchor moiety that then releases the payload inside the endosome. The fusion receptor will be transduced together with the antigen specific CAR

construct, adding no extra steps to the pipeline. In this chapter, the design and characterization of the fusion receptor is first described, followed by its application in termination of the modified CAR T cells and alleviation of CRS like syndrome.

2.2 Materials and Methods

2.2.1 Cell Lines and Human T Cells

RPMI 1640 (Gibco) containing 10% heat-inactivated fetal bovine serum and 1% penicillin-streptomycin was used for the culture of Raji and Jurkat cell lines. DMEM (Gibco) containing 10% heat-inactivated fetal bovine serum and 1% penicillin-streptomycin was used for the culture of MDAMB-231 and MDA-MB-231 $CD19^+$ cells. Peripheral blood mononuclear cells (PBMCs) were isolated by Ficoll density gradient centrifugation (GE Healthcare Lifesciences, #17-5442-02) from human whole blood obtained from healthy volunteers. Pure CD3+ T cells were enriched from PBMCs using an EasySep™ Human T Cell Isolation Kit (STEM CELL technologies, #17951). In detail, 16 ml fresh venous blood were diluted with PBS to 35 ml and carefully layered on top of 15 ml Ficoll. This was centrifuged at 500 g, no break for 30 min. After centrifugation, the middle cloudy part, which consisted of PBMC, was aspirated by pipette to a new 50 ml tube and further washed twice by PBS and centrifugation at 250 g to get rid of the platelets. After washing, the cells were resuspended in PBS at 5 x 10^7/ml and 50 µl EasySep™ Human T Cell negative isolation antibody cocktail was added for each ml and the mixture was incubated at RT for 5 min. After incubation, 40 µl Dextran Strep beads were added for each ml, and then the mixture was toped up to 2.5 ml with medium. The falcon tube containing the mixture was then put inside the magnet, incubated at RT for 3 min. After that, the tube was decanted into a new 50 ml tube with CD3 positive T cells in the supernatant. Human T cells were cultured in a TexMACS™ medium (Miltenyi Biotech Inc., #130-097-196) containing 1% penicillin and

streptomycin sulfate and 2% human serum (Valley Biomedical) in the presence of human IL-2 (100 IU/ml, Miltenyi Biotech Inc.), counted every 2-3 days and maintained at 0.5 x 10^6 cells/ml. All cells were cultured in 5% CO_2 at 37 °C and were regularly tested for contamination of mycoplasma.

2.2.2 Synthesis of Private Passageway Substrates

FK506-Rhodamine: Rhodamine-NHS ester (1.0 equiv.) in dimethylformamide was reacted with Boc-NH-PEG_3-NH_2 (1.2 equiv.) and diisopropylethylamine (3.0 equiv.) for 2 h at room temperature. The product was purified by preparative reverse-phase HPLC with a UV detector. The purified Rhodamine-PEG_3-NH-Boc conjugate (1.0 equiv.) was subjected to Boc deprotection by stirring in a 1:10 TFA-dichloromethane system for 2h. The crude free amine product was then dissolved in dimethylformamide and activated with EDC (2.0 equiv.), HOBT (2.0 equiv.) in the presence of diisopropylethylamine (3.0 equiv.). After 15 minutes, FK506-CO_2H (1.2 equiv., synthesized using the procedure in the reference: Bioorg. Med. Chem., 17 (2009) 5763-5768) was added and the reaction mixture was stirred overnight. The final FK506-Rhodamine conjugate was isolated after purification on preparative reverse-phase HPLC with a UV detector (monitored at a wavelength of 280 nm). The crude product was loaded onto an Xterra RP18 preparative HPLC column (Waters) and eluted with gradient conditions starting with 95% 5 mM sodium phosphate (mobile phase A, pH 7.4) and 5% acetonitrile (mobile phase B) and reaching 0% A and 50% B in 35 min at a flow rate of 12mL/min. The retention time of the product peak = 2.5 min during the gradient (0-50%B) in a 7 min analytical HPLC-MS analysis. ESI m/z = 1539.6. Abbreviations: PEG = polyethylene glycol; EDC = 1-Ethyl-3-(3-dimethylaminopropyl) carbodiimide; HOBT = Hydroxybenzotriazole; HPLC = High Performance Liquid Chromatography.

FITC-AlexFluor647:Fluorescein-5-isothiocyanate (FITC) was added dropwise to a solution of Amino-PEG_3-amine (3 equiv) and DIPEA (5 equiv) in DMSO. The solution was stirred at rt for

1 h to give FITC-PEG_3-amine. The resulting material was purified by preparative reverse-phase high-performance liquid chromatography (yield of 91.9%) with a gradient mobile phase consisting of 20 mM ammonium acetate buffer and 0% to 100% acetonitrile over 30 min (xTerra C18; Waters; 10 μm; 19 × 250 mm). For the synthesis of FITC-PEG_3-Alexa Fluor™ 647, Alexa Fluor™ 647 NHS Ester, FITC-PEG_3-amine (~2 equiv) and DIPEA (~5 equiv) were mixed and dissolved in DMSO. The mixture was stirred at rt for 1 h and purified using the same method as described above (yield of 90.2%). The purified FITC-PEG_3-amine and FITC-PEG_3-Alexa Fluor™ 647 were analyzed by liquid chromatography−mass spectrometry (LC-MS).

FITC-DM4: DM4 (1.0 equiv.) in dimethyl sulfoxide was reacted with 2-(pyridin-2-yldisulfaneyl) ethan-1-amine (1.0 equiv.) and diisopropylethylamine (3.0 equiv.) for 1h at room temperature. The resulting crude product was then reacted with FITC (1.0 equiv.) and the reaction mixture was stirred for 1 h. The final FITC-DM4 conjugate was isolated after purification on preparative reverse-phase HPLC with a UV detector (monitored at wavelength of 280 nm). The crude product was loaded onto an Xterra RP18 preparative HPLC column (Waters) and eluted with gradient conditions starting at 95% 5 mM sodium phosphate (mobile phase A, pH 7.4) and 5% acetonitrile (mobile phase B) and reaching 0% A and 100% B in 10 min at a flow rate of 12mL/min. Retention time of the product peak = 4.23 min during the gradient (0-100%B) in a 7 min analytical HPLC-MS analysis. ESI m/z = 1244.8.

FITC-EC20 head: Protected EC20 head, comprising a peptide sequence β-L-diaminopropionic acid, L-aspartic acid (L-Asp), and L-cysteine (L-Cys), was first synthesized by solid phase peptide synthesis (SPPS) according to a reported method. Next, a polyethylene glycol (PEG) liner Fmoc-N-amido-PEG4-acid was linked to the terminal amine via a formation of an amide bond. Finally, fluorescein isothiocyanate isomer I was conjugated to the sequence catalyzed by DIPEA. The conjugation reaction in each step was performed under an argon atmosphere, and all Fmoc-

protecting groups were removed by 20% piperidine in DMF. The final compound FITC-EC20 head conjugate was cleaved from the resin using a cocktail solution (TFA/TIPS/EtSH/H_2O (92.5:2.5:2.5:2.5)). This cocktail solution also simultaneously deprotected all t-butyl-, trityl- and t-butoxycarbonyl-protecting groups. The cleaved product was precipitated in diethyl ether and dried under vacuum. The crude compound was purified by preparative reverse-phase high-performance liquid chromatography (prep-HPLC) with an eluent consisting of 20 mM ammonium acetate buffer and 0% to 50% acetonitrile over 35 min (xTerra C18; Waters; 10 μm; 19 × 250 mm). The purified FITC-EC20 conjugate was analyzed by liquid chromatography−mass spectrometry (LC-MS) (ESI m/z =959.1).

2.2.3 Preparation of Lentiviral Vectors Encoding anti-CD19 CAR T2A FKBP-FR and anti-CD19 CAR T2A FITC-FR

For co-expression of a classical anti-CD19 CAR together with a private passageway protein in the same human T cell, a lentiviral vector was assembled containing genes for the above two fusion proteins linked via a T2A self-cleaving sequence. For preparation of the sequence of the FKBP containing a private passageway (FKBP-FR), a construct of the following sequences in frame from 5' to 3' end was prepared: residues 1-24 of human Folate Receptor alpha (FRα, NM_016724.2), the entire sequence for human FK506 binding protein 12 (NM_000801.5), the sequence of a flexible peptide linker $(GGGGS)_3$, and the sequence for the remainder of human FR (residues 25-257) (see Figure 2-1). For the co-expression of this sequence in the same vector with the anti-CD19 CAR, the sequence for the anti-CD19 CAR was ligated in frame to the sequence for the T2A self-cleaving peptide, which in turn was ligated in frame to the sequence for FKBP-FR (Figure 2-9). The resulting construct was then inserted into the pHR lentiviral expression vector by restriction enzyme digestion with MluI and NotI and T cells were transfected with the lentiviral vector using standard methods. The anti-fluorescein scFv containing a private

passageway (FITC-FR) was prepared similarly, except the sequence for the human anti-FITC scFv was used instead of the sequence for FKBP in the protocol above.

Lentivirus packaging: low passage 293tn cells (SBI, # LV900A-1) were plated in a 100 mm^3 plate at around 7 x 10^7/plate using a packaging medium (Opti-MEM, 5% FBS, no P/S) at D0. At D1, prewarmed Opti-MEM were used to prepare the lipofectamine mixture as follows: Tube A: expression plasmid 4 μg, packaging mixture (Cellecta, #CPCP-K2A) 10 μg in 20 μl, lipofectamine P3000 (ThermoFisher, #L3000008) 37 μl in 1.5 ml Opti-MEM; Tube B: lipofectamine 3000 42 μl in 1.5 ml Opti-MEM. Tube B were added dropwise to Tube A and the mixture was incubated for 15 min, RT. 6 ml of medium were taken out of the plated cells. The A/B mixture was added dropwise to the plated cells and returned to the incubator. After 6 h, the medium was changed to a fresh packaging medium and the supernatant which contained the lentivirus was then collected at 48 h and/or 72 h. The virus supernatant was filtered by passing through a 0.45 μM PVDF filter. Virus can be stored at -80 ℃ or further concentrated by adding 1/3 volume of lentiX (Clontech, #631232), incubated at 4 ℃ for more than 30 min, and then centrifuged at 4 ℃, 1800 rpm for 1 h. The palleted virus can be resuspended in 1/100 of the original volume of virus packaging medium (pH around 7) and then aliquoted and stored at -80 ℃. Freeze and thaw cycles should be limited, as one cycle reduces the virus titer by a half log.

2.2.4 Use of Lentiviral Vectors Encoding anti-CD19 CAR T2A FKBP-FR and anti-CD19 CAR T2A FITC-FR to Transduce to Human T Cells

For T cell activation, the newly isolated T cells were counted and resuspended at 1 x 10^6/ml with medium, the CD3/CD28 activation beads (ThermoFisher, #11161D) were washed, and added to the cells at 1:1 ratio in a 24-well. For T cell transduction, 4-8 μg/ml polybrene with 10-20 μl concentrated virus was added to 1M activated T cell (TexMACS^{TM} medium w/o serum), centrifuged at 2500 rpm for 1.5 h. Medium was replaced with new TexMACS^{TM} w/ 2-6% Human

Serum the next day to avoid toxicity of polybrene. After 3-5 days of transduction, the T cells were harvested and analyzed by flow cytometry to determine the transduction efficiency.

2.2.5 Analysis of Private Passageway Fusion Receptor Binding and Internalization

For the FK506-Rhodamine binding assay, FKBP-FR Jurkat cells and non-transduced cells (5 x 10^5) were pre-incubated with an FK506-linker (100 fold excess) for 30 min, or with an FK506-Rhodamine (concentration range: from 100 pM to 100 nM) in the presence or absence of FK506-Glucosamine (100 fold excess) for 30 min, at 4 ℃. Cells were then washed 3 times, then resuspended in 2% FBS PBS and submitted for flow cytometry. The binding affinity assays for FITC-AlexFluor 647 were tested similarly, with FITC-Glucosamine for competition. For the Phosphoinositide Phospholipase C (PI-PLC) treatment assay[1], cells were removed from the monolayer by scrapers and washed with PBS, then suspended at 5 x 10^6 cells/ml in 0.025 M Tris-HCl, 0.25 M sucrose, 0.01 M glucose, 1x protease inhibitor cocktail (Roche), pH 7.5. 100 µl of the cell suspension were incubated with 5 units of PI-PLC (ThermoFisher, #P6466) at 37 ℃ for 1 h. The reaction was stopped by cooling it to 4 ℃; cells were then washed and used for FK506-Rhodamine and FITC-AlexFluor 647 staining. Cells were kept at 4 ℃ for the subsequent incubation and washing. FACS Rosseta was used to acquire the fluorescent signal and the compensation was carried out automatically. Results were analyzed using FlowJo software. The GraphPad Prism version 7 software was used to analyze binding affinity.

For the internalization study, 1 x 10^4 FKBP-FR expressing HEK293 cells in 0.5 ml of growth media were seeded in chambered covered glass (ThermoFisher, #155383) and incubated overnight at 37 ℃ for full adherence. The next day, fresh medium containing 50 nM FK506-Rhodamine was added, and the cells were incubated either at 4 ℃ or 37 ℃ for the times indicated. At the end of incubation, the cells were washed with warm cell medium and imaged using a confocal laser

scanning microscope. The internalization assay for the FITC-FR fusion receptor was tested similarly with FITC-AlexFluor 647.

2.2.6 Quantification of Expression Level of Fusion Receptors Using FA-^{99m}Tc

The chelation of FA-^{99m}Tc was prepared according to the previous literature[2]. KB, FKBP-FR Jurkat and FITC-FR Jurkat cells were plated in a 24-well plate and incubated with 50 nM FA-^{99m}Tc at 4 ℃ for 30 min. After incubation, the cells were washed and lysed in a 10% SDS solution, and the radiation level of each sample was then determined with a gamma counter.

2.2.7 Formulation and Labeling of FITC-^{99m}Tc

2 mg FITC-Tc chelating head compound was dissolved in nitrogen sparged water at 1 mg/ml. 1 g tin chloride was dissolved in 100 ml of nitrogen sparged 0.2 N HCl. 2.5 g sodium gluconate and 250 mg EDTA were each dissolved separately in 25 ml nitrogen sparged water. To a new flask, sequentially add 12.5 ml of sodium gluconate solution, 1.5 ml EDTA solution, 0.5 ml tin chloride solution, 5 ml FITC-Tc chelating head compound solution, adjust pH to 6.8 and top it up to 50 ml with nitrogen sparged water. Fill 1ml to each formulation vial and lyophilize for 48h. Store at -80 ℃. To label with radioactive ^{99m} Tc, remove the formulation vial from -80 ℃, place it in a suitable shielding container and equilibrate it to room temperature. Using a shield syringe, inject 1 ml (15 mCi) sodium pertechnetate ^{99m}Tc. Swirl the vial gently to completely dissolve the powder. Allow the vial to stand at RT for 15-20 min and use it within 6 h.

2.2.8 Measurement of Internalized and Membrane-Bound FITC-^{99m}Tc after Various Periods of Continuous Incubation

FITC-^{99m}Tc were synthesized and chelated with technetium similar to FA-^{99m}Tc. To quantitate the amount of cell surface and internalized FITC-^{99m}Tc mediated by the FITC-FR fusion receptor, FITC-FR expressing HEK293 cells were plated in 24-well plates at approximately 30% confluence and allowed to grow for 2 days before the experiment. A certain concentration of

FITC-^{99m}Tc was added to the cultured cells and the cells were incubated for the times indicated in the figures at either 4 or 37 ℃. After incubation, the cells were then washed with PBS and lysed in 0.5 ml of 10% SDS solution. The radiation levels of each sample were then determined with a gamma counter.

2.2.9 Characterization of FITC-FR and FKBP-FR Fusion Receptor Molecular Weights by Western Blotting

FITC-FR or FKBP-FR expression HEK293 cells and KB cells were lysed and centrifuged at 16,000 x g for 10 min at 4 ℃ to remove cell debris. Clear cell lysates were resolved by electrophoresis on 4-20% SDS-PAGE gels and electrophoretically transferred to nitrocellulose filters. The blots were probed with an anti-FRα or anti-actin antibody (1:200 dilution) followed by a horseradish peroxidase conjugated secondary antibody and visualized using an enhanced chemiluminescence method.

2.2.10 FITC-/FK506-Cytotoxic Payload Mediated Killing of Fusion Receptor Positive Cells

For in vitro cell viability assays, CellTiter-Glo™ (Promega, #G7570) was used. FITC-FR or FKBP-FR T cells were incubated with different concentrations (0.1 to 100 nM) of FITC-/FK506 cytotoxic payloads in the absence or presence of competition ligands for 2 h. The cells were then washed twice and supplemented with fresh medium. The cells were cultured for another 72 h. At the endpoint, CellTiter-Glo™ reagent was added to each well at a 1:1 vol/vol ratio and luminescent readings were obtained using a plate reader according to the manufacturer's protocol.

2.2.11 Inhibition of Human T Cell Lysis via Private Passageway Delivery of an Immunosuppressant/Kinase Inhibitor Payload

anti-CD19 FITC-FR or FKBP-FR CAR T cells were co-cultured with CD19 expressing Raji cells at an Effector : Target ratio = 5 : 1 in 96-well plates. FITC-FK506 or FK506-FK506 were added to the anti-CD19 FITC-FR or anti-CD19 FKBP-FR CAR T cells at different concentrations for 2 h, in the absence or presence of competition ligands. The cells were washed and supplemented

with fresh medium and continue cultured for 12 h. At the end of the incubation period, the plates were centrifuged at 350 x g for 10 min and supernatants were analyzed for lactate dehydrogenase release (LDH). For this analysis, CytoONE^{TM} (Promega) and interferon γ (INFγ) levels using human INFγ ELISA kit (BioLegend) were used, according to the manufacture's protocol. Other potential payloads were screened using the same procedure.

2.2.12 Evaluation of FITC-DM4 and FITC-FK506 on FITC-FR CAR T Cell in Raji Tumor Model

Immunodeficient NSG mice (Jackson Laboratory) were implanted intravenously with 2 x 10^6 Raji cells. 7 days after the tumor injection, the mice were injected intravenously with 10^7 FITC-FR anti-CD19 CAR T cells. Body weight was monitored. FITC-DM4 or FITC-FK506 was dosed 7 days after the CAR T cells injection. Cell staining and serum preparation from peripheral blood: mice were put under anesthesia using an isoflurane machine with level 4 flow rate for just 1 min. Blood was drawn quickly by submandibular puncture and collected using an EDTA coated tube. For staining of cell surface markers: fluorescent dye labeled antibodies were added to samples directly, incubated in the dark for 30 min, and then the red blood cells were lysed by adding an RBS lysis buffer (10x, diluted by ddH_2O), RT for 10 min, then washed with a cell staining buffer. When fixation was need, a fix/lysis buffer could be added and incubated in the dark for 10 min, washed with a cell staining buffer, and continued for staining. Human CAR T cell were confirmed by cmyc-APC staining and tested by a flow cytometer with counting beads. For serum preparation: blood containing anti-coagulant EDTA was centrifuged in a swing bucket centrifuge at 1000 g for 10 min. Serum could then be aspirated by pipettes at the top and stored at -20 ℃ for further analysis. To test the cytokine level, INFγ was quantified using a human INFγ ELISA kit (BioLegend).

ELISA procedure: 96-well ELISA plates were coated by incubating each well with 100 µl of a 5 µg/ml capture antibody in a coating buffer (8.4 g $NaHCO_3$, 3.56 g Na_2CO_3, deionized water added to 1.0 L, pH 9.5) at 4 ℃ overnight while covered with adhesion film. The following day, the plates were washed 3x with PBS-Tween (0.01 M PBS with 0.05% Tween-20 at pH 7.4) and blotted dry on paper towels before incubating with a freshly prepared 10% FBS for 1 h at RT. The FBS blocked plates were then washed 4x with PBS-Tween. 100 µl of mice serum dilution (serial dilution by factor of 10) were then added to each well and incubated for 2 h at RT followed by 4x washing. In order to detect cytokines that would have bound to the capture antibodies coated on the wells, the plates were incubated with detection antibody (100 µl at 1:200 dilution) for 1 h and then washed and followed by an HRP labeled secondary antibody (100 µl at 1:1000 dilution) for 1 h at RT. Following another 4x wash, the plates were incubated with a freshly prepared TMB substrate solution. The substrate-HRP reaction was allowed to continue in the dark for 30min at room temperature and subsequently, was stopped by the addition of a 100 µl stop solution (2N HCl). The plate was then read at 450 nm (O.D.) using a 96-well plate reader. Each serum sample was run in triplicate.

2.3 Results

2.3.1 Design of Private Passageway Fusion Receptors

In order to develop a "private passageway" that would allow the delivery of any drug into an engineered therapeutic cell, we hypothesized that the engineered receptor should exhibit the following properties: it should 1) traffic to the cell surface of the desired therapeutic cell, 2) contain a high affinity binding site for a ligand not recognized by any other cell in the body, 3) endocytose constitutively into the therapeutic cell, 4) recycle rapidly back to the cell surface for additional rounds of endocytosis, 5) be comprised of totally human components, and 6) exhibit good stability in vivo. With such an engineered receptor present in the therapeutic cell, any desired drug should be deliverable into that cell by linking the drug via a cleavable spacer to the ligand that recognizes the engineered fusion receptor.

In the studies below, two engineered "private passageway" receptors are described that employ either a human anti-fluorescein scFv (FITC) or a human FK506 binding protein 12 (FKBP12) as the high affinity ligand binding domain (Fig. 2-1). Although many other binding domains could have been selected, the above two were chosen because of their stabilities and high affinities for their specific ligands (i.e. 50 fM[3] and 0.2 nM[4], respectively).

As mentioned in Chapter 1, the FKBP12/FK506 pair has been used extensively for artificially designed chemically induced dimerization and degradation systems. The peptidyl-proline isomerase (PPIases) family consists of FK506-binding protein (FKBP), cyclophilins and parvulins. In humans, there are 18 FKBPs, 24 cyclophilins and 3 parvulins[5]. Among these, FKBP51 and FKBP52 share high to moderate binding affinity of FK506, $K_d^{FK506} \approx 104$ nM and $K_d^{FK506} \approx 23$ nM, respectively, compared to FKBP12 ($K_d^{FK506} \approx 0.2$ nM)[3]. Additionally, none of these two FKBPs are expressed on the cell membrane, resulting in little cross binding activity in the system. The cocrystal structure of FK506 with FKBP (PDB: 1FKF) was solved in 1991 by Stuart Schreiber,

et al[6], while the ternary structure of FK506, FKBP and calcineurin (PDB: 1FKJ), which is the biologically functional complex, was first described by Manuel Navia, et al.[7] 4 years later. Thanks to the information provided by the co-crystal structure, efforts have been made to design synthetic ligands that have a higher affinity to $FKBP12^{F36V}$ than $FKBP^{WT}$[8], as well as to $FKBP51^{F67V}$ [9], which preserve the overall structure of the wild type proteins. The ternary structure also indicated that derivatization of FK506 from the double bond will abolish its binding to calcineurin and therefore deplete its biological function, as confirmed by Schreiber SL et al.[6] using an olefin metathesis reaction. Therefore, we choose FKBP12 as the binding domain and the olefin metathesis derivatized FK506 as the corresponding targeting ligand for our secret passageway fusion receptor. To confirm the generality of the secret passageway system, another binding protein, scFv for FITC, was tested. The scFv for FITC clone 4M5.3 was evolved from 4-4-20 to a femtomolar affinity and humanized to reduce potency for immunogenicity[4]. For the targeting ligand FITC, safety concerns about it being an immunogenic hapten were dismissed by the fact that small molecule haptens by themselves, such as FITC, dinitrophenol (DNP) or trinitrophenol (TNP) were not able to elicit immune reactions, unless being conjugated to immunogenic proteins, such as Keyhole limpet hemocyanin (KLH) and Ovalbumin (OVA)[10]. We have also thoroughly studied the pharmacological properties of a small molecule drug FITC-FA in a clinical setting and observed no immune reactions against FITC during treatment[11-12]. The co-crystal structure of 4M5.3 with FITC (PDB: 1X9Q) provided information on the derivatization site for the FITC molecule to link with potential payloads[4].

To assure that each ligand binding domain would endocytose constitutively into its engineered therapeutic cell type, each ligand binding, FKBP12 or scFv for FITC domain, was tethered via a flexible peptide linker to the glycosylphosphatidylinositol-anchored domain of a human folate

receptor alpha (FRα). Because this domain constitutively enters cells by receptor mediated endocytosis and then rapidly recycles back to the cell surface[13-14], it satisfied both the internalization and recycling requirements mentioned above. Endocytosis is a complicated biological process that takes on several forms. Almost all surface receptors show endocytosis to some extent, but the fast internalization rate of FRα (at the magnitude of 6-12 h) is superior than most of the transmembrane proteins and common for the Glycosylphosphatidylinositol (GPI) anchored protein family[15]. The Low lab has confirmed the internalization rate of both FRα and FRβ using sensitive radioisotope-based imaging agents and found that the FRβ that are expressed mainly on myeloid cells can recycle even faster than FRα[16]. Even more interesting, the rate of FRα recycling does not depend on the folate acid concentration and binding[13], which makes it the ideal candidate for the secret passageway fusion receptor design.

Although grafting of signal peptides to proteins to create transmembrane proteins is widely used in protein engineering, such as the signal peptide of CD8 or GM-CSF at the NH_2-terminus of CAR, no previous report on the use of signal peptides to make de novo GPI anchored proteins has been seen. Most GPI-anchored proteins, including FRα, have a cleaved N-terminal signal that targets them to the Sec61 translocon in the ER[17]. Meantime, the C-terminal of the GPI anchor is also processed in the endoplasmic reticulum (ER) by a transamidation reaction in which the GPI attachment signal is cleaved off concomitantly with addition of the GPI moiety[18-19]. However, the C-terminal signals are poorly conserved and characterized as a polar segment that includes the GPI attachment site followed by a hydrophobic segment end. Therefore, to promote proper trafficking of the de novo synthesized fusion receptor containing FKBP12 or scFv for FITC to the cell surface as a GPI anchored protein, the N-terminal signal peptide from FRα was attached to

the NH_2-terminus of the fusion receptor, leaving the C-terminal signal peptide unchanged (Fig. 2-1 B).

2.3.2 Generation and Characterization of Fusion Receptors

2.3.2.1 Stable Surface Expression of Fusion Receptors in Multiple Cell Lines

To determine whether the above private passageways would exhibit their intended properties, we expressed the fusion constructs in different cell lines and performed assays to evaluate their properties. First, the level of expression of both glycosylphosphatidylinositol-anchored fusion proteins was assayed in Jurkat T cells by incubation of the transfected cells with fluorescent dye conjugates of their respective cognate ligands and measurement of the increase in cell bound fluorescence by flow cytometry. As shown in Fig. 2-2 A, incubation of the FKBP-FR expressing Jurkat cells with FK506-Rhodamine caused a shift of nearly two orders of magnitude in the mean fluorescence intensity of the transfected cells. That this cell-associated fluorescence was mediated by the GPI-anchored FKBP-FR could be readily demonstrated by treating the cells with a GPIdirected phospholipase C (PI-PLC)[20] which showed that the aforementioned shift in fluorescence was abrogated (Fig. 2-2 A). Importantly, as seen in the adjacent panel of Fig. 2-2 A, an analogous outcome was also obtained when the FITC-FR cells were similarly incubated with FITC-AlexaFluor 647.

To explore the structural interference between two moieties within the fusion receptor, two flexible linkers of different length, (G_4S_1) (abbreviated as FF1) or $(G_4S_1)3$ (abbreviated as FF3) were tested. Interestingly, for FKBP-FR, a strong inhibition of FK506 binding with the presence of Folic acid (FA) occurred (starting from 0.1nM, see Fig. 2-3 A) for the shorter linker FF1 (around 15 Å), while methotrexate (MTX), a folate acid analog with much lowered affinity to FRα has no effect. Increasing linker length FF3 (around 45 Å) abolished the interference (Fig. 2-3 B). No interferences were observed between scFv for FITC clone 4M5.3 and FRα with a $(G_4S_1)3$

linker in between in FITC-FR fusion receptor (data not shown). Since the crystal structures of both moieties, FRα[21] and FKBP12, were solved, it will be interesting to learn how the binding of FA blocks the binding pocket of FK506 in the FKBP-FR fusion receptor with a shorter linker.

In situations where the co-expression of a second engineered protein was desired (e.g. a chimeric antigen receptor, (CAR)), the gene for the private passageway was ligated via an oligonucleotide encoding of the T2A self-cleaving peptide[22]. The expression level of inserts has been reported to correlate with their relative position to T2A and the distance away from promoters[23]. Seeking for the optimal expression level of both the fusion receptors and CAR, two constructs were made with fusion receptors positioned either before or after the T2A sequence (Fig. 2-4 A). Interestingly, the position of the fusion receptor before T2A resulted in the failure of the surface translocation of the whole fusion receptor tested by targeting ligand-dye molecule staining (Fig. 2-4 B). One of the possible reasons for this, as indicated by computational predication, is that the 20 amino acids (GSGEGRGSLLTCGDVEENPG) left to the C-terminal of the fusion receptor by the T2A signal after cleavage may have broken the hydrophobic pattern of the C-terminal of GPI attachment signal and interfered with the transamidation reaction (prediction by GPI-SOM: http://gpi.unibe.ch/). Indeed, the other design which has the fusion receptor located behind T2A showed robust expression and surface localization of both the fusion receptor and the CAR. This result indicates that the residual of the T2A sequence has minimal effect on the translocation of the type I transmembrane protein, and the effect of the single amino acid Pro left at the N-terminal of GPI anchoring protein can also be dismissed. The final construct of each secret passageway fusion receptor together with the anti-CD19 CAR is shown in Fig 2-4.

Since the abundance of receptors that present on the surface directly correlates with the potency of receptor mediated drug delivery, several combinations of lentivirus vectors and promoters were tested for proper and efficient expression of the whole insert (CAR-T2A-fusion receptor) in

human T cells using lentivirus. In general, HIV derived lentivirus has a packaging limit of around 9.2kb[24] and for optimal chemical transfection efficiency, the total size of a plasmid should be smaller than 13kb[25] The choice of promoters also significantly affects the final expression level of insert in primary human cells, including T cells. Therefore, two vectors pWPI[26], pHR[27] and two promoters EF1α, PGK that are frequently used in other reported T cell transduction studies were tested. Since no significant difference for promoters between EF1α and PGK at the insert expression level, and the PGK (505 bp) is shorter than EF1α (1179 bp), the PGK promoter was selected. Newly developed promoters, such as PKG100 (truncated PKG, around 100bp)[28], which were designed to have moderate insert expression level with an even shorter sequence to work with the increasing size of the insert for virus transduction in T cells could be tested in future research. In summary, the entire CAR-T2A-fusion receptor construct mentioned above was placed under the control of the PGK promoter of a pHR lentiviral vector, as shown in Fig. 2-4.

Next, to quantitate the level of private passageway expression in the transfected Jurkat cells, the fusion receptor which also contained a functional binding site for folic acid, i.e. allowed the number of FKBP-FR and FITC-FR to be quantitated by measuring the binding of folate-^{99m}Tc to the transfected Jurkat cells. As shown in Fig. 2-2 B, the FKBP-FR transfected cells bound ~48% as much folate-targeted radio imaging agent as the FR-expressing KB cells, while the FITC-FR transfected cells bound ~60% as much as the KB cells. Assuming that the KB cells express ~3 million folate receptors/cell[29], the above data suggests that the transfected Jurkat T cells express between 1.4 and 1.8 million private passageway fusion receptors/cells.

Immunoblots of the transfected cells using an anti-FRα antibody further demonstrated that the expressed fusion receptors had the anticipated molecular weights of 50 and 60 kDa for FKBP-FR and FITC-FR, respectively (Fig. 2-2 C). Antibodies against FKBP12 were also tested for Western

Blotting but gave no signal (data not shown). One possible reason for this result could be the epitope of FKBP12 that recognized by this specific anti-FKBP12 antibody clone was structurally blocked by the FRα.

2.3.2.2 Binding Affinities of Folic Acid, Fluorescein and FK506 For Their Corresponding Binding Domains of the Fusion Receptors

The affinity of each private passageway receptor for its cognate ligand was then determined by quantitating the FA-Rhodamine, FK506-Rhodamine or FITC-AlexaFluor 647 binding to the FKBP-FR, FITC-FR transfected Jurkat cell lines. As shown in Fig. 2-5 A, three fluorescent conjugates bound to their targeted Jurkat cell populations with K_d values of 1nM, 4 nM and 8 nM, respectively. Based on prior experience with other ligand-targeted drug conjugates[30], these affinities are ideal for ligand-targeted drug delivery applications in vivo.

The sustained binding of FK506-Rhodamine to FKBP-FR positive cells that were spiked into anti-clogged whole human blood implies that the peptide linkage between FKBP-FR is resistant to common enzymes residing in the blood and the binding is not affected by macromolecules, such as albumins, in the circulation (Fig. 2-6).

Due to the chemical complexity of FK506, a FK506 analog, SLF, is being explored for substitution as a targeting ligand for the FKBP-FR fusion receptor. SLF is widely used for FKBP binding and has a K_d of 10 nM[31], around 10 times lower than FK506. However, the binding affinity of SLF-FITC to the FKBP-FR fusion receptor is relatively low, around 62 nM (Fig. 2-7). Therefore, the FK506 analog SLF has not been pursued further as a targeting ligand for the FKBP-FR fusion receptor in this study.

2.3.2.3 Internalization of Fusion Receptors

To document the generality of private passageway expression, HEK293 cells were transfected with the same FKBP-FR or FITC-FR lentiviral vectors and the internalization of the same fluorescent conjugates was examined by confocal microscopy. As shown in Fig. 2-8 A, all of the fluorescence remained on the cell surface at 4 ℃ where endocytosis was known to be inhibited[32], whereas many fluorescent puncta were seen within each cell's cytoplasm at 37℃ where endocytosis was permitted. These data demonstrate that the FKBP-FR fusion receptor can internalize its fluorescent cargo by receptor-mediated endocytosis at 37℃. Since similar results were obtained when FITC-FR transfected HEK293 cells were incubated with FITC-AlexaFluor 647. The conclusion was made that both private passageway receptors internalized their bound cargoes at 37 ℃, regardless of the structures of the attached drugs. Internalization has also been tested by sequential FITC-biotin, and Streptavidin-PE staining. FITC-FR cells were first stained with a saturation level of FITC-biotin and washed, followed by Streptavidin-PE staining at different time points (Fig. 2-8 B). Internalized fusion receptor/FITC-biotin complex will reside intracellularly and be hidden from the next step Strep-PE staining. As shown in Fig 2-8 C, FRα in KB cells (positive control) showed periodical recycling of the FRα/FA-biotin complex with a turnover time of around 1 h. The lowest intensity occured approximately 30 min after the FA-biotin incubation and was at a similar intensity as the nonstaining and Strep-PE only. This result implied that almost all receptors previously bound by FA were internalized at around 30 min and then came back to the cell surface at around 1 h. Similarly, FITC-FR positive cells that fixed 30 min after FITC-biotin incubation showed the lowest intensity of a PE signal, indicating that the recycling rate of the FITC-FR fusion receptor is around 1 h, similar to the FRα in KB cells.

Next, to quantitate the internalization of the ligand-drug conjugates at 37 ℃, we attempted to link each ligand to a ^{99m}Tc-chelating agent with the anticipation that it might be possible to measure the uptake of the conjugates as a function of time by gamma counting. Unfortunately, conjugation of the ^{99m}Tc radio-chelating agent to FK506 interfered with ^{99m}Tc chelation, forcing the focus of the study on FITC-^{99m}Tc-chelate conjugate binding and internalization. As shown in Fig 2-9, the binding of FITC-^{99m}Tc in FITC-FR HEK293 cells under both 4 and 37 ℃ saturated below a 50nM concentration, while the final radioactivity level was higher for the cells at 37 ℃ due to a continuous delivery and accumulation of FITC-^{99m}Tc inside the cells through receptor internalization. When incubated with a saturating concentration of FITC-^{99m}Tc and monitored radioactivity at different time points, FITC-FR positive cells were saturated within one hour at 4 ℃, after which point the uptake leveled off due to an absence of receptor internalization. In contrast, uptake of the radio-imaging agent by the same cells continued almost linearly along 6 h of incubation due to constitutive recycling of the fusion receptor at 37 ℃ (Fig 2-9 C).

2.3.3 Inhibition of Cytokine Release Syndrome through Private Passageway Fusion Receptor Mediated Delivery of a Cytotoxic Drug Payload

With the ability to use the private passageway to deliver various imaging agents to differently transfected cell lines now established, the question arose whether functional quantities of a therapeutic drug might be delivered by the same fusion receptor. Because a major need of some CAR T cell therapies has been an ability to terminate CAR T cell activity when they become life threatening, to the next question was to determine whether a transfected therapeutic T cell could be killed by the administration of a cytotoxic payload via the private passageway. As shown in Fig. 2-10, treatment of the FITC-FR containing human T cells with an FITC-linked maytansine (i.e. DM1 and DM4 are microtubule inhibitors commonly used in cytotoxic antibody-drug conjugates[33]) via a disulfide linker resulted in potent killing of the T cells with an IC_{50} of 4.2 nM.

Similar but less potent results were obtained when an FK506-tethered DM1 conjugate was incubated with FKBP-FR. FA linked Tubulysin, another potent microtubule-targeted cytotoxic drug, can also introduce potent and specific killing of FKBP-FR positive T cells by docking with the FRα domain of the fusion receptor, with an IC_{50} of 17.48 nM. Taken together, these data suggest that the suppression of an overactivated T cell response can be mitigated by the targeted killing of the over-activated T cells with a private passageway targeted cytotoxic drug.

2.3.4 Inhibition of Cytokine Release Syndrome through Private Passageway Fusion Receptor Mediated Delivery of Either an Immunosuppressant or Kinase Inhibitor Payload

2.3.4.1 Screening for Potential Small Molecule Inhibitors of CAR T Cell Activity

Because elimination of the therapeutic CAR T cells will terminate the therapy, it seemed prudent to explore whether a more tunable response might be developed where the activity of the CAR T cells would be reduced as needed, but the CAR T cells would not be killed. Since the signaling pathways for CAR and TCR greatly overlap, several commercially available small molecule drugs that are potentially functional in T cell activity were screened in the tumor/CAR T cell co-culture system, and the lysis effect and INFγ level were measured. The ease of chemical modification for the potential payloads should also be considered if similar targets and/or effects present themselves. Detailed function and chemical structure of screened molecules are described below.

- Dasatinib

Dasatinib is an oral broad-spectrum kinase inhibitor of the Abl and Src family, including Lck, which is a central player for downstream TCR signaling. It has been shown to sensitize T cell to inhibition by cyclosporine A or rapamycin when used in combination[34]. During the preparation of this manuscript, the Crystal Mackall group reported on the inhibition effect of Dasatinib on anti-CD19 CAR T cell[35]. In this report, both the CD28 and 4-1BB co-stimulatory domain CARs

were tested, with more discernable effects in the CAR containing CD28. Standard dosing of dasatinib at 100 mg/day in clinic results in maximum serum concentration of 168 nM in patients[36], which is higher than the IC_{50} of around 10 nM tested in their co-culture system.

- PI3K or Akt inhibtor

PI3K/Akt/mTOR pathway regulates cell growth, migration, survival, and many other important cell functions. mTOR is the downstream of PI3K and Akt and blocks of mTOR by rapamycin is a potent inhibitor as T cell activity, partially by inducing the differentiation of CD4 into Treg[37-39]. In contrast, pharmacological inhibition of PI3K in macrophages and dendritic cells has been shown to increase production of proinflammatory cytokines, including IL6, IL12, IL1β and TNFα[40]. Recently, several research groups have been trying to add PI3K inhibitors to the culture medium during the production of CAR T cells, helping to keep CAR T cells at a more memory status and makes them less sensitive to exhaustion before injection (personal communication). This result may relate to the role of the PI3K axis in the induction of anergy in T cells.

- Ibrutinib

Ibrutinib is the first-in-class irreversible kinase inhibitor for Bruton tyrosine kinase (BTK) in B cells, and cross reacts with IL-2 inducible T cell kinase (ITK) in immunosuppressive T helper CD4 T cells, therefore improves the antitumor effect of T cells[41]. Marcela V. Maus, et al.[42] confirmed that the Ibrutinib treatment of CLL not only improves the engraftment but also the therapeutic efficacy of anti-CD19 CAR T cells. Interestingly, although the inhibition of ITK by Ibrutinib is irreversible, a pulse dose of ibrutinib did not alter T cell proliferation or cytotoxicity, even at concentrations higher than those used in clinics.

- Trametinib

MAPK kinase (MEK) is an important player in TCR signaling, therefore, inhibition of MEK should result in decreased CAR T/T cell activity. However, previous research showed that inhibition of MEK by Trametinib, a kinase inhibitor for MEK1/2, protected tumor-infiltrating CD8 T cells from chronic TCR stimulation induced T cell death[43].

- Jak inhibitor

Many cytokines exert their biological functions through Janus kinase (JAK)-Signal Transducers and Activator of Transcription (STAT) pathway in many immune cells, including macrophages, T cells, and NK cells. Inhibitors of JAK, such as Baricitinib, Tofacitinib, and ruxolitinib, have been tested extensively in the treatment of autoimmune diseases, including RA, SLE, Psoriasis, and IBD[44], to lower the effect of inflammatory cytokines. Therefore, inhibition of JAK may lower the activity of CAR T cells as well.

The aforementioned small molecules were then added to the co-culture system of anti-FITC CAR T cells and FRα positive target cells in the presence of an FA-FITC adaptor (Fig. 2-11). As expected, Dasatinib, ITK and Cyclosporin A were all able to down regulate the lysis effect of CAR T cells, while AKT and PI3K appeared to be less effective, consistent with the literature. JAK inhibitors were also less effective; this may be due to the less abundant cytokine levels in the in vitro culture system. Interestingly, MEK1/2 kinase inhibitors showed significant reduction of T cell activity at 10 nM, around 35% lysis effect compare to the untreated group. The detailed mechanism of Trametinib in CAR T cells needs further study.

2.3.4.2 FK506 as a Proof-of-Concept Immunosuppressant Payload

Next, as a proof-of-concept, two of the private passageways were exploited for delivery of FK506, a potent noncytotoxic immunosuppressant of T cells[45]. Thus, as shown in Fig. 5A, delivery of FK506 to FITC-FR expressing CAR T cells was achieved by using a conjugate of

FITC linked to FK506 (upper structure), whereas delivery to FKBP-FR expressing CAR T cells was attained by employing FK506 linked to FK506 (lower structure). Regardless of the private passageway used, both methods allowed for gradual suppression of CAR T cell activity with increasing doses of targeted drug conjugate (Fig. 2-12), as evidenced by both the decline in CAR T cell mediated lysis of CD19+ Raji cells in culture and the decrease in CAR T cell release of interferon gamma (INFγ).

2.3.4.3 Systemic Control of CAR T Cell Number and/or Activity Using Private Passageway Fusion Receptor

Next, to assess the ability of FITC-DM4 and FITC-FK506 for lowering the CAR T cell number and/or the cytokine levels in vivo, NSG mice were systemically inoculated with CD19 expressing Raji cells followed by an anti-CD19 FITC-FR CAR T cell treatment, in order to mimic the Cytokine Release Syndrome (CRS) in acute myeloid leukemia (AML) patients treated in clinics with CAR T cell therapy. Although no severe drop in body weight of the mice was observed, the CAR T cell number as well as the INFγ level from the peripheral blood were elevated significantly upon CAR T cell treatment (Fig. 2-13). The treatment of FITC-DM4 (one dose) dramatically lowered the CAR T cell number and INFγ as expected, in a dose dependent manner, and rescued the mice from overactivated CAR T cells over the course of 10 days after the dose of FITC-DM4 (Fig. 2-13 B). On the other hand, treatment of FITC-FK506 functioned more like a temporal suppressant rather than a termination of CAR T cell activity with a drop of the INFγ level that appeared around 2 h after dosing, but then gradually returned to normal in 24 h (Fig. 2-13 E).

2.4 Discussion

Despite the striking results from clinical trials using T cell based adoptive cell therapy (ACT), concerns about its safety still remain. Cytokine Release Syndrome (CRS), a common side effect in ACT for hematological malignancies, causes a large amount of cytokines to be produced and released, including factor-alpha (TNF-α), interleukin-6 (IL-6), interferon-γ (IFN-γ), etc. Clinical manifestations of CRS include fever, tachycardia, hypotension, and hypoxia, which can be fatal[46]. Moreover, Ruella Macro, et al. recently reported a "CAR B" cell case where the unintended incorporation of the CAR construct into a single leukemic B cell during CAR T cell manufacturing caused the masking of the antigen epitope, resulting in the relapse and final death of the patient[47]. In response to these fatal side effects of current CAR T cell therapy that mainly derive from overactivation and loss-of-control of the adoptive cells, many laboratories have designed suicide gene or ON/OFF switches as a safety switch to be incorporated into the classical CAR constructs. First, to kill the CAR T cells in case of carcinogenesis, a new suicide gene called inducible caspase 9 (iCas9)[48] was developed for better biocompatibility in humans compared to the classical herpes simplex virus thymidine kinase (HSV-tk) which is derived from a virus and may potentially cause immunological reactions[177]. The iCas9 is composed of the pro-apoptotic human caspase 9 protein and the human FK506 binding protein (FKBP). Treatment with the FK506 dimmer, AP1903, induces the dimerization of iCas9 and therefore initiates the intrinsic apoptotic pathway. Another method to eliminate CAR T cells is to express certain markers that can be recognized by clinically approved antibodies, such as a truncated epidermal growth factor receptor (EGFRt)/cetuximab[49] and CD20 mimotopes/rituximab[50]. CAR T cells can be killed similar to tumor cells that overexpress these markers through antibody dependent cell cytotoxicity (ADCC) and/or complement dependent cytotoxicity (CDC) mediated by specific antibodies. Secondly, many

types of small molecule gated ON/OFF switches have been developed. These approaches use small molecules/bispecific protein adaptors to work either as a dimmer inducer to bring together the split activation domains of the CAR construct[51] or as a bridge to control the formation of the immunological synapses between the tumor cell and the CAR T cell[52-54].

While each of the above suicide gene and ON/OFF switch strategies has its unique application, the use of the private passageway fusion receptor developed in this study may have advantages over these approaches. First, instead of modifying the CAR construct with new modules, which may require expression optimization and an immunogenicity test for each different construct, our fusion receptor is expressed independent of the CAR construct, making it possible to be incorporated easily into any CAR T cell design. Secondly, although many current engineering designs can either terminate or control the activity of the CAR T cell, the fusion receptor developed here is truly versatile and capable of exerting different functions. It uses the same cell design by chemically changing the payloads of the targeting ligand-payload conjugates. Thirdly, given the well-established list of immunosuppressant drugs used in clinics[55], targeted delivery of these drugs to the CAR T cell will increase the local drug concentration around the tumor tissue, thereby lowering the dose that is required and diminish the side effects in other immunological sites. It may also be possible to improve the pharmacokinetics of the parental drugs by modifying the structure of the linker and targeting ligands[56]. Finally, the advantages of small molecule drug conjugates over antibody drug conjugates (ADC) that may be used for the control of CAR T cells are also important. Low molecular weight ligand-payload conjugates such as FITC-DM1 (Mr~1200) have better penetration in solid tumors in human cancer patients, while antibody-drug conjugates have revealed significant areas of tumors that remain devoid of antibodies. In addition, a small molecule drug conjugate clears rapidly from receptor negative tissue, in this case, fusion

receptor negative cells, with half-lives around 90 min[57], while the half-lives of antibody-drug conjugates are on the order of days[58], resulting in a higher possibility for pre-mature release of the payload drug. Given the versatile nature of the fusion receptor platform proposed in this study, there are several potential applications of it that warrant further exploration (detailed in chapter 3.3). First, although an overactivation of CAR T cells is the major side effect in hematopoietic cancer treatment, the exhaustion of CAR T cells caused by continuous exposure to antigens and tumor suppressive microenvironments still stands as the biggest obstacle in solid tumor treatment[59-61]. To reprogram and rejuvenate these exhausted CAR T cells, certain immune-agonists and modulators can be specifically delivered through our fusion receptor system. Several potential payloads include TGFβ inhibitors[62-63], SHP1/2 inhibitors[64], DGK inhibitors[65-67], and GSK3b inhibitors, etc Secondly, encouraged by the success of the targeted delivery of microRNA to Folate Receptor alpha (FRα) positive cancer cells by FA-microRNA conjugates developed by the lab conducting the current study[68], it is envisioned that functional microRNAs may also be delivered to fusion receptor positive CAR T cells by linking them to the corresponding targeting ligands, such as FITC and FK506. The broad spectrum of possible payload types, including small molecule, peptides and mRNA, will greatly expand the list of potential signaling pathways and target proteins that can be targeted to modulate CAR T activity[69]. Thirdly, in addition to be used as a platform for drug delivery, the fusion receptor developed in this study can be readily used as a tag for positive T cell selection during the manufacture process of CAR T cells as well as in vivo noninvasive CAR T cell tracking, which is of great interest in clinics[70]. Finally, as mentioned in the introduction, no obvious reasons would prevent the receptor platform presented here from being applied in other adoptive cell therapies, such as stem cell-based therapies. Thus, this platform will not only provide a safety switch, but also exist as a doorway for the delivery of instructions for directed differentiation of implanted stem cells[71].

Although the current design of our fusion receptor is functional, there are optimizations and characterizations of each module that can be explored in the near future. First, several candidate substitutions can be tested for each moiety in the fusion receptor, e.g. anti-DNP scFv and DNP[72] for the ligand binding domain and targeting ligand, other membrane bound proteins, either GPI anchored or transmembrane proteins for the anchor domain; and the type and length of peptide linkers between the two domains. Secondly, although we selected human proteins or humanized scFv for composition of the fusion receptors, there is still a possibility that the whole protein could be immunogenetic. Therefore, detailed MHC prediction and antigen presentation tests need to be done for the fusion receptor design before it is utilized in human patients.

With the recent advances in methods for CRISPR based universal CAR T cells, the standard production of "off-the-shelf" CAR T seems increasingly achievable[73]. Thus, it will be ideal to have private passageway fusion receptors to be incorporated into the design of these universal CAR T cells as a doorway for any instructions that may be needed after they are infused into patients.

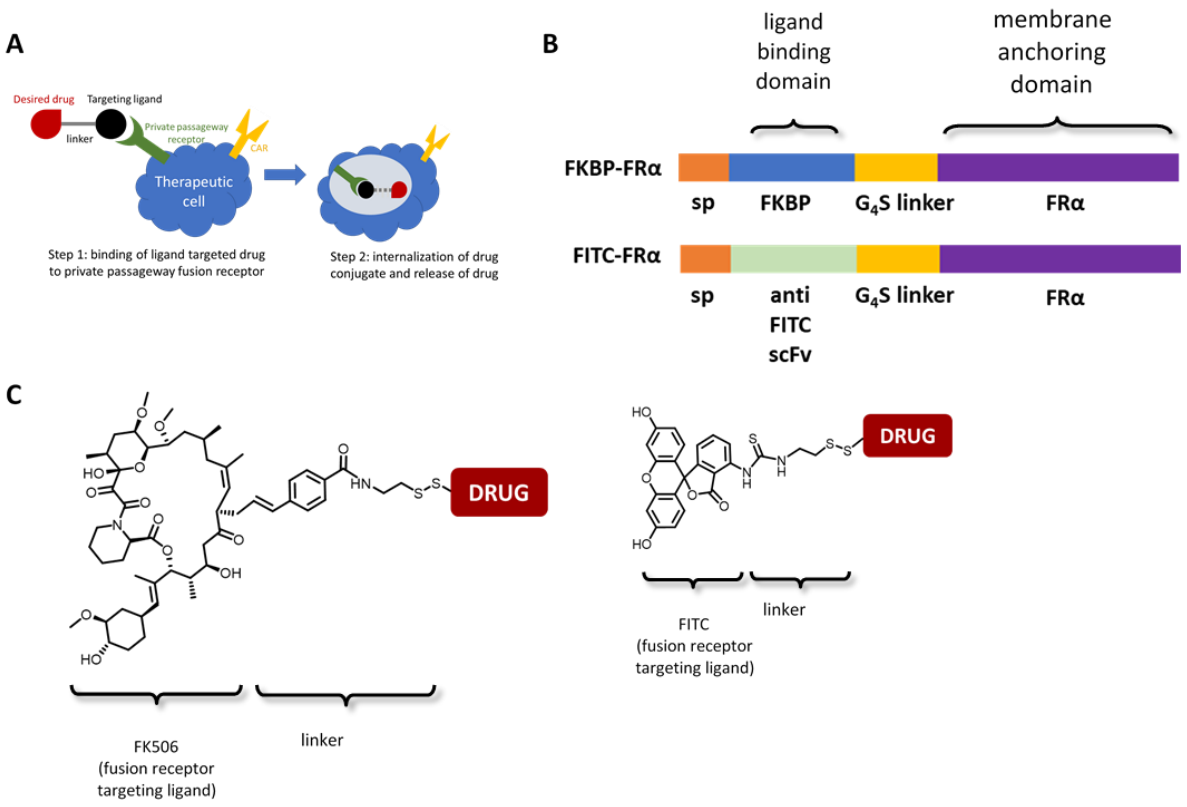

Figure 2-1 Design of FKBP-FR and FITC-FR fusion receptors and corresponding targeting ligands. (A) Diagram to show the working mechanism of the private passageway fusion receptor in CAR T cell therapy. (B) Schematic of FKBP-FR and FITC-FR fusion receptors construct designs, from N to C terminal. (C) Chemical structure of FK506 or FITC linked conjugates showing the derivatization sites. Abbreviation: sp: signal peptide, here refers to human folate receptor alpha (FRα) signal peptide; scFv: short chain variable fragment; G_4S: GGGGS; FITC: fluorescein

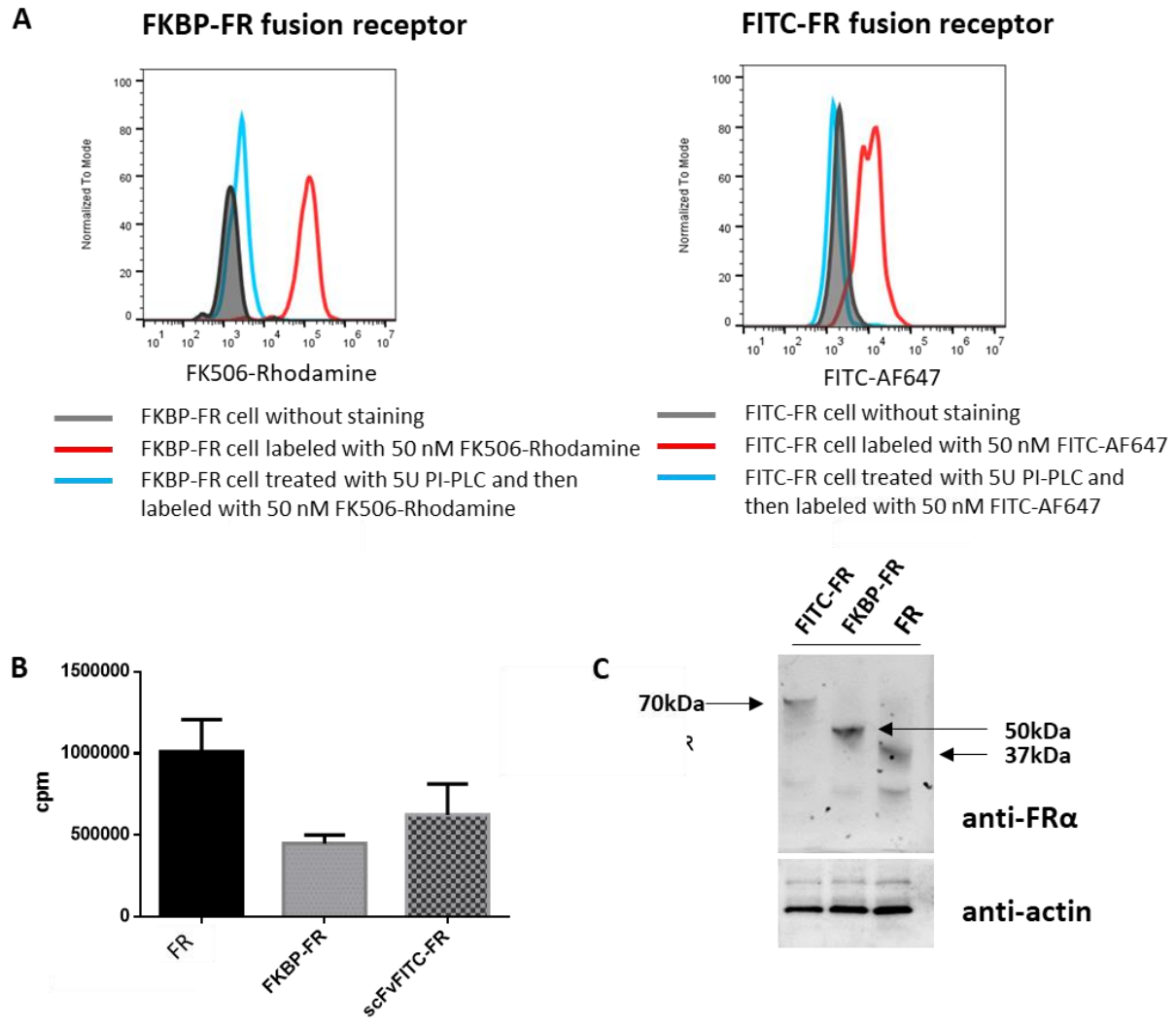

Figure 2-2 Stable expression and localization of FKBP-FR and FITC-FR fusion receptor to the cell surface.
(A) Left, 10 nM FK506-Rhodamine binds to the FKBP-FR fusion receptor and result in a fluorescent shift (red line) compare to non-staining control sample (grey shaded), while Phosphoinositide Phospholipase C (PI-PLC) treatment (blue line) abolished this binding. Right, similar results with FITC-AlexFluor 647. (B) The relative expression level of fusion receptors on Jurkat cells compare to FRα on KB cells (dark: FRα in KB cell, grey: FKBP-FR in Jurkat, patterned: FITC-FR in Jurkat). Bar graphs represent mean ± s.d. n = 3. Data shown are the represent data from two independent experiments. (C) Western blot of FKBP-FR and FITC-FR detected by FRα antibody.

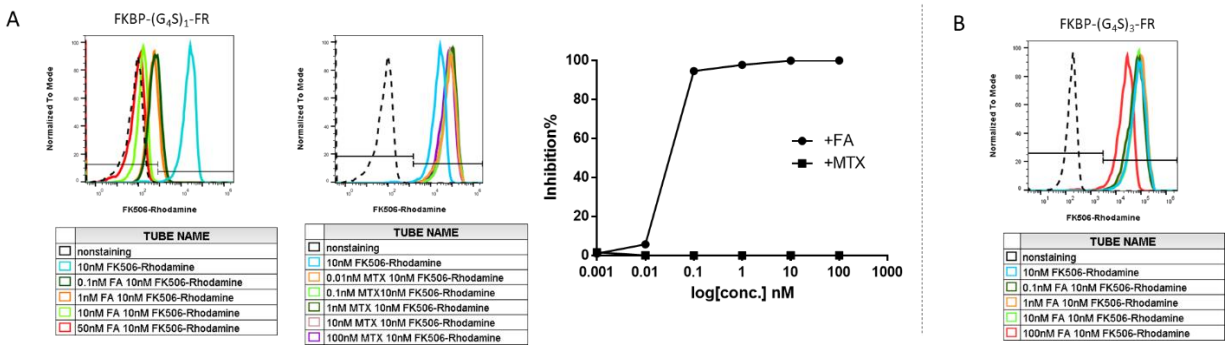

Figure 2-3 Structural interference between FR and FKBP in FKBP-FR fusion receptor.
(A) Inhibition of FK506-Rhodamine binding to FKBP by different concentration of Folic Acid (FA) in FKBP-$(G_4S)_1$-FR fusion receptor (left) while no effect is observed when Methotrexate (MTX) is used (middle). Inhibition percentage by FA and MTX quantified by Mean Fluorescent Intensity (MFI) shift (right). (B) the inhibition of FK506-Rhodamine binding to FKBP by FA is abolished in FKBP-$(G_4S)_3$-FR.

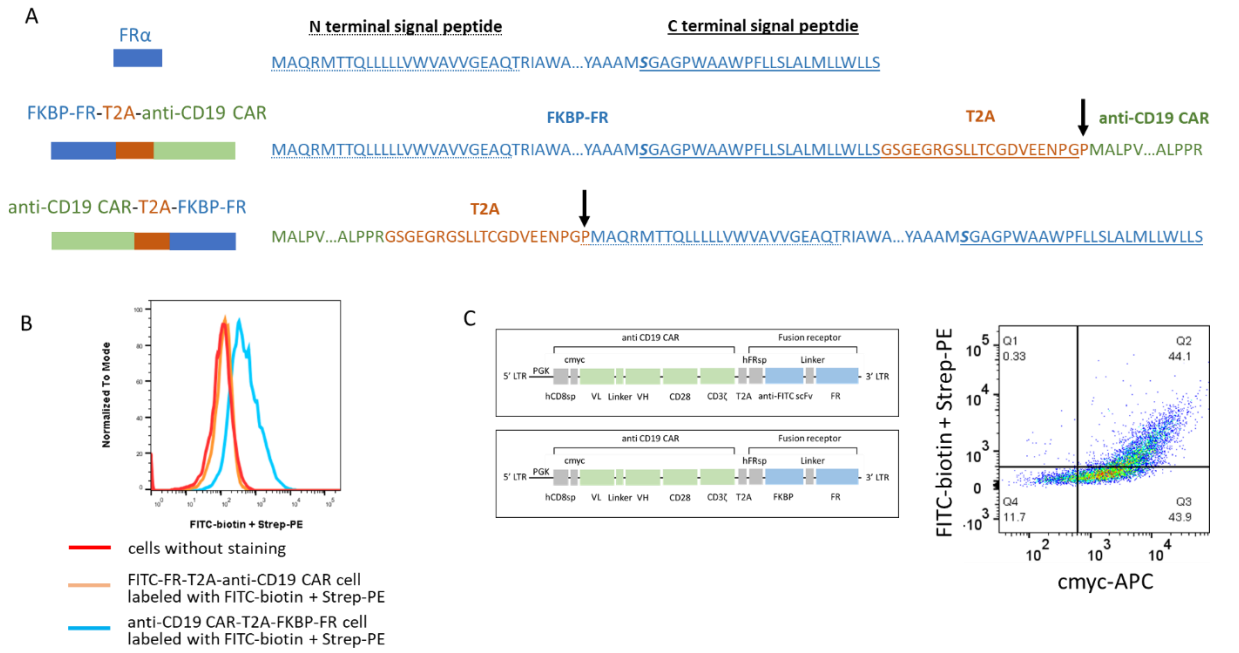

Figure 2-4 Optimization of co-expression of fusion receptor and anti-CD19 CAR using a T2A self-cleavage linker in between.

(A) Design of two versions of FKBP-FR-T2A-anti-CD19 CAR construct. Top, FRα (blue colored) with N terminal signal peptide (dot line) and C terminal signal peptide (solid line) of GPI anchor protein underlined. The potential GPI anchoring site Ser is in bold and Italic. Middle, version 1: FKBP-FR fusion receptor (blue colored) is positioned before T2A (red colored), followed by anti-CD19 CAR (green colored). Cutting site of T2A peptide between Gly and Pro is indicated by the arrow, potential C terminal signal peptide of the new GPI anchoring protein (FKBP-FR-part of T2A) is underlined (solid line). Bottom, version 2: the position of FKBP-FR and anti-CD19 CAR is switched regard to T2A with FKBP-FR fusion receptor locates after T2A. (B) Staining of FITC-FR co-expressed with anti-CD19 CAR in both versions by FITC-biotin + Strep-PE. Version 1 (yellow line) does not show positive staining compare to negative control, indicates potential failure of GPI anchoring, while version 2 (blue line) shows clear shift. (C) Left, final construct of FITC-FR-T2A-anti-CD19 and FKBP-FR-T2A-anti-CD19; Right, double staining of FITC-FR by FITC-biotin + Strep-PE and anti-CD19 by cmyc-APC. Abbreviation: hCD8sp, signal peptide of human CD8; VL, variable light chain; VH, variable heavy chain; hFRsp, signal peptide of human FRα.

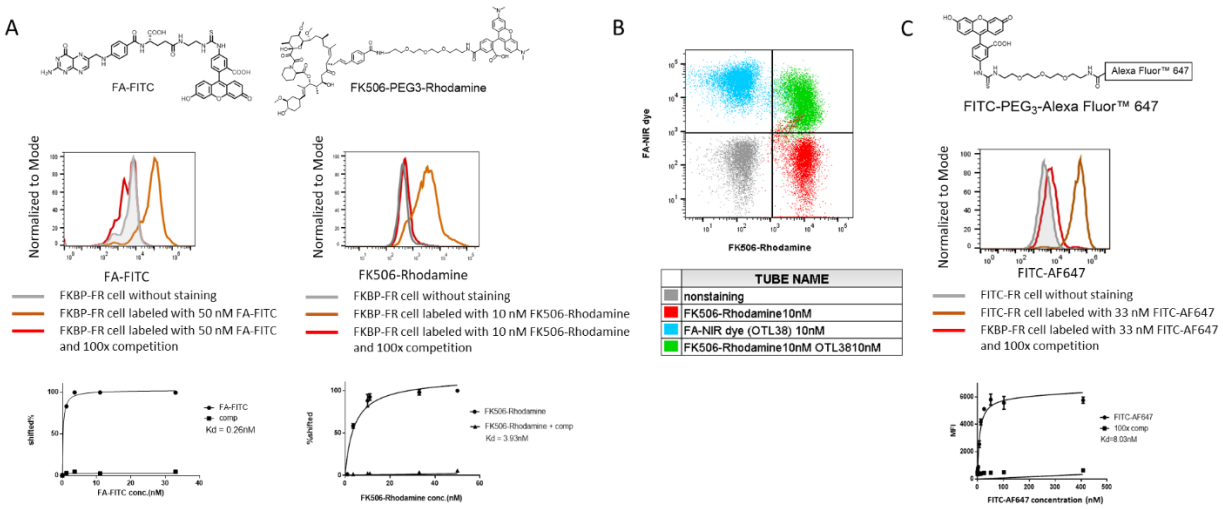

Figure 2-5 Private passageway fusion receptors preserve good binding affinity for the corresponding targeting ligands property.
(A) Evaluation of binding affinity of FA-FITC (left) and FK506-Rhodamine (right) for FKBP-FR fusion receptor. (B) Double staining of FA-NIR dye (OTL38) and FK506-Rhodamine for FKBP-FR fusion receptor. (C) Evaluation of binding affinity of FITC-AlexFluor 647 for FITC-FR fusion receptor (left);

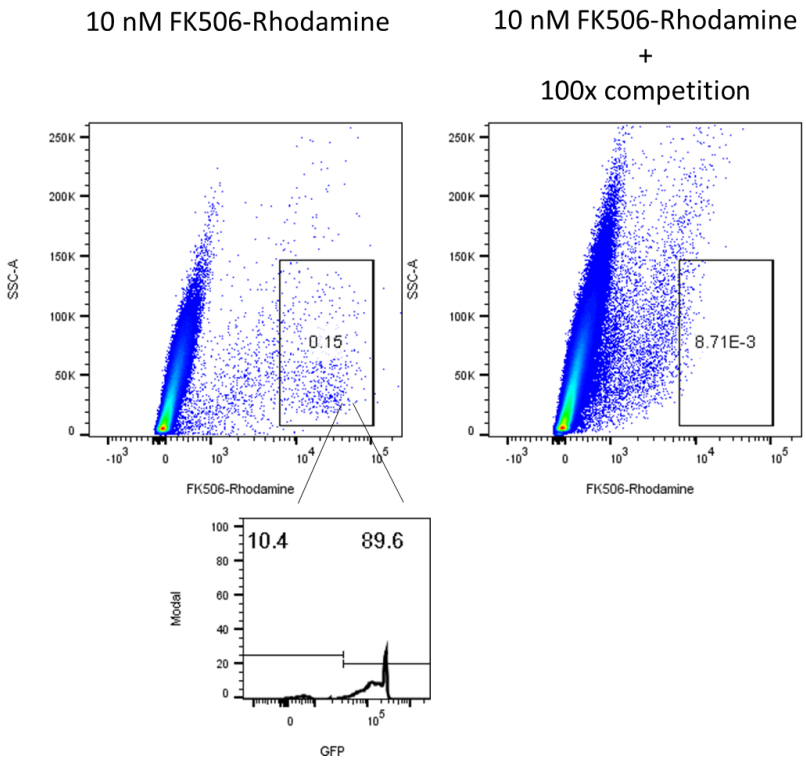

Figure 2-6 Preservation and specificity of the binding of FK506-Rhodmaine to FKBP-FR fusion receptor in whole blood.
FKBP-FR fusion receptor positive Jurkat cells (GFP positive) were spiked into whole human blood and incubated with 10 nM FK506-Rhodamine for 30min in the absence (left) or presence (right) of 100-fold competition. Insert: 90% of the FK506-Rhodamine positive population are GFP positive Jurkat cells.

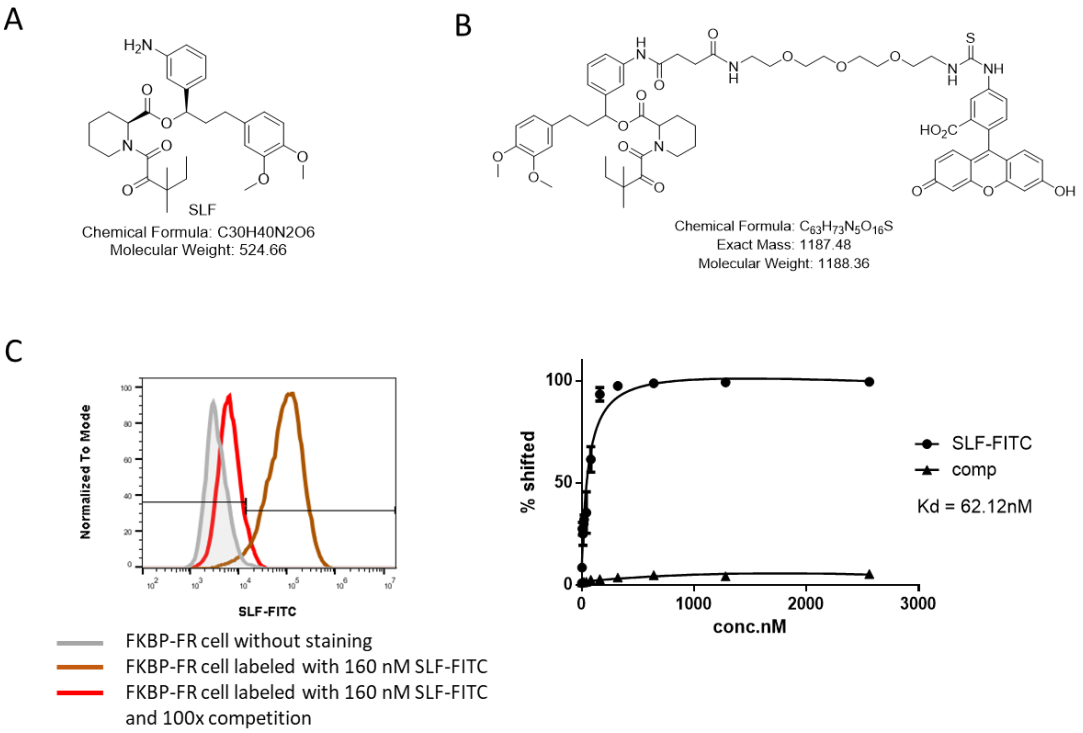

Figure 2-7 Structure and binding affinity of SLF-FITC for FKBP-FR fusion receptor.
(A) Chemical structure and MW of SLF, a FK506 analog. (B) Chemical structure and MW of SLF-FITC. (C) Binding affinity of SLF-FITC against FKBP-FR fusion receptor tested in a cell-based assay. Left, a representative flow cytometry data of FKBP-FR cells labeled with 160 nM SLF-FITC; Right, binding curve of SLF-FITC.

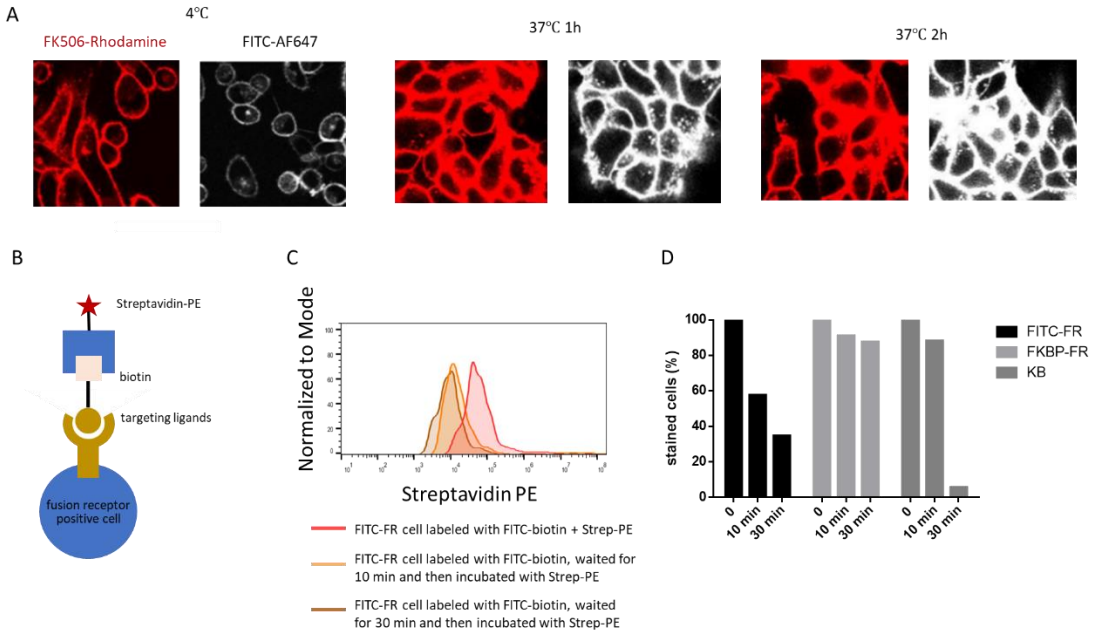

Figure 2-8 Evaluation and Quantification of FITC-FR and FKPB-FR fusion receptors internalization.

(A) Internalization of FKBP-FR or FITC-FR fusion receptors in HEK293 detected by FK506-Rhodamine or FITC-AF647 cells, respectively, using confocal microscopy at 4 ℃ and 37 ℃. (B) Diagram of indirect labeling of fusion receptors (FITC-FR, FKBP-FR) by sequential incubation of targeting ligand-biotin (FITC-biotin, FK506-biotin) followed by Streptavidin-PE. (C) Representative flow cytometry data of FITC-FR internalization detected by FITC-biotin and Streptavidin PE. Around half of the FITC-FR fusion receptor/FITC-biotin complexes on the cell surface were internalized and excluded from the cell membrane after 10 min incubation, shown as the loss of PE signal upon Strep-PE staining. (D) Quantification of internalization rate of both FITC-FR and FKBP-FR fusion receptors by the percentage of population shift over PE intensity at 0 min. FRα on KB cells and FA-biotin conjugate are used as a positive control.

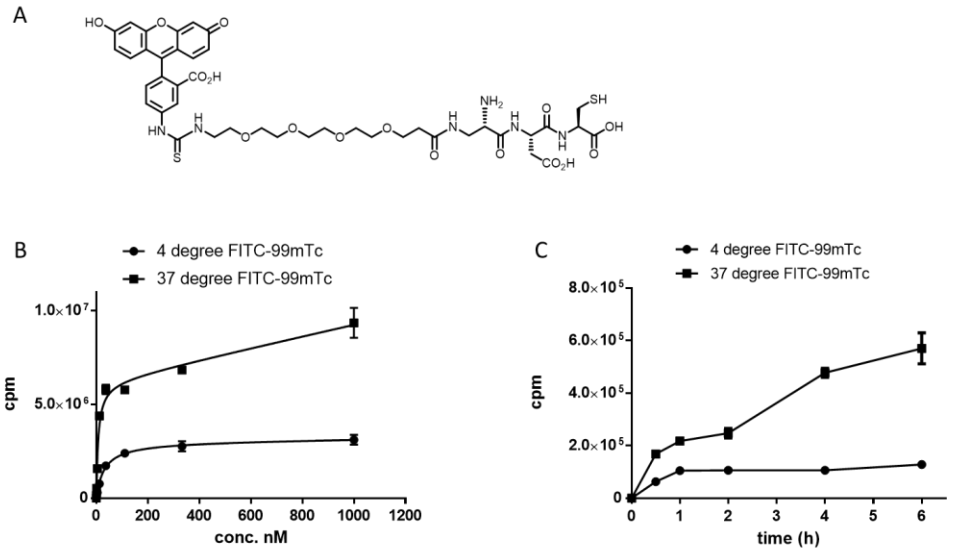

Figure 2-9 Quantification of FITC-FR fusion receptor internalization by FITC-^{99m}Tc.
(A) Chemical structure of FITC-EC20 head. (B) Cell binding and accumulation of FITC-^{99m}Tc in FITC-FR cells. FITC-FR cells were incubated with increasing concentration of FITC-^{99m}Tc under 4 ℃ and 37 ℃, and then radioactivity was determined by gamma counter. Both groups showed exponent increase of ligand binding below 50nM, radiotracer intensity of cells incubated at 4 ℃ become plateau after that while cells incubated at 37 ℃ continue to increase due to more internalization. (C) FITC-FR cells were incubated with FITC-^{99m}Tc at 50 nM under 4 ℃ and 37 ℃ for the times indicated, and then radioactivity was determined by gamma counter, radiotracer intensity increase fast for both groups within 30min, after that radiotracer intensity become plateau for cells at 4 ℃, while continues to increase for cells at 37 ℃ due to increased internalization. Graphs represent mean ± s.d. n = 3. Data shown are the represent data from two independent experiments.

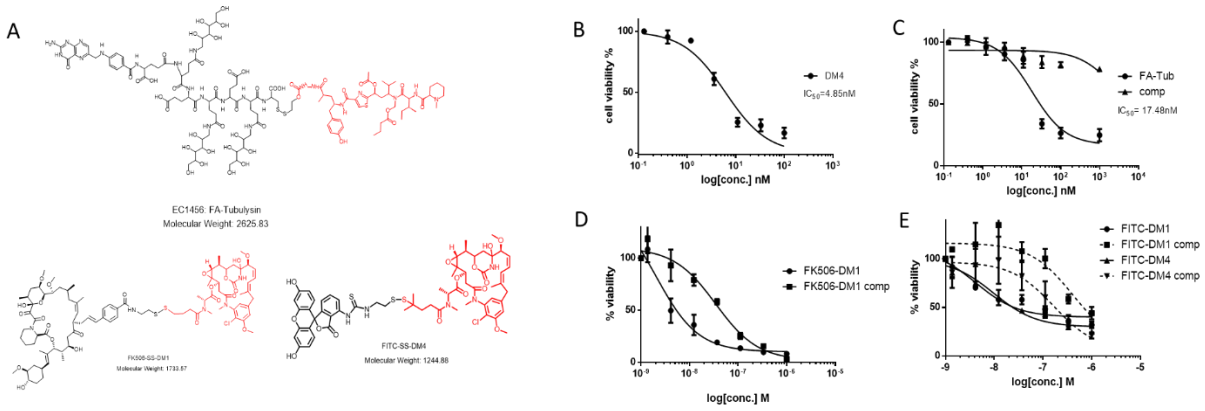

Figure 2-10 Effect of FITC-cytotoxic payload on FITC-FR positive human T cells.
(A) Chemical Structure of FA-Tubulysin, FK506-DM1 and FITC-DM4 with disulfide bond releasable linker. (B) human T cells were incubated with different concentrations of DM4 free drugs. (C-D) FKBP-FR human T cells were incubated with different concentration of FA-Tubulysin (C) or FK506-DM1 (D). (E) FITC-FR human T cells were incubated with different concentrations of FITC-DM1 or FITC-DM4 in the absence or presence of 100-fold competition. Conjugates were incubated for 2 h, washed away and continued culture for 72 h before viability was measured by LDH assay. Graphs represent mean ± s.d. n = 3. Data shown are the represent data from two independent experiments.

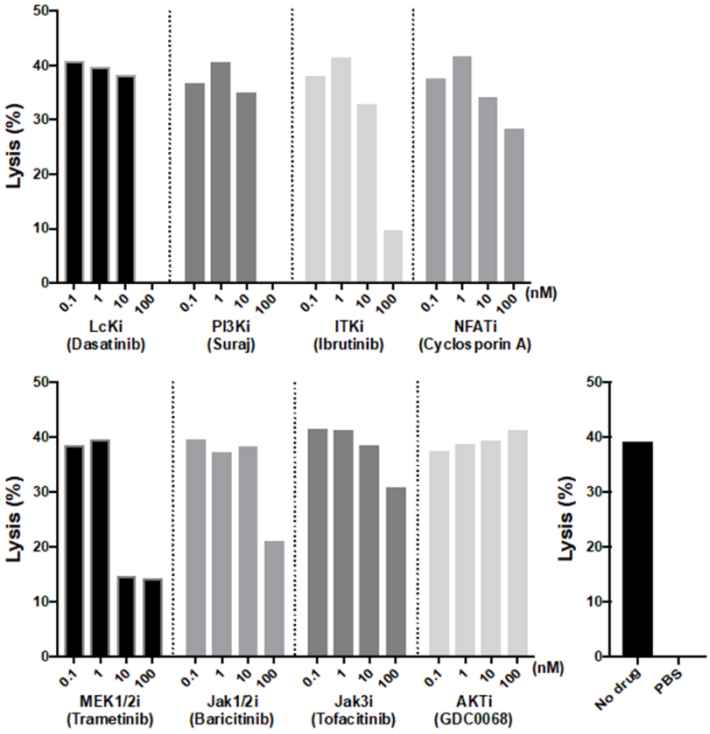

Figure 2-11 Screening of potential payloads for inhibition of CAR T cell lysis effect.

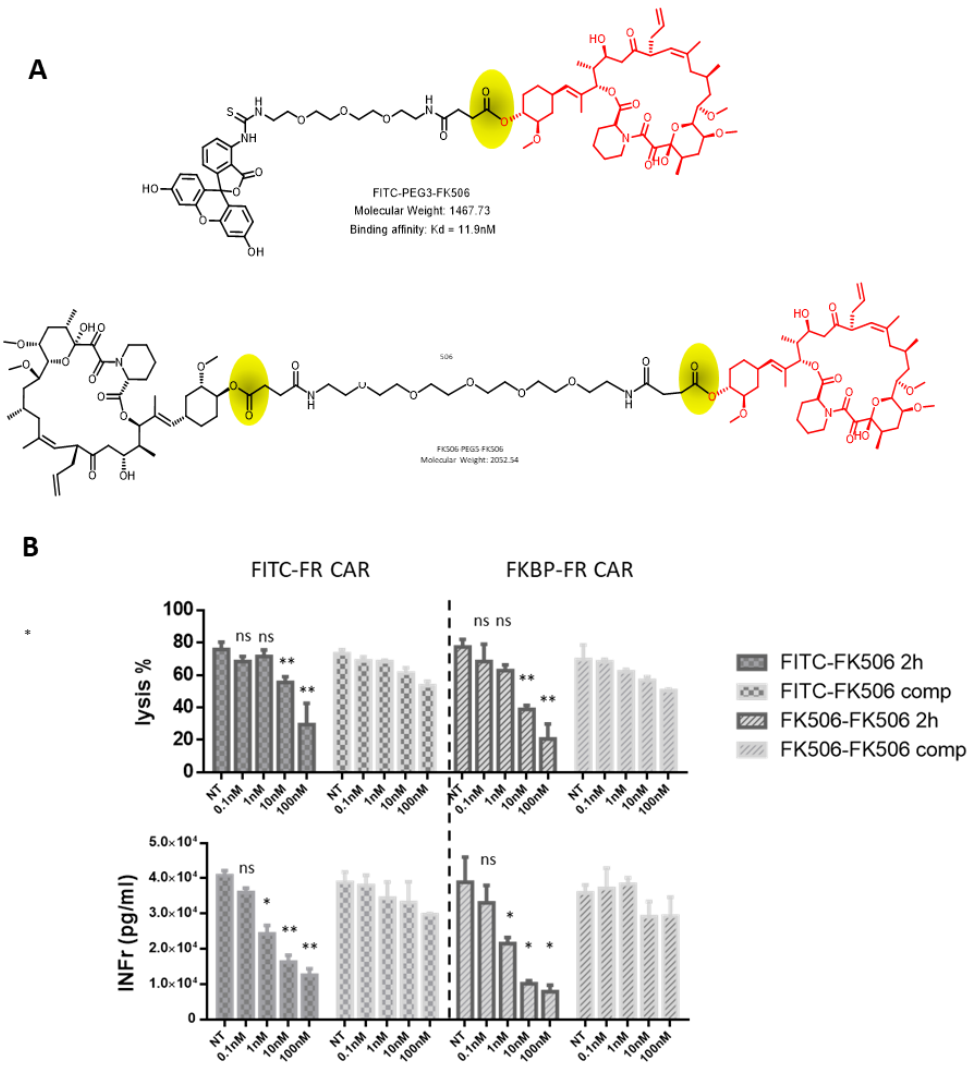

Figure 2-12: Effect of targeting ligand-immunosuppressant conjugates on fusion receptor positive anti-CD19 CAR T cells.
(A) Structure of FITC-PEG3-FK506 and FK506-PEG5-FK506. (B) FITC-FR or FKBP-FR anti-CD19 CAR T cells were incubated with different concentrations of FITC-FK506 or FK506-FK506, respectively, in the absence or presence of 100-fold FITC-Glucosamine or FK506-linker as competition. Conjugates were incubated for 2 h, washed away and continued culture for 12 h before lysis effect and INFγ level were measured as described in Method. Bar graphs represent mean ± s.d. n = 3. Data shown are the represent data from two independent experiments. * denotes a p-value < 0.05, ** < 0.01, ns = not significant.

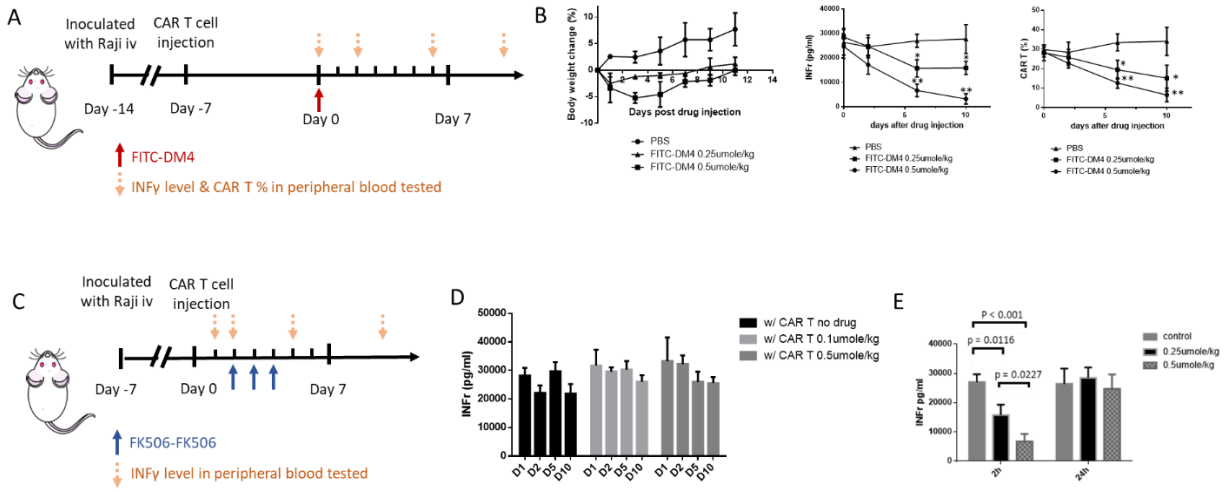

Figure 2-13 FITC-DM4 and FITC-FK506 alleviate the CRS by decreasing CAR T cell number and/or cytokine release level in mice bearing Raji tumor cell.
(A) NSG mice were inoculated with $2x10^6$ Raji cells intravenously and treated with $1x10^7$ anti-CD19 CAR T or anti-CD19 FITC-FR CAR T cells at days 7, FITC-DM4 (0.25 μmole/kg or 0.5 μmole/kg) was dosed for anti-CD19 FITC-FR CAR T group at days 14. (B) Left, Body weight change was monitored for each group after drug dosing. Middle and right, INFγ level and CAR T number before (zero point) and after FITC-DM4 along treatment. (C) Similar Raji tumor model with FITC-FK506 dosed 2 days after CAR T injection. (D) INFγ level at 2 h and 24 h after treatment of FITC-FK506. n = 5 mice per group. All data represent mean ± s.e.m. Data shown are the represent data from two independent experiments. * denotes a p-value < 0.05, ** < 0.01, ns = not significant.

2.5 References

1. Luhrs, C.; Slomiany, B. L., A human membrane-associated folate binding protein is anchored by a glycosyl-phosphatidylinositol tail. *Journal of Biological Chemistry* **1989,** *264* (36), 21446-21449.

2. Leamon, C. P.; Parker, M. A.; Vlahov, I. R.; Xu, L. C.; Reddy, J. A.; Vetzel, M.; Douglas, N., Synthesis and biological evaluation of EC20: a new folate-derived, (99m)Tc-based radiopharmaceutical. *Bioconjugate chemistry* **2002,** *13* (6), 1200-10.

3. Kozany, C.; Marz, A.; Kress, C.; Hausch, F., Fluorescent probes to characterise FK506-binding proteins. *Chembiochem : a European journal of chemical biology* **2009,** *10* (8), 1402-10.

4. Midelfort, K. S.; Hernandez, H. H.; Lippow, S. M.; Tidor, B.; Drennan, C. L.; Wittrup, K. D., Substantial energetic improvement with minimal structural perturbation in a high affinity mutant antibody. *Journal of molecular biology* **2004,** *343* (3), 685-701.

5. Dunyak, B. M.; Gestwicki, J. E., Peptidyl-Proline Isomerases (PPIases): Targets for Natural Products and Natural Product-Inspired Compounds. *Journal of medicinal chemistry* **2016,** *59* (21), 9622-9644.

6. Clemons, P. A.; Gladstone, B. G.; Seth, A.; Chao, E. D.; Foley, M. A.; Schreiber, S. L., Synthesis of calcineurin-resistant derivatives of FK506 and selection of compensatory receptors. *Chemistry & biology* **2002,** *9* (1), 49-61.

7. Wilson, K. P.; Yamashita, M. M.; Sintchak, M. D.; Rotstein, S. H.; Murcko, M. A.; Boger, J.; Thomson, J. A.; Fitzgibbon, M. J.; Black, J. R.; Navia, M. A., Comparative X-ray structures of the major binding protein for the immunosuppressant FK506 (tacrolimus) in unliganded form and in complex with FK506 and rapamycin. *Acta crystallographica. Section D, Biological crystallography* **1995,** *51* (Pt 4), 511-21.

8. Clackson, T.; Yang, W.; Rozamus, L. W.; Hatada, M.; Amara, J. F.; Rollins, C. T.; Stevenson, L. F.; Magari, S. R.; Wood, S. A.; Courage, N. L.; Lu, X.; Cerasoli, F., Jr.; Gilman, M.; Holt, D. A., Redesigning an FKBP-ligand interface to generate chemical dimerizers with novel specificity. *Proceedings of the National Academy of Sciences of the United States of America* **1998,** *95* (18), 10437-42.

9. Feng, X.; Sippel, C.; Bracher, A.; Hausch, F., Structure-Affinity Relationship Analysis of Selective FKBP51 Ligands. *Journal of medicinal chemistry* **2015,** *58* (19), 7796-806.

10. Swaminathan, A.; Lucas, R. M.; Dear, K.; McMichael, A. J., Keyhole limpet haemocyanin - a model antigen for human immunotoxicological studies. *Br J Clin Pharmacol* **2014,** *78* (5), 1135-42.

11. Predina, J. D.; Newton, A. D.; Keating, J.; Dunbar, A.; Connolly, C.; Baldassari, M.; Mizelle, J.; Xia, L.; Deshpande, C.; Kucharczuk, J.; Low, P. S.; Singhal, S., A Phase I Clinical Trial of Targeted Intraoperative Molecular Imaging for Pulmonary Adenocarcinomas. *Ann Thorac Surg* **2018,** *105* (3), 901-908.

12. Lu, Y.; Xu, L. C.; Parker, N.; Westrick, E.; Reddy, J. A.; Vetzel, M.; Low, P. S.; Leamon, C. P., Preclinical pharmacokinetics, tissue distribution, and antitumor activity of a folate-hapten conjugate-targeted immunotherapy in hapten-immunized mice. *Molecular cancer therapeutics* **2006,** *5* (12), 3258-67.

13. Bandara, N. A.; Hansen, M. J.; Low, P. S., Effect of receptor occupancy on folate receptor internalization. *Molecular pharmaceutics* **2014,** *11* (3), 1007-13.

14. Saha, S.; Anilkumar, A. A.; Mayor, S., GPI-anchored protein organization and dynamics at the cell surface. *Journal of lipid research* **2016,** *57* (2), 159-75.

15. Rijnboutt, S.; Jansen, G.; Posthuma, G.; Hynes, J. B.; Schornagel, J. H.; Strous, G. J., Endocytosis of GPI-linked membrane folate receptor-alpha. *The Journal of cell biology* **1996,** *132* (1-2), 35-47.

16. Yang, J.; Chen, H.; Vlahov, I. R.; Cheng, J. X.; Low, P. S., Evaluation of disulfide reduction during receptor-mediated endocytosis by using FRET imaging. *Proceedings of the National Academy of Sciences of the United States of America* **2006,** *103* (37), 13872-7.

17. Zimmermann, R.; Eyrisch, S.; Ahmad, M.; Helms, V., Protein translocation across the ER membrane. *Biochimica et biophysica acta* **2011,** *1808* (3), 912-24.

18. Galian, C.; Bjorkholm, P.; Bulleid, N.; von Heijne, G., Efficient glycosylphosphatidylinositol (GPI) modification of membrane proteins requires a C-terminal anchoring signal of marginal hydrophobicity. *The Journal of biological chemistry* **2012,** *287* (20), 16399-409.

19. Luhrs, C. A.; Slomiany, B. L., A human membrane-associated folate binding protein is anchored by a glycosyl-phosphatidylinositol tail. *The Journal of biological chemistry* **1989,** *264* (36), 21446-9.

20. Mortara, R. A.; Minelli, L. M.; Vandekerckhove, F.; Nussenzweig, V.; Ramalho-Pinto, F. J., Phosphatidylinositol-specific phospholipase C (PI-PLC) cleavage of GPI-anchored surface molecules of Trypanosoma cruzi triggers in vitro morphological reorganization of trypomastigotes. *The Journal of eukaryotic microbiology* **2001,** *48* (1), 27-37.

21. Wibowo, A. S.; Singh, M.; Reeder, K. M.; Carter, J. J.; Kovach, A. R.; Meng, W.; Ratnam, M.; Zhang, F.; Dann, C. E., 3rd, Structures of human folate receptors reveal biological trafficking states and diversity in folate and antifolate recognition. *Proceedings of the National Academy of Sciences of the United States of America* **2013,** *110* (38), 15180-8.

22. Liu, Z.; Chen, O.; Wall, J. B. J.; Zheng, M.; Zhou, Y.; Wang, L.; Ruth Vaseghi, H.; Qian, L.; Liu, J., Systematic comparison of 2A peptides for cloning multi-genes in a polycistronic vector. *Scientific reports* **2017,** *7* (1), 2193.

23. Jones, S.; Peng, P. D.; Yang, S.; Hsu, C.; Cohen, C. J.; Zhao, Y.; Abad, J.; Zheng, Z.; Rosenberg, S. A.; Morgan, R. A., Lentiviral vector design for optimal T cell receptor gene expression in the transduction of peripheral blood lymphocytes and tumor-infiltrating lymphocytes. *Human gene therapy* **2009,** *20* (6), 630-40.

24. Lentivirus Fact Sheet.

25. Kim, T. K.; Eberwine, J. H., Mammalian cell transfection: the present and the future. *Analytical and bioanalytical chemistry* **2010,** *397* (8), 3173-8.

26. Gaire, J.; Lee, H. C.; Ward, R.; Currlin, S.; Woolley, A. J.; Coleman, J. E.; Williams, J. C.; Otto, K. J., PrismPlus: a mouse line expressing distinct fluorophores in four different brain cell types. *Scientific reports* **2018,** *8* (1), 7182.

27. Morrissey, M. A.; Williamson, A. P.; Steinbach, A. M.; Roberts, E. W.; Kern, N.; Headley, M. B.; Vale, R. D., Chimeric antigen receptors that trigger phagocytosis. *Elife* **2018,** *7*.

28. Brogdon, J.; Ebersbach, H. E.; Glass, D.; Huber, T.; Jascur, J.; June, C. H.; Lee, J.; Mannick, J.; Milone, M. C.; Murphy, L., Phosphoglycerate kinase 1 (pgk) promoters and methods of use for expressing chimeric antigen receptor. Google Patents: 2018.

29. Low, P. S.; Henne, W. A.; Doorneweerd, D. D., Discovery and development of folic-acid-based receptor targeting for imaging and therapy of cancer and inflammatory diseases. *Acc Chem Res* **2008,** *41* (1), 120-9.

30. Srinivasarao, M.; Low, P. S., Ligand-Targeted Drug Delivery. *Chemical reviews* **2017,** *117* (19), 12133-12164.

31. Marinec, P. S.; Chen, L.; Barr, K. J.; Mutz, M. W.; Crabtree, G. R.; Gestwicki, J. E., FK506-binding protein (FKBP) partitions a modified HIV protease inhibitor into blood cells and prolongs its lifetime in vivo. *Proceedings of the National Academy of Sciences of the United States of America* **2009,** *106* (5), 1336-41.

32. Paulos, C. M.; Turk, M. J.; Breur, G. J.; Low, P. S., Folate receptor-mediated targeting of therapeutic and imaging agents to activated macrophages in rheumatoid arthritis. *Adv Drug Deliv Rev* **2004,** *56* (8), 1205-17.

33. Chen, H.; Lin, Z.; Arnst, K. E.; Miller, D. D.; Li, W., Tubulin Inhibitor-Based Antibody-Drug Conjugates for Cancer Therapy. *Molecules* **2017,** *22* (8).

34. Schade, A. E.; Schieven, G. L.; Townsend, R.; Jankowska, A. M.; Susulic, V.; Zhang, R.; Szpurka, H.; Maciejewski, J. P., Dasatinib, a small-molecule protein tyrosine kinase inhibitor, inhibits T-cell activation and proliferation. *Blood* **2008,** *111* (3), 1366-77.

35. Weber, E. W.; Lynn, R. C.; Sotillo, E.; Lattin, J.; Xu, P.; Mackall, C. L., Pharmacologic control of CAR-T cell function using dasatinib. *Blood advances* **2019,** *3* (5), 711.

36. Dasatinib: dosing/administration. **2018,** *In: Micromedex (lane.stanford.edu) [electronic version]* (Ann Arbor, MI: Truven Health Analytics.), http://www.micromedexsolutions.com.

37. Delgoffe, G. M.; Kole, T. P.; Zheng, Y.; Zarek, P. E.; Matthews, K. L.; Xiao, B.; Worley, P. F.; Kozma, S. C.; Powell, J. D., The mTOR kinase differentially regulates effector and regulatory T cell lineage commitment. *Immunity* **2009,** *30* (6), 832-44.

38. Strauss, L.; Whiteside, T. L.; Knights, A.; Bergmann, C.; Knuth, A.; Zippelius, A., Selective survival of naturally occurring human CD4+CD25+Foxp3+ regulatory T cells cultured with rapamycin. *Journal of immunology* **2007,** *178* (1), 320-9.

39. Ardeshna, K. M.; Pizzey, A. R.; Devereux, S.; Khwaja, A., The PI3 kinase, p38 SAP kinase, and NF-kappaB signal transduction pathways are involved in the survival and maturation of lipopolysaccharide-stimulated human monocyte-derived dendritic cells. *Blood* **2000,** *96* (3), 1039-46.

40. Williams, D. L.; Li, C.; Ha, T.; Ozment-Skelton, T.; Kalbfleisch, J. H.; Preiszner, J.; Brooks, L.; Breuel, K.; Schweitzer, J. B., Modulation of the phosphoinositide 3-kinase pathway alters innate resistance to polymicrobial sepsis. *Journal of immunology* **2004,** *172* (1), 449-56.

41. Long, M.; Beckwith, K.; Do, P.; Mundy, B. L.; Gordon, A.; Lehman, A. M.; Maddocks, K. J.; Cheney, C.; Jones, J. A.; Flynn, J. M.; Andritsos, L. A.; Awan, F.; Fraietta, J. A.; June, C. H.; Maus, M. V.; Woyach, J. A.; Caligiuri, M. A.; Johnson, A. J.; Muthusamy, N.; Byrd, J. C., Ibrutinib treatment improves T cell number and function in CLL patients. *The Journal of clinical investigation* **2017,** *127* (8), 3052-3064.

42. Fraietta, J. A.; Beckwith, K. A.; Patel, P. R.; Ruella, M.; Zheng, Z.; Barrett, D. M.; Lacey, S. F.; Melenhorst, J. J.; McGettigan, S. E.; Cook, D. R.; Zhang, C.; Xu, J.; Do, P.; Hulitt, J.; Kudchodkar, S. B.; Cogdill, A. P.; Gill, S.; Porter, D. L.; Woyach, J. A.; Long, M.; Johnson, A. J.; Maddocks, K.; Muthusamy, N.; Levine, B. L.; June, C. H.; Byrd, J. C.; Maus, M. V., Ibrutinib enhances chimeric antigen receptor T-cell engraftment and efficacy in leukemia. *Blood* **2016,** *127* (9), 1117-27.

43. Ebert, P. J. R.; Cheung, J.; Yang, Y.; McNamara, E.; Hong, R.; Moskalenko, M.; Gould, S. E.; Maecker, H.; Irving, B. A.; Kim, J. M.; Belvin, M.; Mellman, I., MAP Kinase Inhibition Promotes T Cell and Anti-tumor Activity in Combination with PD-L1 Checkpoint Blockade. *Immunity* **2016,** *44* (3), 609-621.

44. Winthrop, K. L., The emerging safety profile of JAK inhibitors in rheumatic disease. *Nat Rev Rheumatol* **2017,** *13* (4), 234-243.

45. Minguillon, J.; Morancho, B.; Kim, S. J.; Lopez-Botet, M.; Aramburu, J., Concentrations of cyclosporin A and FK506 that inhibit IL-2 induction in human T cells do not affect TGF-beta1 biosynthesis, whereas higher doses of cyclosporin A trigger apoptosis and release of preformed TGF-beta1. *Journal of leukocyte biology* **2005,** *77* (5), 748-58.

46. Porter, D.; Frey, N.; Wood, P. A.; Weng, Y.; Grupp, S. A., Grading of cytokine release syndrome associated with the CAR T cell therapy tisagenlecleucel. *Journal of hematology & oncology* **2018,** *11* (1), 35.

47. Ruella, M.; Xu, J.; Barrett, D. M.; Fraietta, J. A.; Reich, T. J.; Ambrose, D. E.; Klichinsky, M.; Shestova, O.; Patel, P. R.; Kulikovskaya, I., Induction of resistance to chimeric antigen receptor T cell therapy by transduction of a single leukemic B cell. *Nature medicine* **2018,** *24* (10), 1499.

48. Straathof, K. C.; Pule, M. A.; Yotnda, P.; Dotti, G.; Vanin, E. F.; Brenner, M. K.; Heslop, H. E.; Spencer, D. M.; Rooney, C. M., An inducible caspase 9 safety switch for T-cell therapy. *Blood* **2005,** *105* (11), 4247-54.

49. Paszkiewicz, P. J.; Frassle, S. P.; Srivastava, S.; Sommermeyer, D.; Hudecek, M.; Drexler, I.; Sadelain, M.; Liu, L.; Jensen, M. C.; Riddell, S. R.; Busch, D. H., Targeted antibody-mediated depletion of murine CD19 CAR T cells permanently reverses B cell aplasia. *The Journal of clinical investigation* **2016,** *126* (11), 4262-4272.

50. Valton, J.; Guyot, V.; Boldajipour, B.; Sommer, C.; Pertel, T.; Juillerat, A.; Duclert, A.; Sasu, B. J.; Duchateau, P.; Poirot, L., A Versatile Safeguard for Chimeric Antigen Receptor T-Cell Immunotherapies. *Scientific reports* **2018,** *8* (1), 8972.

51. Wu, C. Y.; Roybal, K. T.; Puchner, E. M.; Onuffer, J.; Lim, W. A., Remote control of therapeutic T cells through a small molecule-gated chimeric receptor. *Science* **2015,** *350* (6258), aab4077.

52. Tamada, K.; Geng, D.; Sakoda, Y.; Bansal, N.; Srivastava, R.; Li, Z.; Davila, E., Redirecting gene-modified T cells toward various cancer types using tagged antibodies. *Clinical cancer research : an official journal of the American Association for Cancer Research* **2012,** *18* (23), 6436-45.

53. Ma, J. S.; Kim, J. Y.; Kazane, S. A.; Choi, S. H.; Yun, H. Y.; Kim, M. S.; Rodgers, D. T.; Pugh, H. M.; Singer, O.; Sun, S. B.; Fonslow, B. R.; Kochenderfer, J. N.; Wright, T. M.; Schultz, P. G.; Young, T. S.; Kim, C. H.; Cao, Y., Versatile strategy for controlling the specificity and activity of engineered T cells. *Proceedings of the National Academy of Sciences of the United States of America* **2016,** *113* (4), E450-8.

54. Lee, Y. G.; Marks, I.; Srinivasarao, M.; Kanduluru, A. K.; Mahalingam, S. M.; Liu, X.; Chu, H.; Low, P. S., Use of a Single CAR T Cell and Several Bispecific Adapters Facilitates Eradication of Multiple Antigenically Different Solid Tumors. *Cancer research* **2019,** *79* (2), 387-396.

55. Wiseman, A. C., Immunosuppressive Medications. *Clin J Am Soc Nephrol* **2016,** *11* (2), 332-43.

56. Yura, H.; Yoshimura, N.; Hamashima, T.; Akamatsu, K.; Nishikawa, M.; Takakura, Y.; Hashida, M., Synthesis and pharmacokinetics of a novel macromolecular prodrug of Tacrolimus (FK506), FK506-dextran conjugate. *Journal of controlled release : official journal of the Controlled Release Society* **1999,** *57* (1), 87-99.

57. Tummers, Q. R.; Hoogstins, C. E.; Gaarenstroom, K. N.; de Kroon, C. D.; van Poelgeest, M. I.; Vuyk, J.; Bosse, T.; Smit, V. T.; van de Velde, C. J.; Cohen, A. F.; Low, P. S.; Burggraaf, J.; Vahrmeijer, A. L., Intraoperative imaging of folate receptor alpha positive ovarian and breast cancer using the tumor specific agent EC17. *Oncotarget* **2016,** *7* (22), 32144-55.

58. Mankarious, S.; Lee, M.; Fischer, S.; Pyun, K. H.; Ochs, H. D.; Oxelius, V. A.; Wedgwood, R. J., The half-lives of IgG subclasses and specific antibodies in patients with primary immunodeficiency who are receiving intravenously administered immunoglobulin. *J Lab Clin Med* **1988,** *112* (5), 634-40.

59. Eyquem, J.; Mansilla-Soto, J.; Giavridis, T.; van der Stegen, S. J.; Hamieh, M.; Cunanan, K. M.; Odak, A.; Gonen, M.; Sadelain, M., Targeting a CAR to the TRAC locus with CRISPR/Cas9 enhances tumour rejection. *Nature* **2017,** *543* (7643), 113-117.

60. Mognol, G. P.; Spreafico, R.; Wong, V.; Scott-Browne, J. P.; Togher, S.; Hoffmann, A.; Hogan, P. G.; Rao, A.; Trifari, S., Exhaustion-associated regulatory regions in CD8(+) tumor-infiltrating T cells. *Proceedings of the National Academy of Sciences of the United States of America* **2017,** *114* (13), E2776-E2785.

61. Sen, D. R.; Kaminski, J.; Barnitz, R. A.; Kurachi, M.; Gerdemann, U.; Yates, K. B.; Tsao, H. W.; Godec, J.; LaFleur, M. W.; Brown, F. D.; Tonnerre, P.; Chung, R. T.; Tully, D. C.; Allen, T. M.; Frahm, N.; Lauer, G. M.; Wherry, E. J.; Yosef, N.; Haining, W. N., The epigenetic landscape of T cell exhaustion. *Science* **2016,** *354* (6316), 1165-1169.

62. Vong, Q.; Nye, C.; Hause, R.; Clouser, C.; Jones, J.; Burleigh, S.; Borges, C. M.; Chin, M. S. Y.; Marco, E.; Barrera, L., Inhibiting TGFβ signaling in CAR T-cells may significantly enhance efficacy of tumor immunotherapy. Am Soc Hematology: 2017.

63. Chen, M. L.; Pittet, M. J.; Gorelik, L.; Flavell, R. A.; Weissleder, R.; von Boehmer, H.; Khazaie, K., Regulatory T cells suppress tumor-specific CD8 T cell cytotoxicity through TGF-beta signals in vivo. *Proceedings of the National Academy of Sciences of the United States of America* **2005,** *102* (2), 419-24.

64. Watson, H. A.; Wehenkel, S.; Matthews, J.; Ager, A., SHP-1: the next checkpoint target for cancer immunotherapy? *Biochemical Society transactions* **2016,** *44* (2), 356-62.

65. Riese, M. J.; Wang, L. C.; Moon, E. K.; Joshi, R. P.; Ranganathan, A.; June, C. H.; Koretzky, G. A.; Albelda, S. M., Enhanced effector responses in activated CD8+ T cells deficient in diacylglycerol kinases. *Cancer research* **2013,** *73* (12), 3566-77.

66. Prinz, P. U.; Mendler, A. N.; Masouris, I.; Durner, L.; Oberneder, R.; Noessner, E., High DGK-alpha and disabled MAPK pathways cause dysfunction of human tumor-infiltrating CD8+ T cells that is reversible by pharmacologic intervention. *Journal of immunology* **2012,** *188* (12), 5990-6000.

67. Moon, E. K.; Wang, L. C.; Dolfi, D. V.; Wilson, C. B.; Ranganathan, R.; Sun, J.; Kapoor, V.; Scholler, J.; Pure, E.; Milone, M. C.; June, C. H.; Riley, J. L.; Wherry, E. J.; Albelda, S. M., Multifactorial T-cell hypofunction that is reversible can limit the efficacy of chimeric antigen receptor-transduced human T cells in solid tumors. *Clinical cancer research : an official journal of the American Association for Cancer Research* **2014,** *20* (16), 4262-73.

68. Orellana, E. A.; Tenneti, S.; Rangasamy, L.; Lyle, L. T.; Low, P. S.; Kasinski, A. L., FolamiRs: Ligand-targeted, vehicle-free delivery of microRNAs for the treatment of cancer. *Science translational medicine* **2017,** *9* (401).

69. Karlsson, H.; Svensson, E.; Gigg, C.; Jarvius, M.; Olsson-Stromberg, U.; Savoldo, B.; Dotti, G.; Loskog, A., Evaluation of Intracellular Signaling Downstream Chimeric Antigen Receptors. *PloS one* **2015,** *10* (12), e0144787.

70. Rashidian, M.; Keliher, E. J.; Bilate, A. M.; Duarte, J. N.; Wojtkiewicz, G. R.; Jacobsen, J. T.; Cragnolini, J.; Swee, L. K.; Victora, G. D.; Weissleder, R.; Ploegh, H. L., Noninvasive imaging of immune responses. *Proceedings of the National Academy of Sciences of the United States of America* **2015,** *112* (19), 6146-51.

71. Lairson, L. L.; Lyssiotis, C. A.; Zhu, S.; Schultz, P. G., Small molecule-based approaches to adult stem cell therapies. *Annual review of pharmacology and toxicology* **2013,** *53*, 107-25.

72. Eshhar, Z.; Ofarim, M.; Waks, T., Generation of hybridomas secreting murine reaginic antibodies of anti-DNP specificity. *Journal of immunology* **1980,** *124* (2), 775-80.

73. Graham, C.; Jozwik, A.; Pepper, A.; Benjamin, R., Allogeneic CAR-T Cells: More than Ease of Access? *Cells* **2018,** *7* (10).

CHAPTER 3. IN VIVO LOCATIONLIZATION AND REJUVENATION OF CAR T CELLS USING A PRIVATE PASSAGEWAY FUSION RECEPTOR

3.1 Introduction

Chimeric antigen receptor (CAR) T cell therapies have recently experienced substantial success in the treatment of several types of hematopoietic cancers. In the meantime, one should also recognize that some of the lymphoma and most solid tumor cases still have a very low response rate or a high relapse rate with CAR T cell therapies. This mainly result from one or combinations of the following three reasons: 1. Emergence of antigen negative cancer cell colonies under the selection pressure of CAR T cells, as seen in the case of CD19 negative ALL relapse treated with anti-CD19 CAR T cells; 2. Hindered initial homing and proliferation of CAR T cells in solid tumor due to the aberrant tumor vasculature, dense stromal barrier and suppressive microenvironment; 3. Gradual exhaustion and lowered lysis effect of CAR T cells after continuous tumor antigen exposure. Assuming loss of antigen is not present for a given solid tumor patient (validated by biopsy sampling), the causes of a potential failure of a CAR T cell therapy are most likely to result from the latter two reasons. Therefore, to increase CAR T cells efficacy in solid tumors, practical methods for in vivo evaluation and rejuvenation of CAR T cells are highly desired.

Here we describe the novel design of a private passageway fusion receptor in CAR T cells as a universal platform to achieve both objectives. This FITC-FR fusion receptor is composed of two parts, scFv against FITC as the ligand binding domain at the N terminal and FRα as the GPI anchoring and internalizing domain at the C terminal. When independently expressed on CAR T cells, the FITC-FR fusion receptor can be specifically targeted by a FITC-radio-imaging agent for a noninvasive evaluation of the initial localization and proliferation of CAR T cells in solid tumors.

In addition to that, to overcome the exhaustion status of CAR T cells in the suppressive tumor microenvironment, immuno-agonists which normally cause strong autoimmunity side effects can now be systemically dosed in a FITC targeted form, and safely delivered to FITC-FR positive CAR T cells.

3.2 Materials and Methods

3.2.1 Cell Lines and Human T Cells

DMEM (Gibco) containing 10% heat-inactivated fetal bovine serum and 1% penicillin-streptomycin was used for the culture of MDAMB-231 and MDA-MB-231 $CD19^+$ cells. Peripheral blood mononuclear cells (PBMCs) were isolated by Ficoll density gradient centrifugation (GE Healthcare Lifesciences, #17-5442-02) from human whole blood obtained from healthy volunteers. Pure CD3+ T cells were enriched from PBMCs using an EasySep™ Human T Cell Isolation Kit (STEM CELL technologies, #17951).

3.2.2 Biodistribution and SPECT Imaging of Fusion Receptor Positive T Cells Detected by FITC-^{99m}Tc

The preparation and formation of FITC-99mTc is described in Chapter 2.2.2 and 2.2.7. To visualize and quantify the biodistribution of the fusion receptor targeting ligand, the MDA-MB-231 breast cancer cells solid tumor model was used. MDA-MB-231 were transduced with lentivirus encoding a gene for human CD19 (NM_001178098.1). 10^6 MDA-MB-231 CD19+ cells were subcutaneously implanted in immunodeficient NSG (Jackson Laboratory). The growth of tumors was measured using a caliper, and the tumor volumes were calculated as ½(L x W2) where L was the longest axis of the tumor and W was the axis perpendicular to L. After the tumor reached 100mm^3, 10^7 anti-CD19 FITC-FR CAR T cells were intravenously injected into the mice. 2 weeks after the CAR T cells injection, 200 μCi FITC-^{99m}Tc (prepared according to chapter 2.2.11) in 100 μl solution was intravenously injected to each mouse and a whole-body image was taken with

a Kodak Imaging Station (In-Vivo FX, Eastman Kodak Company) in combination with a CCD camera and Kodak molecular imaging software (version 4.0). Radio images: illumination source = radio isotope, acquisition time = 3 min, f-stop = 4, focal plane = 5, FOV = 160, binning = 4. White light images: illumination source = white light transillumination, acquisition time = 0.05 s, f-stop = 16, focal plane = 5, FOV = 160 with no binning. The kidneys were shielded by lead when needed. Following the imaging, the mice were dissected, and major organs were collected into pre-weighed gamma-counter tubes. CPM values were decay corrected.

3.2.3 Evaluation of Potential Payloads for in vitro Rejuvenation of Exhausted CAR T Cells

anti-CD19 CAR T cells were co-incubated with $CD19^+$ Raji cell at 1:1 ratio in 12-well plate at density of 2 x 10^6 CAR T and 2 x 10^6 Raji per well, new Raji cell were added every 12 h for 3 times, Raji cell population, lysis effect and co-inhibitory receptors were then tested to confirm the exhaustion of the CAR T cells. Both flow cytometry and luciferase-based assays were used to quantify the lysis effect. To test the rejuvenating efficacy of the potential payloads, this cell mixture was then transferred to 96-well plate, around 2 x 10^5 cells per well, and different concentration of drugs were added. After 12 h, Raji cell population, lysis effect and co-inhibitory receptors were tested again and compared to the PBS treatment group.

3.2.4 Evaluation of FITC-TLR7 Agonist on FITC-FR CAR T Cell in MDA-MB-231 Tumor Model

NSG mice were subcutaneously implanted with MDA-MB-231 $CD19^+$ cells, 20M CAR T cells with FITC-FR fusion receptor were infused through intravenous injection once the tumor size reached 50 mm^3. Releasable FITC-TLR7 agonist is dosed every other day at 5 nmole/mice, starting at day 20 after CAR T cell injection and continued for 20 days. Tumor volume was measured for no CAR T cell control group, CAR T cell only group and CAR T cell + FITC-TLR7 agonist group. At the endpoint of the study, tumors were digested using the following protocol and CAR T cells

within in tumor tissue were characterized by flow cytometry for total number and co-inhibitory molecules levels at the endpoint of the study. Tumor digestion: subcutaneous tumor tissues were dissected from the mouse, cut into pieces (to avoid location bias, it's better to dissect the whole tumor), incubate with 10 ml digestion buffer (100 ml: 100 mg collagenase, 10 mg Hyaluronidase, 20 mg Dexyonuclease, RPMI w/o FBS) for 1 h. After digestion, the supernatant was passed through a 40 μM nylon strainer, and the flow through was centrifuged and washed by PBS at 400 g. Cells were counted and ready for subsequent flow cytometry staining.

3.3 Results

3.3.1 Evaluation of Fusion Receptor Positive CAR T Cells Homing in Solid Tumor by a FITC-^{99m}Tc Radio-Imaging Agent

Although there are more than one-hundred CAR T cell therapy clinical trials currently going on for solid tumors, little or none methods have been developed for the direct characterization of CAR T cells homing and proliferation. CAR T cells and cytokine levels in peripheral blood are great indicators for efficacy in hematopoietic cancer treatment, but not always indicative for solid tumors. Tissue biopsy are most often biased and intrusive, therefore should be avoided when possible. Since radio-imaging is a widely used, sensitive and nonintrusive tool for disease diagnosis and monitor in clinics, we set out to design a novel FITC-radio-imaging agent for the visualization of CAR T cells in solid tumors.

Technetium (^{99m}Tc), the major radio-imaging nuclide used clinically[1-3], was selected and attached to the targeting ligand FITC via a peptide-based chelator, EC20 head (Fig. 3-1 A). A FITC-EC20 head compound was first synthesized through azide-DBCO based Cu-free Click reaction. However, this ligand was unable to chelate with ^{99m}Tc efficiently for unknown reasons (data not shown). A modified FITC-EC20 head compound with a PEG_3 linker was then synthesized through solid phase and displayed complete chelation with ^{99m}Tc. Therefore, the

modified FITC-EC20 head is used for future study. The binding affinity of FITC-^{99m}Tc for FITC-FR fusion receptor is around 2.82 nM, measured by cell-based assays, similar with FITC-AF647 (Fig. 3-1 B).

As a proof-of-concept, to visualize anti-CD19 FITC-FR CAR T cells in a solid tumor model using FITC-^{99m}Tc, mice were implanted with MDA-MB-231 overexpressing CD19 as a xenograft on the shoulder followed by anti-CD19 FITC-FR CAR T cell treatment. FITC-^{99m}Tc was systemically injected into these mice to track the CAR T cells and evaluate if there are any background signals from other major organs. The whole-body imaging taken 4 h after injection showed that ^{99m}Tc radiotracer accumulated mainly around the tumor site, with little or no radioactivity in other tissues except kidneys and liver (Fig 3-1 D). The in vivo specificity of FITC-targeted imaging agent was further tested by prior administration of excess cold FITC-EC20 head or FITC-Glucosamine before FITC-^{99m}Tc administration. Competition group showed almost no radiotracer uptake in tumor tissue, confirming the specificity of FITC for FITC-FR fusion receptor. A detailed biodistribution study was also conducted after imaging the animals. As shown in Fig. 3-1 E, mice from both 4 h and 24 h post injection groups shown high and specific accumulation of FITC-^{99m}Tc radiotracer in tumor tissues, while much lower signals were found in other major organs except kidneys. The high non-competitive signal in kidney was resulted from the secretion of unbound FITC-^{99m}Tc conjugates. Considering the relatively small portion of CAR T cells compare to tumor cells and stroma cells in tumor tissues (around 20% of total cells in tumor tissue at this tumor size), the sensitivity of FITC-^{99m}Tc is good and comparable with previous targeted radio-imaging agents. Taken together, these results confirmed the in vivo specificity and sensitivity of FITC-^{99m}Tc for the FITC-FR fusion receptor CAR T cells.

3.3.2 Evaluation of the Ability of Phosphatase Inhibitors and TLR7 Agonists to Rejuvenate Exhausted CAR T cells

As mentioned in Chapter 1, one major limitation of CAR T cell therapies in solid tumors is their tendency to become exhausted after repeated stimulation with cancer antigens. This phenomenon however, is not specific to CAR T cells, but has been described in both chronic virus infections[4] and tumor infiltration lymphocytes[5]. The reversibility of the exhausted phenotype of T cells has been proven in studies where T cells isolated from the solid tumor tissue show a higher INFγ secretion and a killing effect if kept away from antigens ("rested") overnight before re-stimulation[57]. However, it would will be more appealing if rejuvenation could be achieved in a more clinically relevant way using commercially available therapeutics: either to block the inhibitory signaling or to activate the T cells through other pathways. Antibodies targeting checkpoint inhibitors (i.e. PD-1, CTLA-4, etc.) have shown some success in solid tumors in-clinic[151], however, two or more targets in combination often have been found to be necessary. Moreover, antibody therapy also suffers from poor penetration in solid tumors and this may have led to less reports for the combination therapy of CAR T cells and checkpoint blockades (ICB) in solid tumors.

The inhibition of the phosphatases, such as SHP1/2 and TC-PTP, that mediate TCR deactivation, is a potential way to block tonic CAR T signaling. SHP1/2 phosphatase is responsible for mediating the signal from PD-1 and other exhaustion markers. Data has shown that SHP1/2 phosphatase inhibitor or silencing can increase the activity of T cells and CAR T cells[6-9]. TC-PTP is known to be an important player in T cell activity signaling. Mice harboring a T cell specific TC-PTP deficiency have increased susceptibility to inflammation and autoimmunity due to heightened antigen-driven T cell activation[10]. TC-PTP inactivates Src family kinase downstream of the TCR, thereby contributing to the threshold of TCR activation[11].

Although both knockout experiments and small molecule inhibitors of these phosphatases have shown potent effect on lowering TCR threshold and increasing T cell activity, none of them have been used in CAR T therapy.

Another approach to rejuvenate the T cells is to augment their activity through the engagement of antigen independent innate immune receptors. It has been known that certain pathogen pattern recognition (PPR) receptors, including toll like receptors (TLR), do express on non-myeloid cell populations, including T cells, and can be activated in a similar way[12-16]. Research has also shown that co-stimulation of TLR7/8 agonists and TCR signaling can activate CD8 T cells and increase INFγ secretion[13]. However, due to the strong side effects of systemic dosing of TLR agonists[17-22], none of these agonists have been used in CAR T therapy to reactivate the T cell or change the immunosuppressive microenvironment. The employment of TLR agonists for cancer immunotherapy is also hindered by the controversial effect of TLR agonists on the tumor cells. Therefore, a targeted delivery of the potential payloads to the CAR T cell is highly desired. A potent TLR7 agonist was found in the literature[23-24] (Fig. 3-3 A), which is around 40 fold stronger than the FDA approved imiquimod[25].

To set up an in vitro screening model, as shown in Fig. 3-2, anti-CD19 CAR T cells were exposed to 4 rounds of addition of CD19 positive Raji cells, and became exhausted as marked by gradual decreased lysis activity as well as increased co-inhibitory markers in an in vitro co-culture model. It's worth noticing that the culture medium is important for the introduction of CAR T exhaustion and needs to be kept the same without new replenish or change during the whole process. It indicates that the soluble components that are released by cancer cells and/or CAR T cells into the medium, most likely immunosuppressive cytokines and modulators (adenosine etc.),

play a pivotal role in this process. It also suggests that the exhaustion of CAR T cells generated by this in vitro model is at a rather pliable than irreversible status.

Treatment of the TLR7 agonist and PTP1b (highly homologous to TC-PTP[26]) inhibitor[27] of choice with the already exhausted CAR T cells was shown to be able to reactivate them compared to the no treatment group (Fig. 3-3). No significant changes, however, were observed in the expression level of co-inhibitory markers except for Tim3. As shown by Fig 3-3, the PTP1b inhibitor in general does not show as strong of a reactivation effect as the TLR7 agonist. This result could be due to the current in vitro screening model where "Reversion" rather than "Prevention" of exhaustion is studied, and the phosphatases are already "silenced" at the exhausted status, therefore their inhibition will have little to no effect. A modified screening model for a future study will test the effects of phosphatase inhibitors and other drugs with a focus on the "prevention" of exhaustion by adding the drugs at the beginning of all cultures and keeping the rest of the settings the same. In this way, it may be possible to see whether the inhibition of phosphatase can lower the tonic signaling of CAR T while still keeping a functional killing effect. We will mainly focus on TLR7 agonist for the following study.

Since TLR7 is one of the 4 TLR family members that resides inside the endosome, it is speculated that a non-releasable linker between the TLR7 agonist and our secret passageway targeting ligand would preserve its TLR7 agonist function[28]. To achieve that, several TLR7 agonist analogs were prepared and tested to find the proper derivatization sites for linkage. As shown in Fig. 3-4, the TLR7 agonist with a CH_2OH extension at the piperidine ring has an even higher activity compared to the parent drug. Therefore, this derivative site will be used for a non-releasable conjugate. A disulfide bond linked self-immolative form also has been synthesized. In order to understand the distance needed for this TLR7 agonist to reach its own target, three

different lengths of linker (PEG3, 6, 16) between the FITC and TLR7 agonist were made for the non-releasable FITC-TLR7. As shown in Fig. 3-5 C, all of the non-releasable forms had some effect, while the PEG_6 compound showed the best dose-dependent response. These results indicate that TLR7 agonists may dock with TLR7 either by reaching out while binding with FITC-FR or jumping between TLR and FITC-FR, under which conditions the length of the linker in between is not a crucial factor (Fig. 3-5 D-E). Since the non-releasable FITC-TLR7 is trapped inside the endosome and the volume of each endosome is much smaller than the cytosol, the intra-endosome TLR7 can gets to its functional concentration much faster and quicker, resulting in a smaller IC_{50}.

3.3.3 Evaluation of the Ability of FITC-TLR7 Agonists to Rejuvenate Exhausted CAR T Cells in a Solid Tumor Model

Next, the focus of this study was directed to the targeted delivery of the TLR7 agonist for the rejuvenation of CAR T cells in a mouse solid tumor model using our secret passageway. To keep it consistent with previous studies, the FITC-FR anti-CD19 CAR was used and CD19 antigen was overexpressed in an MDA-MB-231 breast cancer cell line (Fig. 3-6). To mimic the exhaustion status of the CAR T cells in vivo, a subcutaneous implanted xenograft of CD19+ MDA-MB-231 in NSG mice was used as the solid tumor model. Preliminary data showed that 20M of FITC-FR anti-CD19 CAR T cells (around 50% positive) were able to reduce the growth rate of tumor compared to no CAR T control, while the addition of FITC-TLR7 (releasable form) further lowered the tumor volume at a later stage. Interestingly, digestion of the tumor tissue at the end-point of the study showed both LAG3 and Tim3 markers dropped in the CAR T + FITC-TLR7 group compared to the CAR T-only group. No toxicities were seen for the repeated dosing of FITC-TLR7 judged by body weight change.

At least two causes could be responsible for the less significant difference between the CAR T + FITC-TLR7 and CAR T-only group: First and foremost, the overall efficacy of single treatment

anti-CD19 CAR T against $CD19^{+}$MDA-MB-231 is already good judged by the controlled tumor growth, high CAR T number in tumor tissue and low exhaustion markers on CAR T cells. For future work, a solid tumor model with a more suppressive and harsher tumor microenvironment is needed to differentiate the effect of targeted TLR7 agonists. This could be achieved by: 1. delaying the CAR T treatment until the tumor grows to a bigger size, around 150 mm^3; 2. switching to a more CAR T resistant tumor cell line, such as ovarian cancer cell line KB cell; 3. establishing the solid tumor xenograft in a humanized NSG mice model which has a more complete immune system; 4. introducing a subcurative dose of CAR T cells. Secondly, as reported by literature, due to the induced tolerance phenomena of TLR7, the pharmacological effect of TLR7 agonist greatly depends on dosing frequency and amount, presenting a bell-shaped curve as the concentration continues. Therefore, a systemic evaluation of several dosing schemes with different dosing frequencies and doses may be necessary for our targeted delivery approach.

3.4 Discussion

Current efforts in noninvasive tracking of CAR T cells for clinical usage can be categorized as direct and indirect labeling. Direct labeling (or passive labeling) refers to exogenous labeling with MRI-based contrast agents or PET or SPECT radioprobes. For example, intravenously injected ^{111}In labeled CAR T cells provides high-resolution images and reveals the short residence of CAR T cells in lung short after injection (around 3 h), followed by major accumulation in liver and secondary lymphoid organs and low tissue penetration in solid tumors[29]. However, the signal is temporary for direct labeling and will disappear base on the isotope's half-life. It's also not incorporated at gene level, therefore cannot represent cell conditions, such as viability and proliferation. For indirect labeling, reporter genes encoding surface proteins, channels or enzymes that are detectable or bind imaging probes are incorporated into target cell's genome. Classical reporters such as herpes simplex virus thymidine kinase (HSV-TK) reporter[30] and human sodium iodide symporter (hNIS)[31] have been explored for CAR T cells imaging. Although the immunogenicity problem is solved for hNIS compared to HSV-TK, it still suffers from specificity problems, as hNIS is naturally expressed in thyroid, stomach, salivary glands and lactating breast[32], resulting in potential high background signals from these tissues. Another type of indirect imaging involves targeting the endogenous or artificially expressed surface proteins on CAR T cells. For example, Peter M. Smith-Jones, et al. co-expressed somatostatin receptor type 2 (SSTR2) on CAR T cells and imaged the cells with allium-68-labeled octreotide analog (^{68}Ga-DOTATOC), which is a FDA-approved SPECT imaging probe for neuroendocrine tumors[33-34]. Limitation for this type of approach also involves the lack of specificity of the targeted surface protein, since SSTR2 are known to be expressed on other immune cells.

The FITC-^{99m}Tc mediated imaging of FITC-FR fusion receptor positive CAR T cells described here has several advantages compare to the mentioned ones above. First, there are no other cells in humans and mice express the FITC scFv on the cell surface, except for the fusion receptor modified CAR T cells around the tumor tissues, therefore, the specificity of FITC-^{99m}Tc ligand is guaranteed. Secondly, the molecule weight of FITC-EC20 head compound is around 1000, which is much smaller than an antibody or peptide-based probe. This gives us a better tissue penetration in solid tumor, faster clearance in fusion receptor negative tissues and a better PK/PD profile, all of these contribute to a higher sensitivity and signal to noise ratio (S/N) of the imaging. Thirdly, due to the modular construction of FITC-^{99m}Tc, the PK/PD profile can be easily modified via alteration of the PEG linker in between for lower background signals. For example, previous research in current lab has shown that a FA based NIR dye probe with a PEG_{12} linker in between gives less liver uptake compare to the PEG_3 one without any sacrifice in binding affinity (Sakkarapalayam M. Mahalingam, unpublished data). Other types of linkers with variable levels of rigidity or hydrophilicity can also be incorporated to improve the binding affinity of the whole conjugate or according to the choice of different chelating heads (Fig. 3-7).

Nevertheless, the FITC-^{99m}Tc based visualization of CAR T cells described here can be further improved from several aspects for future study. First, as shown in Fig. 3-1, there is competable and relatively high uptake in liver compare to other organs from the biodistribution data. This could result from the CAR T cells reside in liver, or due to the nonspecific engulf by Kufer cells towards amino acid based chelating head. Therefore, non-amino acid-based chelation heads, such as NOTA, DOTA and DTPA or increased length of PEG linker (as mentioned above) can be used to potentially lower the background signals from liver. Secondly, although ^{99m}Tc is used here for its wide usage and availability in clinics, it has relatively short half-life (around 6 h) that may not

be suitable for CAR T cell tracking. Other radio-imaging nuclide such as ^{64}Cu and ^{67}Ga can be explored in future study[35].

For the FITC-TLR7 agonist directed rejuvenation of exhausted CAR T cells, detailed studies are needed to fully understand the mechanism for the increased efficacy of the combinational therapy. First, for a similar study carried out in current lab using anti-FITC CAR T cells and FITC-TLR7 agonist in a KB solid tumor model, human CD3 IHC staining indicates that addition of FITC-TLR7 agonist not only increased the number of infiltrating CAR T cells, but also promoted a sparse distribution pattern of CAR T cells in the tumor tissue compare to the CAR T cells only group. This implies that TLR7 agonist is capable to turn an immune cold tumor to a hot condition by directly targeting the T cells. It's reasonable to expect similar mechanisms to be presented for the FITC-FR fusion receptor CAR T cells, since the targeting ligand and payload are the same. Secondly, since TLR7 agonists have strong proinflammatory effects on myeloid cells, while all of the current studies were carried out in NSG mice with a compromised immune system, it will be interesting and more clinical revelent to see whether FITC-TLR7 will act on other immune cells or not except FITC-FR CAR T cells in a humanized NSG or immunocompetent mice model. Thirdly, it has been recently confirmed that transcriptional factor Tox is a driver for the exhaustion status of T cells and silencing of it results in lack of T_{EX} generation[36-37]. Therefore, ongoing work in current lab includes characterization of the level changes of certain transcription factors before and after FITC-TLR7 treatment as well as their potential interactions with the TLR7-MyD88-NF-κB[38] pathway. The list of candidate transcription factors includes: Tox, Tox2, Nr4a2[39] and etc.

Other than TLR7 agonist, there are several other potential payloads that may revert/prevent the exhaustion of CAR T cells as described below. Some of the targets may not have agonists or inhibitors with IC_{50} suitable for our targeted drug delivery approach for now, but

are still worth noticing and may be explored through other inhibitory mechanisms, such as CRISPR or targeted microRNA delivery approaches.

- STING agonist

The Simulator of IFN Genes (STING) is a master adaptor involved in cytosolic DNA sensing and the following IFN-β production. STING associates weakly to sdDNA, but strongly binds the endogenous cyclic dinucleotide GMP-AMP (cGAMP) synthesized by the cGMP-AMP synthase (sGAS). It is predominantly expressed in macrophages, T cells, a variety of DCs, endothelial cells, and select fibroblasts and epithelial cells. Studies of STING have mainly focused on its function in macrophages and dendritic cells, and recently some groups have noticed the direct effect of STING activation in T cells[40]. It is possible that a STING agonist will have a similar pro-inflammatory effect on T cells. ADU-S100 is one of the many STING agonists that has been pursued in clinics.

- DGK-α inhibitor

Diacylglycerol Kinase-α (DGK-α) converts diacylglycerol (DAG), a second messenger in TCR signaling together with IP3, to phosphatidic acid (PA). DGK is more highly expressed in CD8TIL than in CD8-NIL, and its inhibition promotes ERK phosphorylation and lytic degranulation[41]; it also restores lytic functions of CAR TIL that are isolated from in vivo[5].

- TGFβRI (ALK5) inhibitor

TGFβ is known for its immunosuppressive function in many immune cells, such as the T cell, B cell, and macrophages. The blockage of TGFβ type I receptor (TGFβRI, also called ALK5) in T cells reverts the immunosuppressive environment of the tumor[42]. Small molecule inhibitors have been pursued with galunisertib (LY2157299 monohydrate) and EW-7197 tested in clinics[43-44].

- EZH2 inhibitor

Enhancer of Zeste Homolog 2 (EZH2) is a histone H3K27 methyltransferase with a strong correv with the Treg function. Genetic or pharmacological disruption of EZH2 drove acquisition of proinflammatory function of tumor infiltrating Treg[45]. Since exhausted CTL in chronic virus infections is also characterized by unique epigenetic changes[174], it is possible that EZH2 inhibitors will be able to reverse this exhaustion status. Several small molecules of EZH2 inhibitors have been developed, including CPI1205, EPZ6438 and GSK126.

In summary, the FITC-FR fusion receptor and the corresponding FITC targeted radio-imaging agents and immune-agonists payloads provide a universal platform for the monitor and control of CAR T cells homing and persistence in solid tumor. This approach can be easily incorporated into CAR T cells for any antigens since the FITC-FR fusion receptor is independently expressed to the CAR construct. The modular design of targeting ligand-payload conjugates also make it easier for the switching and modification. This approach combines the benefits of cell therapy and small molecule-based targeted drug delivery and may requires extra characterization of both the engineered cells and the corresponding ligands. The success of CAR T cells in solid tumor is most likely to require the combination of multiple approaches targeting other players within the microenvironment as well, such as breaking down of the extracellular matrix by PI3K kinase inhibitors, reprograming of anti-inflammatory M2 macrophages to a proinflammatory M1 phenotype and upregulation of the decreased MHC molecules level on cancer cells. Therefore, it is guaranteed that more and more combinational therapy studies will be conducted both preclinically and clinically. However, at the same time, a careful examination and control of the CAR T cell itself cannot be neglected and should be optimized by using simple but robust systems like FITC-FR fusion receptors in preclinical research first before it reaches to humans.

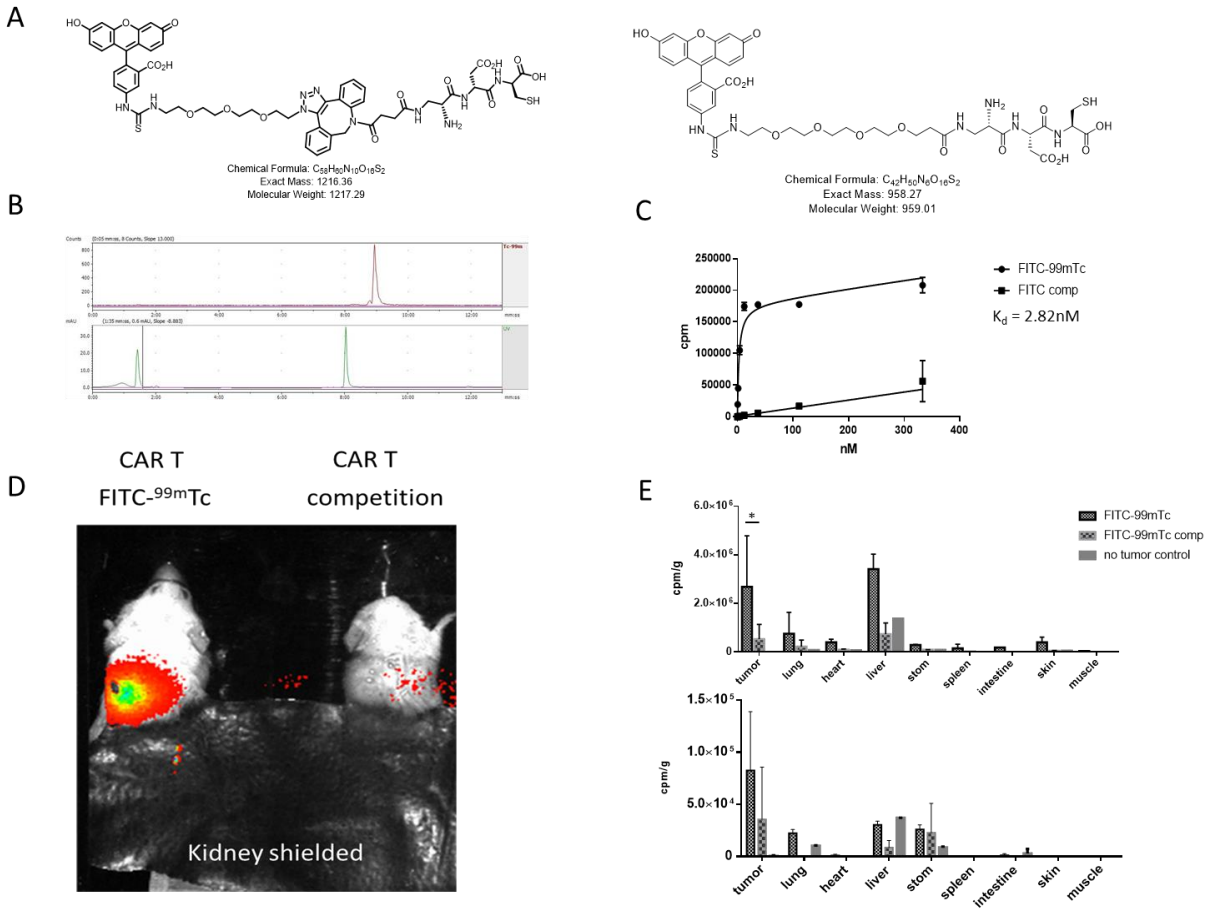

Figure 3-1 in vivo localization of CAR T cells using FITC-^{99m}Tc imaging agents.
(A) Chemical structure of FITC-EC20 head compounds. (B) Radio-HPLC shows complete chelating of FITC-^{99m}Tc. (C) Evaluation of binding affinity of FITC-^{99m}Tc in FITC-FR expressing cells. (D) Overlay of whole-body radioimages on white light images of mice bearing MDA-MB-231 CD19+ tumors and treated with anti-CD19 FITC-FR CAR T cells 4h after administration of FITC-^{99m}Tc. (E) Biodistribution of FITC-^{99m}Tc 4 h (upper) and 24 h (lower) post injection in major organs with kidney excluded. Bar graphs represent mean ± s.d. n = 3. Data shown are the represent data from two independent experiments.

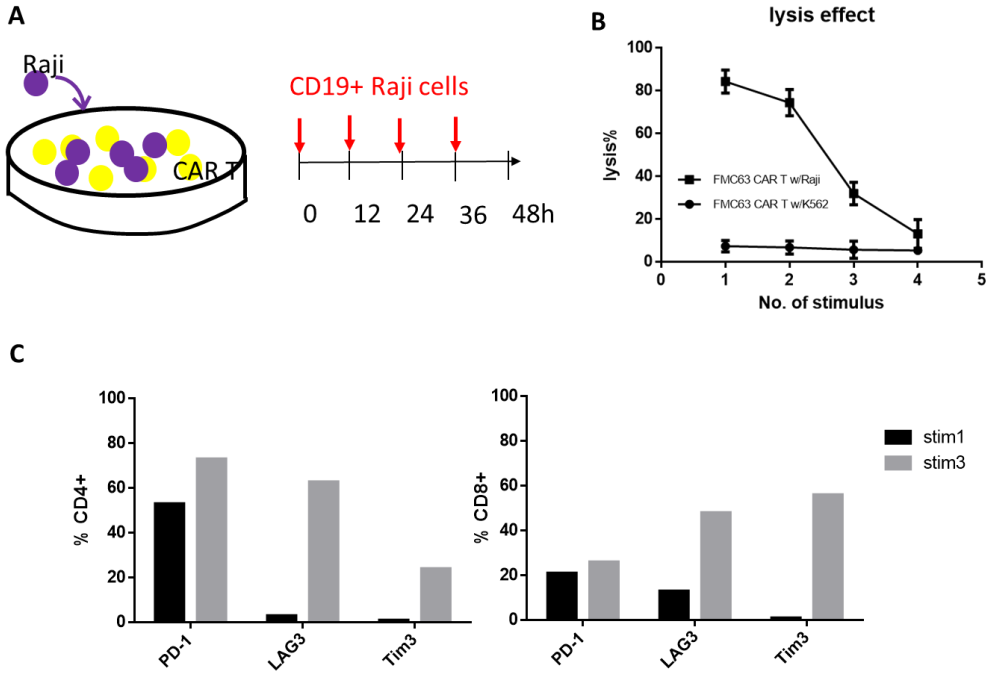

Figure 3-2 in vitro model for the induction of CAR T cell exhaustion.
(A) $CD19^{+}$ Raji and anti-CD19 CAR T cells were co-cultured at 1:1 ratio with fresh Raji cells added every 12 h. (B) Lysis effect of CAR T cells gradually decreased as the number of stimulus (number of Raji cell addition) increases. $CD19^{-}$K562 cells were used as control. (C) Expression level change of co-inhibitory molecules, PD-1, LAG3 and Tim3 for stim1 and stim3 in CD4 and CD8 positive CAR T cells.

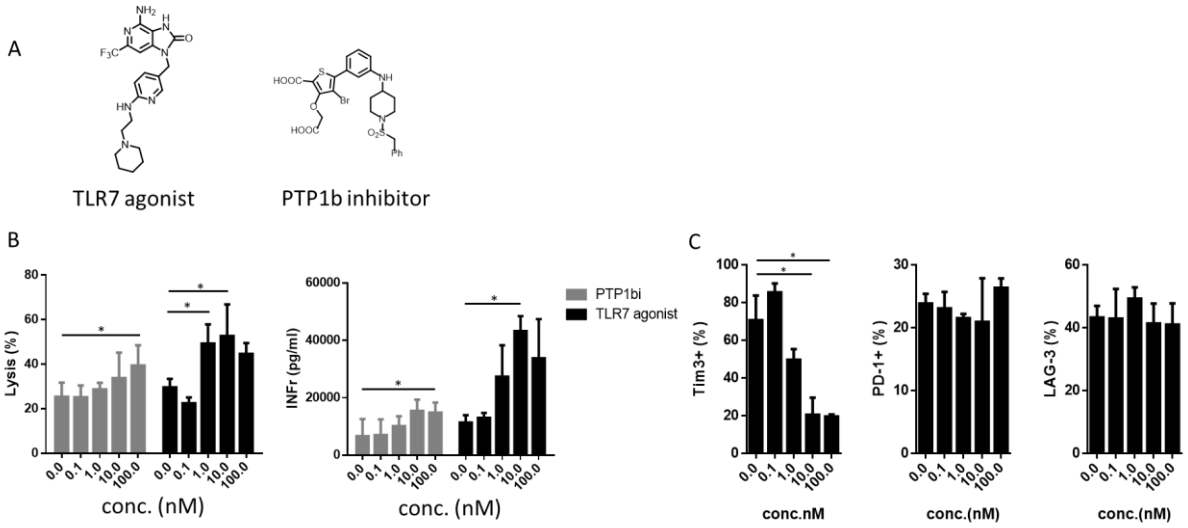

Figure 3-3 Evaluation of TLR7 agonist and PTP1b inhibitor effect on rejuvenation of exhausted CAR T cells.

(A) Chemical structure of TLR7 agonist and PTP1b inhibitor. (B-C) Exhausted CAR T cells were incubated with different concentrations of TLR7 agonist and PTP1b inhibitor monitored by lysis effect and INFγ (B) and expression level of PD-1 LAG-3 and Tim3 after incubation (C). * denotes a p-value < 0.05, ** < 0.01, ns = not significant.

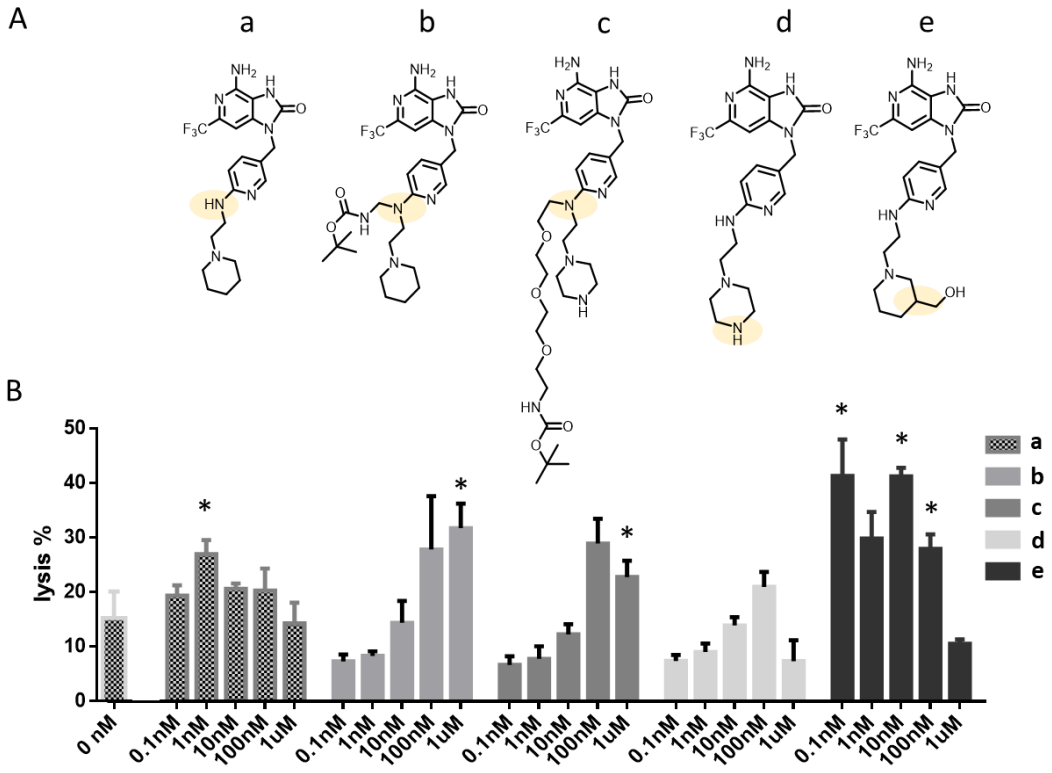

Figure 3-4 Evaluation of potential derivatization sites of the TLR7 agonist for non-releasable ligand targeted delivery.
(A) Chemical structure of the TLR7 agonist analogs. (B) Exhausted CAR T cells were incubated with different concentration of TLR7 analogs and lysis effect was measured and compared to non-treated group.

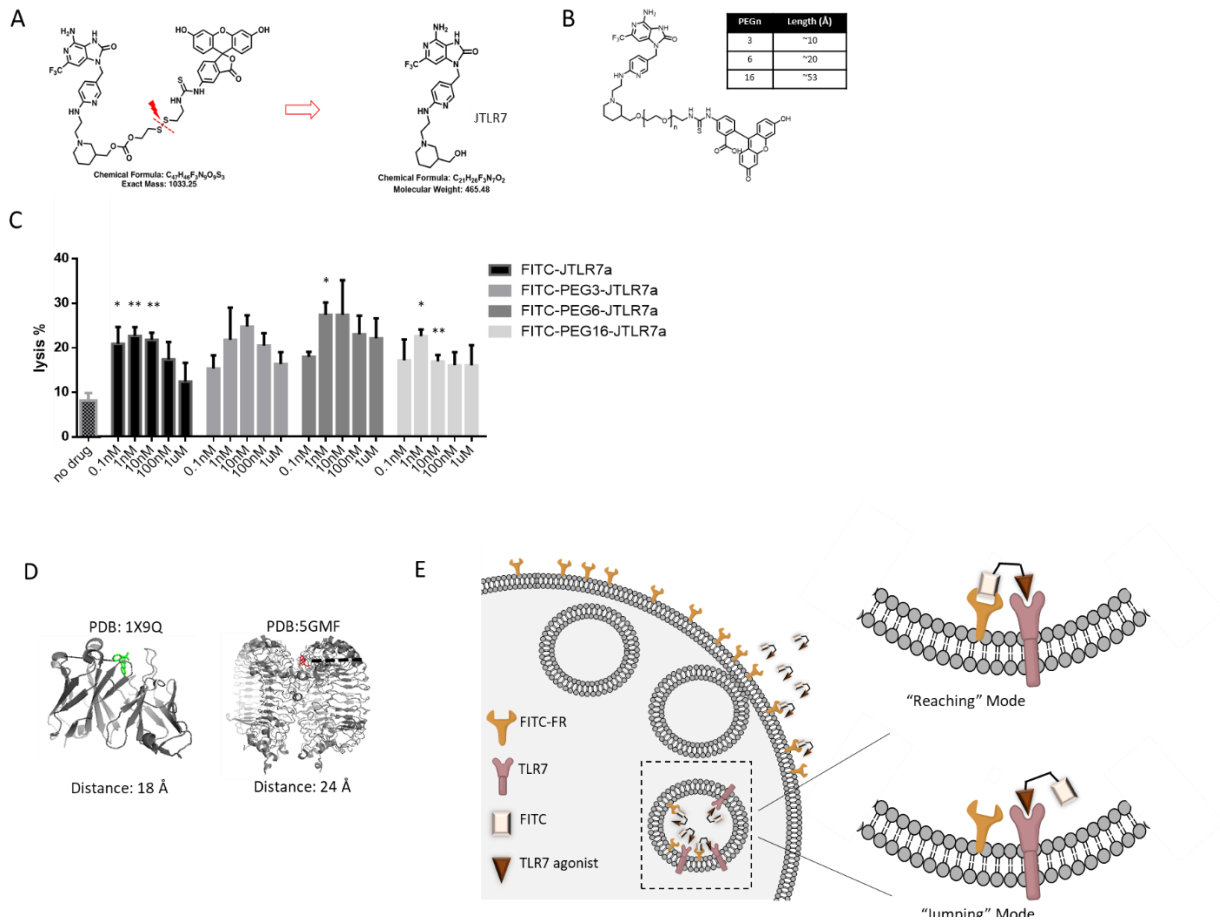

Figure 3-5 Design and evaluation of releasable and non-releasable targeted delivery of TLR7 agonist using FITC as a targeting ligand.
(A) TLR7 agonist analog, JTLR7 (with CH_2OH) is linked to FITC in a self-immolative disulfide bond, unmodified TLR7 agonist analog will be released once the disulfide bond breaks inside endosome. (B) Chemical structure of non-releasable FITC-JTLR7 agonists with different PEG length of linker in between. (C) Exhausted CAR T cells were incubated with different concentration of releasable FITC-TLR7 and non-releasable FITC-JTLR7 agonists and lysis effect was measured and compared to non-treated group. * denotes a p-value < 0.05, ** < 0.01, ns = not significant. (D) Left, crystal structure of FITC (green) binding with FITC scFv (grey) (PDB: 1X9Q, left), the distance between FITC to the edge of FTIC scFv is measured to be around 18 Å. Right, similarly, crystal structure of R-848 (red) binding with TLR7 (grey) (PDB:5GMF) is shown with distance between R-848 and the edge of TLR7 around 24 Å. (E) Diagram illustrating the two possible working mechanisms, "Reaching" or "Jumping" Mode, for the non-releasable FITC-TLR7 agonists.

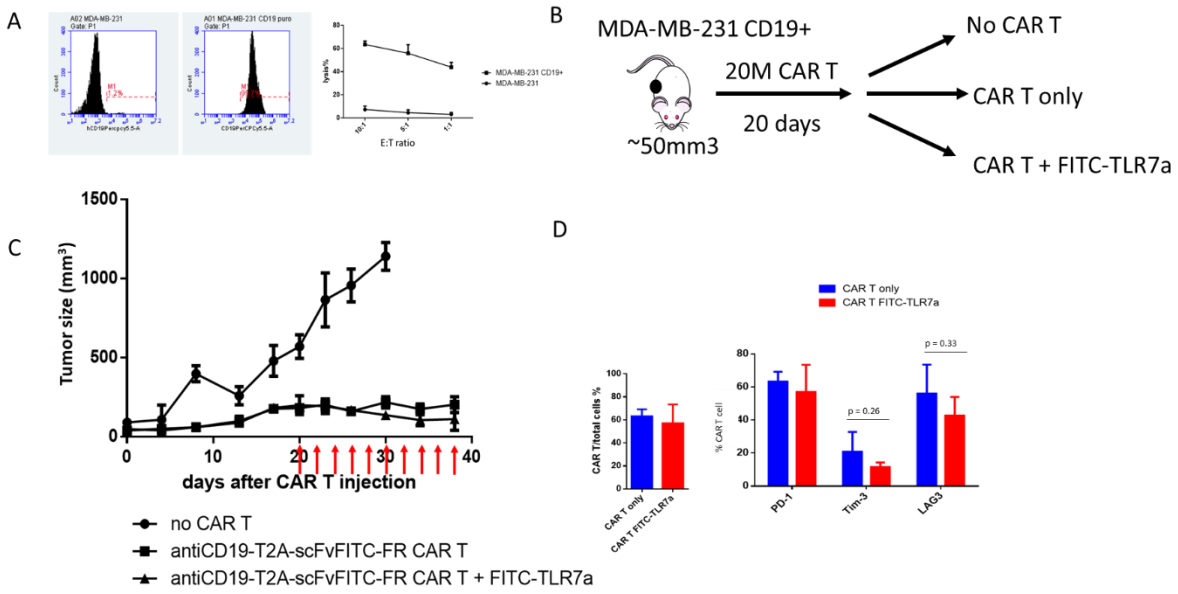

Figure 3-6 Evaluation of a potential rejuvenation effect of the releasable FITC-TLR7 agonist in an MDA-MB-231 CD19^{+} solid tumor model.

(A) Left, overexpression of CD19 in MBA-MB-231 breast cancer cell; Right, lysis of MDA-MB-231 CD19^{+} cells by anti-CD19 CAR T cells. (B) NSG mice were subcutaneously implanted with MDA-MB-231 CD19^{+} cells followed by 20M CAR T cells with FITC-FR fusion receptor once the tumor size reached 50 mm^{3}, releasable FITC-TLR7 agonist is dosed every other day start at day 20 after CAR T cell injection and continued for 20 days. (C) Tumor volume was measured for no CAR T cell control, CAR T cell only and CAR T cell + FITC-TLR7 agonist group. (D) CAR T cells within in tumor tissue were characterized by flow cytometry for total number and co-inhibitory molecules levels at the endpoint of the study.

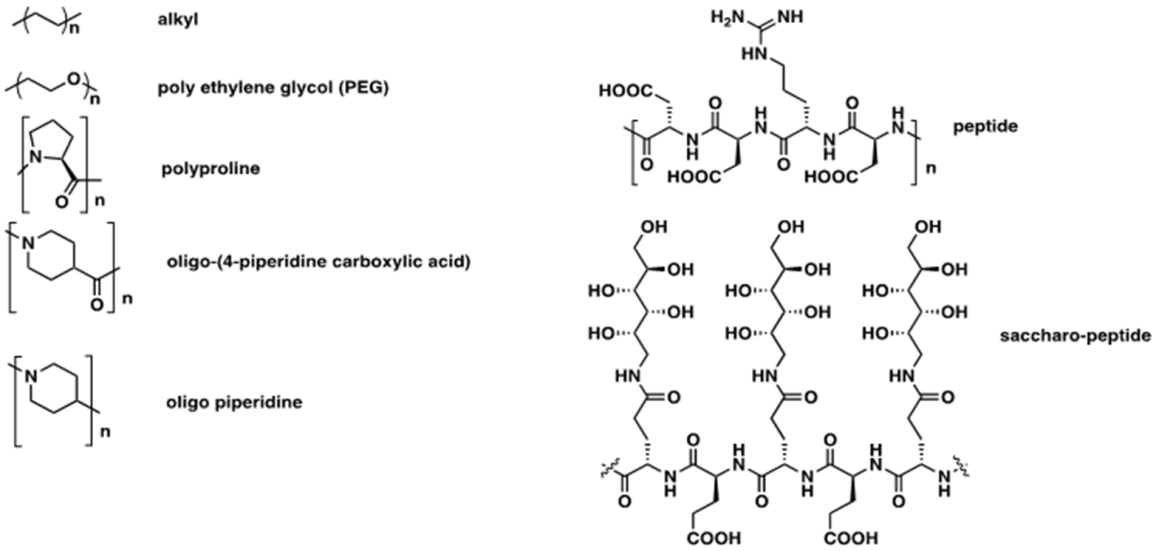

Figure 3-7 Chemical linkers of variable rigidity and hydrophobicity available for usage in the design of targeting ligand-payload conjugates.

3.5 References

1. Kniess, T.; Laube, M.; Wust, F.; Pietzsch, J., Technetium-99m based small molecule radiopharmaceuticals and radiotracers targeting inflammation and infection. *Dalton transactions* **2017,** *46* (42), 14435-14451.

2. Kularatne, S. A.; Zhou, Z.; Yang, J.; Post, C. B.; Low, P. S., Design, synthesis, and preclinical evaluation of prostate-specific membrane antigen targeted (99m)Tc-radioimaging agents. *Molecular pharmaceutics* **2009,** *6* (3), 790-800.

3. Henne, W. A.; Rothenbuhler, R.; Ayala-Lopez, W.; Xia, W.; Varghese, B.; Low, P. S., Imaging sites of infection using a 99mTc-labeled folate conjugate targeted to folate receptor positive macrophages. *Molecular pharmaceutics* **2012,** *9* (5), 1435-40.

4. Kahan, S. M.; Wherry, E. J.; Zajac, A. J., T cell exhaustion during persistent viral infections. *Virology* **2015,** *479-480*, 180-93.

5. Moon, E. K.; Wang, L. C.; Dolfi, D. V.; Wilson, C. B.; Ranganathan, R.; Sun, J.; Kapoor, V.; Scholler, J.; Pure, E.; Milone, M. C.; June, C. H.; Riley, J. L.; Wherry, E. J.; Albelda, S. M., Multifactorial T-cell hypofunction that is reversible can limit the efficacy of chimeric antigen receptor-transduced human T cells in solid tumors. *Clinical cancer research : an official journal of the American Association for Cancer Research* **2014,** *20* (16), 4262-73.

6. Stefanova, I.; Hemmer, B.; Vergelli, M.; Martin, R.; Biddison, W. E.; Germain, R. N., TCR ligand discrimination is enforced by competing ERK positive and SHP-1 negative feedback pathways. *Nature immunology* **2003,** *4* (3), 248-54.

7. Lorenz, U., SHP-1 and SHP-2 in T cells: two phosphatases functioning at many levels. *Immunological reviews* **2009,** *228* (1), 342-59.

8. Watson, H. A.; Wehenkel, S.; Matthews, J.; Ager, A., SHP-1: the next checkpoint target for cancer immunotherapy? *Biochemical Society transactions* **2016,** *44* (2), 356-62.

9. Hebeisen, M.; Baitsch, L.; Presotto, D.; Baumgaertner, P.; Romero, P.; Michielin, O.; Speiser, D. E.; Rufer, N., SHP-1 phosphatase activity counteracts increased T cell receptor affinity. *The Journal of clinical investigation* **2013,** *123* (3), 1044-56.

10. Wiede, F.; Shields, B. J.; Chew, S. H.; Kyparissoudis, K.; van Vliet, C.; Galic, S.; Tremblay, M. L.; Russell, S. M.; Godfrey, D. I.; Tiganis, T., T cell protein tyrosine phosphatase attenuates T cell signaling to maintain tolerance in mice. *The Journal of clinical investigation* **2011,** *121* (12), 4758-74.

11. Pike, K. A.; Hatzihristidis, T.; Bussieres-Marmen, S.; Robert, F.; Desai, N.; Miranda-Saavedra, D.; Pelletier, J.; Tremblay, M. L., TC-PTP regulates the IL-7 transcriptional response during murine early T cell development. *Scientific reports* **2017,** *7* (1), 13275.

12. Wiedemann, G. M.; Jacobi, S. J.; Chaloupka, M.; Krachan, A.; Hamm, S.; Strobl, S.; Baumgartner, R.; Rothenfusser, S.; Duewell, P.; Endres, S.; Kobold, S., A novel TLR7 agonist reverses NK cell anergy and cures RMA-S lymphoma-bearing mice. *Oncoimmunology* **2016,** *5* (7), e1189051.

13. Caron, G.; Duluc, D.; Fremaux, I.; Jeannin, P.; David, C.; Gascan, H.; Delneste, Y., Direct stimulation of human T cells via TLR5 and TLR7/8: flagellin and R-848 up-regulate proliferation and IFN-gamma production by memory CD4+ T cells. *Journal of immunology* **2005,** *175* (3), 1551-7.

14. Wille-Reece, U.; Flynn, B. J.; Lore, K.; Koup, R. A.; Miles, A. P.; Saul, A.; Kedl, R. M.; Mattapallil, J. J.; Weiss, W. R.; Roederer, M.; Seder, R. A., Toll-like receptor agonists influence the magnitude and quality of memory T cell responses after prime-boost immunization in nonhuman primates. *The Journal of experimental medicine* **2006,** *203* (5), 1249-58.

15. Zarember, K. A.; Godowski, P. J., Tissue expression of human Toll-like receptors and differential regulation of Toll-like receptor mRNAs in leukocytes in response to microbes, their products, and cytokines. *Journal of immunology* **2002,** *168* (2), 554-61.

16. Hornung, V.; Rothenfusser, S.; Britsch, S.; Krug, A.; Jahrsdorfer, B.; Giese, T.; Endres, S.; Hartmann, G., Quantitative expression of toll-like receptor 1-10 mRNA in cellular subsets of human peripheral blood mononuclear cells and sensitivity to CpG oligodeoxynucleotides. *Journal of immunology* **2002,** *168* (9), 4531-7.

17. Strominger, N. L.; Brady, R.; Gullikson, G.; Carpenter, D. O., Imiquimod-elicited emesis is mediated by the area postrema, but not by direct neuronal activation. *Brain Res Bull* **2001,** *55* (3), 445-51.

18. Harrison, L. I.; Astry, C.; Kumar, S.; Yunis, C., Pharmacokinetics of 852A, an imidazoquinoline Toll-like receptor 7-specific agonist, following intravenous, subcutaneous, and oral administrations in humans. *Journal of clinical pharmacology* **2007,** *47* (8), 962-9.

19. Dudek, A. Z.; Yunis, C.; Harrison, L. I.; Kumar, S.; Hawkinson, R.; Cooley, S.; Vasilakos, J. P.; Gorski, K. S.; Miller, J. S., First in human phase I trial of 852A, a novel systemic toll-like receptor 7 agonist, to activate innate immune responses in patients with advanced cancer. *Clinical cancer research : an official journal of the American Association for Cancer Research* **2007,** *13* (23), 7119-25.

20. Dummer, R.; Hauschild, A.; Becker, J. C.; Grob, J. J.; Schadendorf, D.; Tebbs, V.; Skalsky, J.; Kaehler, K. C.; Moosbauer, S.; Clark, R.; Meng, T. C.; Urosevic, M., An exploratory study of systemic administration of the toll-like receptor-7 agonist 852A in patients with refractory metastatic melanoma. *Clinical cancer research : an official journal of the American Association for Cancer Research* **2008,** *14* (3), 856-64.

21. Perkins, H.; Khodai, T.; Mechiche, H.; Colman, P.; Burden, F.; Laxton, C.; Horscroft, N.; Corey, T.; Rodrigues, D.; Rawal, J.; Heyen, J.; Fidock, M.; Westby, M.; Bright, H., Therapy with TLR7 agonists induces lymphopenia: correlating pharmacology to mechanism in a mouse model. *J Clin Immunol* **2012,** *32* (5), 1082-92.

22. Hasham, M. G.; Baxan, N.; Stuckey, D. J.; Branca, J.; Perkins, B.; Dent, O.; Duffy, T.; Hameed, T. S.; Stella, S. E.; Bellahcene, M.; Schneider, M. D.; Harding, S. E.; Rosenthal, N.; Sattler, S., Systemic autoimmunity induced by the TLR7/8 agonist Resiquimod causes myocarditis and dilated cardiomyopathy in a new mouse model of autoimmune heart disease. *Dis Model Mech* **2017,** *10* (3), 259-270.

23. Katie, J.; David, N., The discovery of a novel prototype small molecule TLR7 agonist for the treatment of hepatitis C virus infection. *MedChemComm* **2011,** *2* (3), 185-189.

24. Jones, P.; Pryde, D. C.; Tran, T. D.; Adam, F. M.; Bish, G.; Calo, F.; Ciaramella, G.; Dixon, R.; Duckworth, J.; Fox, D. N.; Hay, D. A.; Hitchin, J.; Horscroft, N.; Howard, M.; Laxton, C.; Parkinson, T.; Parsons, G.; Proctor, K.; Smith, M. C.; Smith, N.; Thomas, A., Discovery of a highly potent series of TLR7 agonists. *Bioorganic & medicinal chemistry letters* **2011,** *21* (19), 5939-43.

25. Hemmi, H.; Kaisho, T.; Takeuchi, O.; Sato, S.; Sanjo, H.; Hoshino, K.; Horiuchi, T.; Tomizawa, H.; Takeda, K.; Akira, S., Small anti-viral compounds activate immune cells via the TLR7 MyD88-dependent signaling pathway. *Nature immunology* **2002,** *3* (2), 196-200.

26. Iversen, L. F.; Moller, K. B.; Pedersen, A. K.; Peters, G. H.; Petersen, A. S.; Andersen, H. S.; Branner, S.; Mortensen, S. B.; Moller, N. P., Structure determination of T cell protein-tyrosine phosphatase. *The Journal of biological chemistry* **2002,** *277* (22), 19982-90.

27. Wilson, D. P.; Wan, Z. K.; Xu, W. X.; Kirincich, S. J.; Follows, B. C.; Joseph-McCarthy, D.; Foreman, K.; Moretto, A.; Wu, J.; Zhu, M.; Binnun, E.; Zhang, Y. L.; Tam, M.; Erbe, D. V.; Tobin, J.; Xu, X.; Leung, L.; Shilling, A.; Tam, S. Y.; Mansour, T. S.; Lee, J., Structure-based optimization of protein tyrosine phosphatase 1B inhibitors: from the active site to the second phosphotyrosine binding site. *Journal of medicinal chemistry* **2007,** *50* (19), 4681-98.

28. Ignacio, B. J.; Albin, T. J.; Esser-Kahn, A. P.; Verdoes, M., Toll-like Receptor Agonist Conjugation: A Chemical Perspective. *Bioconjugate chemistry* **2018,** *29* (3), 587-603.

29. Parente-Pereira, A. C.; Burnet, J.; Ellison, D.; Foster, J.; Davies, D. M.; van der Stegen, S.; Burbridge, S.; Chiapero-Stanke, L.; Wilkie, S.; Mather, S.; Maher, J., Trafficking of CAR-engineered human T cells following regional or systemic adoptive transfer in SCID beige mice. *J Clin Immunol* **2011,** *31* (4), 710-8.

30. Dobrenkov, K.; Olszewska, M.; Likar, Y.; Shenker, L.; Gunset, G.; Cai, S.; Pillarsetty, N.; Hricak, H.; Sadelain, M.; Ponomarev, V., Monitoring the efficacy of adoptively transferred prostate cancer-targeted human T lymphocytes with PET and bioluminescence imaging. *Journal of nuclear medicine : official publication, Society of Nuclear Medicine* **2008,** *49* (7), 1162-70.

31. Emami-Shahri, N.; Foster, J.; Kashani, R.; Gazinska, P.; Cook, C.; Sosabowski, J.; Maher, J.; Papa, S., Clinically compliant spatial and temporal imaging of chimeric antigen receptor T-cells. *Nature communications* **2018,** *9* (1), 1081.

32. Bruno, R.; Giannasio, P.; Ronga, G.; Baudin, E.; Travagli, J. P.; Russo, D.; Filetti, S.; Schlumberger, M., Sodium iodide symporter expression and radioiodine distribution in extrathyroidal tissues. *J Endocrinol Invest* **2004,** *27* (11), 1010-4.

33. Vedvyas, Y.; Shevlin, E.; Zaman, M.; Min, I. M.; Amor-Coarasa, A.; Park, S.; Park, S.; Kwon, K. W.; Smith, T.; Luo, Y.; Kim, D.; Kim, Y.; Law, B.; Ting, R.; Babich, J.; Jin, M. M., Longitudinal PET imaging demonstrates biphasic CAR T cell responses in survivors. *JCI insight* **2016,** *1* (19), e90064.

34. Zhang, H.; Moroz, M. A.; Serganova, I.; Ku, T.; Huang, R.; Vider, J.; Maecke, H. R.; Larson, S. M.; Blasberg, R.; Smith-Jones, P. M., Imaging expression of the human somatostatin receptor subtype-2 reporter gene with 68Ga-DOTATOC. *Journal of nuclear medicine : official publication, Society of Nuclear Medicine* **2011,** *52* (1), 123-31.

35. Bhattacharyya, S.; Dixit, M., Metallic radionuclides in the development of diagnostic and therapeutic radiopharmaceuticals. *Dalton transactions* **2011,** *40* (23), 6112-28.

36. Khan, O.; Giles, J. R.; McDonald, S.; Manne, S.; Ngiow, S. F.; Patel, K. P.; Werner, M. T.; Huang, A. C.; Alexander, K. A.; Wu, J. E.; Attanasio, J.; Yan, P.; George, S. M.; Bengsch, B.; Staupe, R. P.; Donahue, G.; Xu, W.; Amaravadi, R. K.; Xu, X.; Karakousis, G. C.; Mitchell, T. C.; Schuchter, L. M.; Kaye, J.; Berger, S. L.; Wherry, E. J., TOX transcriptionally and epigenetically programs CD8(+) T cell exhaustion. *Nature* **2019**.

37. Alfei, F.; Kanev, K.; Hofmann, M.; Wu, M.; Ghoneim, H. E.; Roelli, P.; Utzschneider, D. T.; von Hoesslin, M.; Cullen, J. G.; Fan, Y.; Eisenberg, V.; Wohlleber, D.; Steiger, K.; Merkler, D.; Delorenzi, M.; Knolle, P. A.; Cohen, C. J.; Thimme, R.; Youngblood, B.; Zehn, D., TOX reinforces the phenotype and longevity of exhausted T cells in chronic viral infection. *Nature* **2019**.

38. Kawai, T.; Akira, S., Signaling to NF-kappaB by Toll-like receptors. *Trends in molecular medicine* **2007,** *13* (11), 460-9.

39. Chen, J.; Lopez-Moyado, I. F.; Seo, H.; Lio, C. J.; Hempleman, L. J.; Sekiya, T.; Yoshimura, A.; Scott-Browne, J. P.; Rao, A., NR4A transcription factors limit CAR T cell function in solid tumours. *Nature* **2019,** *567* (7749), 530-534.

40. Larkin, B.; Ilyukha, V.; Sorokin, M.; Buzdin, A.; Vannier, E.; Poltorak, A., Cutting Edge: Activation of STING in T Cells Induces Type I IFN Responses and Cell Death. *Journal of immunology* **2017,** *199* (2), 397-402.

41. Prinz, P. U.; Mendler, A. N.; Masouris, I.; Durner, L.; Oberneder, R.; Noessner, E., High DGK-alpha and disabled MAPK pathways cause dysfunction of human tumor-infiltrating CD8+ T cells that is reversible by pharmacologic intervention. *Journal of immunology* **2012,** *188* (12), 5990-6000.

42. Gorelik, L.; Flavell, R. A., Immune-mediated eradication of tumors through the blockade of transforming growth factor-β signaling in T cells. *Nature medicine* **2001,** *7* (10), 1118.

43. Herbertz, S.; Sawyer, J. S.; Stauber, A. J.; Gueorguieva, I.; Driscoll, K. E.; Estrem, S. T.; Cleverly, A. L.; Desaiah, D.; Guba, S. C.; Benhadji, K. A.; Slapak, C. A.; Lahn, M. M., Clinical development of galunisertib (LY2157299 monohydrate), a small molecule inhibitor of transforming growth factor-beta signaling pathway. *Drug design, development and therapy* **2015,** *9*, 4479-99.

44. Jin, C. H.; Krishnaiah, M.; Sreenu, D.; Subrahmanyam, V. B.; Rao, K. S.; Lee, H. J.; Park, S. J.; Park, H. J.; Lee, K.; Sheen, Y. Y.; Kim, D. K., Discovery of N-((4-([1,2,4]triazolo[1,5-a]pyridin-6-yl)-5-(6-methylpyridin-2-yl)-1H-imidazol-2 -yl)methyl)-2-fluoroaniline (EW-7197): a highly potent, selective, and orally bioavailable inhibitor of TGF-beta type I receptor kinase as cancer immunotherapeutic/antifibrotic agent. *Journal of medicinal chemistry* **2014,** *57* (10), 4213-38.

45. Wang, D.; Quiros, J.; Mahuron, K.; Pai, C. C.; Ranzani, V.; Young, A.; Silveria, S.; Harwin, T.; Abnousian, A.; Pagani, M.; Rosenblum, M. D.; Van Gool, F.; Fong, L.; Bluestone, J. A.; DuPage, M., Targeting EZH2 Reprograms Intratumoral Regulatory T Cells to Enhance Cancer Immunity. *Cell reports* **2018,** *23* (11), 3262-3274.

VITA

Boning Zhang was born and grew up in Beijing, China. She attended Peking University Health Science Center as an undergraduate and completed one-year internship at Beijing Third Hospital as a part of the training. After completing a Bachelor degree in Basic Medicine, Boning came to US for her Ph.D. study at Purdue University PULSe Program. After one-year rotation, she joined Prof. Philip Low's lab in Chemistry Department. During her time at Low lab, she worked on several projects, including development of antibody based NIR dye imaging agents for MUC1 positive tumors, design of ankyrin-based scaffold protein library for MUC1 targeting, folate-rhamnose directed immunotherapy for cancer, zanamivir-DNP directed immunotherapy for influenza infectious disease as well as her thesis work of designing a private passageway fusion receptor for the control of CAR T cells. She completed her Doctor of Philosophy degree in August 2019.

PUBLICATIONS

Zhang, B., Napoleo, J., Liu X, Srinivasarao, M and Low, P.S., Sensitive Manipulation of CAR T Cell Activity with a Private Passageway Fusion Receptor, in submission.

Low, P.S., **Zhang, B.** and Srinivasarao, M. Purdue Research Foundation, 2018. Targeted ligandpayload based drug delivery for cell therapy. PCT/US2018/018557

Zhang, B., J. V. Napoleon and P. Low (2019). "Abstract 2316: Systemic Control of CAR T Cell Activity Using a Secret Passageway Fusion Receptor." Cancer Research 79(13 Supplement): 2316-2316.

Liu, X., **Zhang, B.**, Wang, Y., Hamour, H.S. and Low, P.S., Neuraminidase-targeted immunotherapy of influenza: repurposing zanamivir as a targeting ligand for delivery of an attached immunogenic hapten to virus/virus-infected cells, manuscript in preparation.